The Mechanisms of Alpha Herpesvirus Intracellular Trafficking and Exocytosis

by

Melissa Hope Bergeman

A Dissertation Presented in Partial Fulfillment
of the Requirements for the Degree
Doctor of Philosophy

Approved March 2023 by the
Graduate Supervisory Committee:

Ian Hogue, Chair
Arvind Varsani
Brenda Hogue
Robert Roberson

ARIZONA STATE UNIVERSITY

May 2023

ABSTRACT

Alpha herpesviruses are a family of neuroinvasive viruses that infect multiple vertebrate species. Alpha herpesviruses are responsible for human and livestock infections, most notably Herpes Simplex Virus (HSV), Varicella Zoster virus (VZV), and Pseudorabies Virus (PRV). PRV is a potent swine virus that can infect other mammals, and results in lethal encephalitis that can be devastating to livestock and of great financial expense to farmers. HSV, types 1 and 2, and VZV are widespread throughout the global human population, with estimates of the HSV-1 burden at about 60% of people worldwide. The hallmark of alpha herpesvirus infection is a persistent, lifelong infection that can reactivate throughout the lifespan of the host. Currently, the precise mechanisms of how these viruses undergo intracellular trafficking to emerge from the infected cell in epithelial tissues is not well understood. Many insights have been made with PRV in animal neurons, both in culture systems and animal models, about the viral genes and host factors involved in these processes. However, understanding of these mechanisms, and the interplay between viral and host proteins, in the human pathogen HSV-1 is even more lacking. Using recombinant fluorescent virus strains of HSV-1 and Total Internal Reflection Microscopy to image the transport of mature viral progeny in epithelial cells, it was determined that the egress of HSV-1 uses constitutive cellular secretory pathways. Specifically, the viral progeny traffic from the *trans*-Golgi network to the site of exocytosis at the plasma membrane via Rab6a secretory vesicles. This work will contribute to the understanding of how alpha herpesviruses complete their lifecycles in host cells, particularly at the sites where infection initially occurs and can spread to a new organism. Knowledge of these processes may lead to the development of therapeutics or prophylactics to reduce the burden of these viruses.

DEDICATION

For Steven, Bethany, and Geffen, my family;

Michael Ayres and Jo Ann Jennings Ayres, my parents;

Mara, Washburn, Riley, the feline editors-in-chief who slept on the job to ensure that I did not.

ACKNOWLEDGMENTS

Thank you to my husband Steven for all of his support as I made a drastic change in careers and started all over with a whole different field. You have never doubted me, and only provided comfort and encouragement along this entire journey. I could not have done it without you.

Thank you to my parents Michael and Jo Ann, who have always fostered my drive for education and learning, and most importantly gave me the space to be curious, imaginative, and just the right amount of stubborn as I grew up. Without that, I would not have been able to become the person I am today.

Thank you to Bethany and Geffen. Best friends does not even begin to describe us; going on thirty years, we're nothing but sisters. Here's to thirty more, because no matter how far flung around the world we are, we always know where home is.

Thank you to my advisor and mentor, Dr. Ian Hogue, for all the guidance, advice, troubleshooting, recommendations, and pure opportunities you have given me over these five years. I am honored to have been so readily welcomed to your lab and to have helped build such a sense of community and camaraderie as the Hogue Lab got its start.

Thank you to all my fellow Hoguites: Wesley Tierney, Kim Velarde, Kayla Borg, Michaella Hernandez, and Ian Vicino. It would not have been half as fun without you all as my lab, as you made it a good place to be even on the worst days where it seemed the science would never work.

Thank you to my committee for all of their advice, critiques, and guidance on how to produce the best science that I could.

Thank you to Mae and Michelle, for giving me the support and encouragement as all three of us made major career changes at the same time. Here's to the 3 M's.

Thank you to Christine Bradshaw. You've come so far, and you're only going to go further. You helped me realize that I should not have given up on science. So here we are: we did it!

Thank you to Ali Varfai for telling me about LaTeX. It was a week's learning curve but made this final document a fraction of the hassle it would have been otherwise.

And last, but certainly not least, to my Desert View High School Jaguars: Keep it up, Minions. You're doing alright.

TABLE OF CONTENTS

Page

LIST OF TABLES vii

LIST OF FIGURES viii

CHAPTER

1 INTRODUCTION TO ALPHA HERPESVIRUSES 1

1.1 Herpes Virus Families and Their Pathogenicity 1

1.2 Alpha Herpesvirus Structure and Host Infection Cycle 2

1.3 Viral Replication Cycle In Host Cells 3

1.4 Alpha Herpesvirus Egress 7

1.5 Current Treatments for Alpha Herpesviruses 8

1.6 Current Development and Use of Alpha Herpesvirus Vaccines 9

1.7 Alpha Herpesvirus Vectors 12

1.8 Open Alpha Herpesvirus Research Directions 14

2 VISUALIZING VIRAL INFECTION: FLUORESCENT ALPHA HERPESVIRUS RESEARCH 20

2.1 Fluorescent Proteins: A New Spotlight on Microscopy 20

2.2 Viral Imaging 21

2.3 Fluorescent PRV Research Approaches 22

2.4 Case Study of Using Fluorescent PRV to Infer Host-Virus Interactions 25

2.5 Use of Fluorescent HSV-1 Viruses 28

3 LIVE-CELL FLUORESCENCE MICROSCOPY OF HSV-1 CELLULAR EGRESS BY EXOCYTOSIS 33

3.1 Abstract 33

3.2 Introduction 34

CHAPTER Page

3.3 Results 37

3.4 Discussion 43

3.5 Materials and Methods 44

BIBLIOGRAPHY 57

4 HERPES SIMPLEX VIRUS 1 (HSV-1) USES THE RAB6 POST-GOLGI SECRETORY PATHWAY FOR VIRAL EGRESS 67

4.1 Abstract 67

4.2 Introduction 68

4.3 Results 70

4.4 Discussion 76

4.5 Materials and Methods 78

BIBLIOGRAPHY 88

5 DISCUSSION 94

5.1 Summary of Results 94

5.2 Future Directions: Rab6 in Neurons 96

5.3 Future Directions: Rab6 and Other Rab Protein Interactions 97

5.4 Future Directions: Rab and ERC1 98

5.5 Motor Transport 98

5.6 Concluding Remarks 99

REFERENCES 102

APPENDIX

A COAUTHOR PERMISSION FOR PREVIOUSLY PUBLISHED WORK IN CHAPTER 3 120

APPENDIX Page

B COAUTHOR PERMISSION FOR PREVIOUSLY PUBLISHED WORK IN CHAPTER 4 122

LIST OF TABLES

Table Page

3.1. PCR Primer Sequences 56

LIST OF FIGURES

Figure Page

1.1. HSV-1 Virion 16

1.2. Linear HSV-1 Genome 17

1.3. HSV-1 Infection Cycle Inside Human Host 18

1.4. HSV-1 Replication Cycle 19

2.1. gE, gI, and US9 Expression in PRV Recombinants. 30

2.2. Growth Kinetics and Plaque Sizes of PRV Recombinants 31

2.3. Recombinant PRV Exocytosis and Particle Velocity 32

3.1. HSV-1 Egress and gM-pHluorin Insert 49

3.2. PCR of gM-pHluorin Insert 50

3.3. pHluorin Expression and Impact on Viral Replication 51

3.4. TIRF Microscopy of HSV-1 Exocytosis 52

3.5. Single Virus Particle Exocytosis of HSV-1 and PRV 53

3.6. HSV-1 Exocytosis in Primary REF Cells 54

3.7. Accumulations of Progeny Virus Particles 55

4.1. Rab6a Secretory Pathway 82

4.2. Rab6a and HSV-1 Cotrafficking 83

4.3. Endogenous and Exogeous Rab6a with HSV-1 Infection 84

4.4. Rab6a and HSV-1 Accumulate at Exocytosis Sites 85

4.5. HSV-1 Undergoes Exocytosis from Rab6a Secretory Vesicles 86

4.6. HSV-1 Does Not Undergo Exocytosis from Rab5a Vesicles 87

Chapter 1

INTRODUCTION TO ALPHA HERPESVIRUSES

1.1 Herpes Virus Families and Their Pathogenicity

The herpesviridae family comprises three distinct sub-families: the gamma herpesviruses, the beta herpesviruses, and the alpha herpesviruses [1, 2]. The viruses in these sub-families infect a broad number of species, have a broad spectrum of tissue tropisms and produce lifelong infections in their hosts. The herpes viruses were formerly classified into families based on the cell types in which they establish latent, lifelong infections and the length of their replication cycles, but have more recently begun to be classified by genetic sequencing and homology [2, 3]. Gamma herpesviruses infect and remain latent in lymphoid cells [2]. The beta herpesviruses are slow-replicating viruses that produce cytomegaly, and their latent tissue tropisms include secretory glands, kidney, and lymphoreticular cells [2]. Alpha herpesviruses, by contrast, have rapid replication cycles and are neuroinvasive, establishing latency in the peripheral nervous system (PNS) [2, 4].

Notable members of the alpha herpesvirus family that are of particular interest due to their human or livestock hosts are the Herpes Simplex Viruses (HSV), Varicella Zoster Virus (VZV), Pseudorabies Virus (PRV), and Bovine Herpes Virus (BHV) [5]. BHV and PRV are bovine and suid herpesviruses, respectively, while HSV and VZV are distinctly human pathogens [2, 5, 6]. Rare instances of PRV infecting humans have been documented in recent years in Chinese pork farmers and slaughterhouse workers who come into regular contact with pigs and their bodily tissues [7]. Herpes

B virus, whose primary host is macaques, can infect humans with a high mortality rate and cases are primarily only seen in veterinary or research personnel working with these animals [2, 8]. In humans, there are two distinct simplex viruses: HSV-1 and HSV-2. Globally HSV-1 infects the majority of adults, with estimates running to two out of three persons worldwide [4, 5, 9, 10].

Alpha herpesviruses establish a lifelong infection for the host, with alternating periods of latency and reactivation [4, 5, 9]. Active HSV-1 infection typically produces oral or genital lesions [4]. Most infections with HSV-1 are minor and, while they may be irritating with recurrent outbreaks of lesions, are typically not life-threatening. However in some cases the virus, due to its neuroinvasive properties, can pass from the PNS and into the central nervous system (CNS), resulting in herpes encephalitis in very young or immunocompromised patients [4, 11]. HSV-1 can also infect the eye, causing herpes keratitis, which can lead to blindness in the affected eye [4]. Systemic/disseminated herpes is a grievous infection in neonates and can also be fatal [4].

1.2 Alpha Herpesvirus Structure and Host Infection Cycle

Alpha herpesviruses are enveloped, double stranded DNA viruses [2, 12]. The icosahedral nucleocapsid core contains the viral genome with approximately 150 kilobase pairs of DNA [2, 13]. A layer of tegument protein surrounds the nucleocapsid and is in turn enclosed in a lipid envelope with glycoproteins of various functions related to egress, attachment, and entry (Figure 1.1) [2, 12, 14]. Like other alpha herpesviruses, the HSV-1 genome is packaged in a linear manner and consists of two unique sections that are flanked by repeat sections, and as one unique segment is

longer than the other, these are respectively named the Unique Long (UL) and Unique Short (US) regions (Figure 1.2) [15–17]. Viral gene expression is then derived from both of the UL and US regions during replication.

Infection with alpha herpesviruses, particularly PRV and HSV-1, begins at epithelial tissues in mucosal surfaces [2]. The virus then gains access to the PNS via sensory and autonomic neurons that innervate these tissues, first entering at or near the peripheral nerve endings [2, 4, 5]. The virus can then spread through the network of connected neurons in the peripheral nervous system [2, 5, 18]. The virus establishes latency in sensory neurons, primarily in the trigeminal ganglia (TG) that innervate the head and dorsal root ganglia (DRG) that innervate the rest of the body. Typically, in natural infections of healthy hosts, viral infection does not lead to CNS disease, although asymptomatic or subclinical infection of the CNS may occur. However, spread into the central nervous system is fatal for most mammals infected with PRV, and human HSV-1 encephalitis is always serious and carries a high risk of fatality [2, 5, 19]. Upon reactivation, alpha herpesviruses traffic through the PNS and back to epithelial tissues, resulting in characteristic herpetic or zosteriform lesions (Figure 1.3). These lesions facilitate spread from one mammalian host to another, or from person to person in the case of HSV-1 [2, 4, 5].

1.3 Viral Replication Cycle In Host Cells

In HSV-1, four viral glycoproteins are essential for viral entry [20, 21]. Glycoprotein D (gD) binds cellular receptors to initiate the entry process [22, 23]. Receptors vary across cell types, and include herpes virus entry mediator (HVEM), 3-0-sulfated heparan sulfate, and nectin-1 [20–23]. After receptor binding, glycoprotein B (gB)

mediates envelope fusion with the host cell's plasma membrane [24]. The glycoprotein H/L (gH/L) heterodimer forms a complex with gB and gD, and are also required for entry [25].

After fusion between the viral envelope and plasma membrane, the tegument layer is disassembled, and dynein motors deliver the nucleocapsid along microtubules to the nucleus, where viral mRNA synthesis and DNA replication occurs [23, 26]. Tegument proteins UL36 and UL37 are thought to be the main viral factors that recruit dynein motors, but other viral proteins, like VP26, UL14, and ICP0 may also facilitate capsid delivery to the nucleus [23]. UL6, UL25, and UL36 assist with capsid with docking at nuclear pores [23, 27, 28]. The capsid vertex specific component, consisting of UL25, UL17, and UL36, binds and stabilizes the capsid at the nuclear pore complex during viral genome delivery [29]. Once the capsid docks at the nuclear pore complex, UL36 is cleaved to release the viral genome from the capsid into the nucleus [30]. With successful delivery of the viral genome, viral gene expression and genome replication can begin (Figure 1.4).

HSV-1 gene expression is divided into three main categories: immediate-early, early, and late genes [15, 31, 32], all of which are transcribed by host RNA polymerase II [17]. Immediate-early genes are driven by strong constitutively active promoters, and immediate-early gene products transactivate the early genes. The proteins synthesized from early mRNAs are primarily enzymes and regulatory proteins that are required for DNA synthesis and replication [15, 17]. Immediate-early gene expression peaks between 2-4 hours post infection (hpi) [17]. Early gene expression drives nucleotide metabolism, initiates DNA replication, and comprises some of the envelope glycoproteins [15]. In the nucleus, early proteins form replication centers and initiate replication of the viral genome [33]. While early viral proteins are required for DNA replication, this process

also relies on many host factors [34]. Early gene expression is detectable as early as 3 hpi and reaches its peak at 5-7 hpi. DNA replication is detectable as early as 3 hpi, but continues until about 15 hpi [17]. Late genes mostly encode structural proteins, including capsid proteins, tegument proteins, and some membrane proteins [33]. A few viral gene products guide the assembly and egress of viral capsids, but are not incorporated into mature virions. For example, the UL33 protein is essential for capsids to complete assembly and DNA packaging, but is not detected in mature virions [35].

During replication, the viral genome circularizes for rolling circle replication [36, 37] (Figure 1.4). UL6 forms the unique portal vertex through which DNA is inserted into the capsid [38, 39]. The terminase complex cleaves the viral DNA concatemers produced from replication into single, discrete genomes during packaging [39]. Intranuclear capsids are categorized as B capsids, which contain scaffold proteins; A capsids, which are empty and lacking an HSV genome; and C capsids, which contain a complete HSV genome [13]. During DNA packaging, the capsid vertex specific complex (including UL25 and UL17) binds to capsids and these proteins are required for capsids to maintain their structural integrity and retain viral DNA, which is under high pressure [40, 41]. Once packaged, capsids must exit the nucleus to complete assembly and egress.

To exit the nucleus, a nuclear egress complex (NEC) forms to alter the nuclear membrane and allow membrane scission to release capsids [42]. UL25 drives the formation of the NEC, which is a hexagonal scaffold around the capsid [43]. NEC proteins coat the interior of budding nuclear vesicles that contain capsids, and they constrict the membrane neck during budding to release the capsid-containing vesicle from the nucleus into the perinuclear space [42, 44]. During nuclear egress, viral

capsids obtain what is known as the "primary envelope", derived from the inner nuclear membrane, and this primary envelope is then removed during subsequent steps of replication [44]. UL31 and UL34 proteins assist viral budding into the perinuclear space and are essential components of the NEC [44].

Upon nuclear egress, capsids and tegument begin to associate. Tegument consists of many viral and host proteins, including UL36, UL37, US3 proteins [45]. The tegument layer forms in a chain-like cascade: UL36 binds UL48, UL48 in turn binds UL46, UL47, UL49, and envelope proteins during secondary envelopment [46–51]. Tegument complexes can also assemble in the absence of capsids, leading to the formation of non-infectious light or L-particles [52, 53]. Once they have acquired tegument, capsids traffic along microtubules via kinesin motors [45].

During these stages of HSV infection, the microtubule organizing center (MTOC) undergoes reorganization and microtubules are elongated from nucleating sites at the *trans*-Golgi towards the plasma membrane [54–56]. In order to counteract host cell defenses against this increase in microtubule growth, US3 protein inactivates glycogen synthase kinase 3 and depresses cytoplasmic linker associated proteins [54]. Microtubules also form tunneling nanotubes, a potential avenue of direct cell-cell spread for HSV, under direction of US3 [57, 58]. VP22 assists in microtubule elongation by bundling and hyperacetylating them [59–61]. Thus the host cell is prepared for the intracellular trafficking and egress of virus progeny.

Kinesin motors carry capsids that are coated with tegument to the site of secondary envelopment, in which the immature virus particle acquires an envelope to become a complete infectious virion [46]. The specific organelle from which envelopes are obtained, and where secondary envelopment occurs, is currently not fully understood. It is known, though, that capsids localize to *cis*- and *medial*-Golgi compartments

during this stage of infection [62, 63]. Tegument proteins UL36 and UL37 may serve as the link between the capsid, the tegument, and *trans*-Golgi network (TGN) membranes by directing capsid movement to the site of secondary envelopment [62–65]. UL37-null virus particles do not associate with the TGN or undergo successful envelopment, whereas those which do express competent UL37 complete these steps [66]. Envelopment occurs through the association of envelope and tegument proteins, with lipids and viral proteins comprising the viral envelope [46, 66].

HSV requires host ESCRT machinery for envelopment, which mediates membrane scission. It remains unclear how viral structural proteins recruit cellular ESCRT complexes, but UL51 may mimic cellular ESCRT by interacting with gE and gI [66, 67].

1.4 Alpha Herpesvirus Egress

After envelopment, virus particles must be transported to the plasma membrane for exocytosis (Figure 1.4). Several membrane glycoproteins coordinate the recruitment and employment of various host factors and complexes in order to complete virus particle transport and egress. Two notable examples are glycoprotein E (gE) and glycoprotein I (gI). gE and gI may assist in trafficking to the TGN, and gE-gI null viruses do not sort to basal surfaces of polarized epithelial cells [67]. Virus proteins UL7 and UL51 help the cell maintain focal adhesions by stabilizing them so that virus particles may spread to neighboring cells [55].

Host factors that have been noted in alpha herpesvirus egress are Rab6 and Rab8 [68, 69]. Rab proteins are small GTPases, meaning that they are molecular switches that turn on or off by binding GTP or hydrolyzing it to GDP, respectively. Humans

express over 60 different types, which bind to particular membranes and regulate vesicle transport. Dynein and kinesin motors are indirectly regulated by Rabs, and kinesins are direct Rab effector proteins [70]. In the context of HSV-1 infection, Rab6 has been implicated as a potential host factor as knockdowns of Rab6 have resulted in lower viral titers, reduced viral glycoprotein transport, and inhibited the late stages of viral replication [71].

In Vero (African green monkey kidney) cells, virus particles egress at preferential sites, accumulating at these areas of the plasma membrane [72]. These hotspots are thought to be where the cell adheres to its substrate and neighboring cells, and they may be associated with cellular focal adhesion complexes [72]. In human fetal DRGs, synaptic vesicle markers Rab3A, SNAP25, and GAP43 indicate that egress may occur from synaptic vesicles or synaptic vesicle precursors, which may explain the specific spread of alpha herpesviruses between synaptically-connected neurons [73, 74].

1.5 Current Treatments for Alpha Herpesviruses

Antiviral therapies are the main line of treatment for severe cases of HSV-1 and HSV-2 infections, particularly for neonatal herpes or herpes encephalitis [75]. Antivirals also can be administered orally or topically for recurrent outbreaks of genital and labial herpes [75]. Acyclovir and valacyclovir are the main antivirals used for human herpes infections, and they are guanosine analogs that disrupt DNA replication and thereby halt viral replication. Hydrocortisone can also be administered in conjunction with antivirals to reduce inflammation and to soothe the inflamed tissues at the outbreak site. A newer generation antiviral is penicyclovir. It is another

guanosine analog, but has the advantage of reducing the risk of viral spread from person to person during an active outbreak [75].

A major limitation of antivirals is that they must be started early, typically within the first eight hours of symptom onset or they have minimal to no effect during an outbreak of new oral or genital lesions [75]. While penicyclovir can reduce transmission, it does so only by ∼50%. Finally, there have been extremely rare cases of antiviral resistance, with resistance increased significantly in immunocompromised patients. This is likely due to the fact that these patients have an increase in both frequency and severity of outbreaks. With each outbreak comes viral replication and the potential for genetic mutation that could lead to antiviral resistance, particularly as the antivirals can place selective pressure on the actively replicating virus [75].

The same class of antivirals that are employed against human herpes viruses are also effective against PRV. However, as PRV is primarily a veterinary pathogen, treating animals, especially the large numbers found in livestock herds, is impractical from a logistical and financial point of view. Vaccination for PRV remains the primary method of control, especially in China and other east Asian countries as discussed further below.

1.6 Current Development and Use of Alpha Herpesvirus Vaccines

Vaccines have been successfully developed and used for two alpha herpesviruses: VZV in humans and PRV in swine. Currently there is no FDA approved vaccine available for HSV-1 or HSV-2 [76, 77]. Alpha herpesvirus vaccines fall into three categories: subunit, replication incompetent, and live attenuated [76–78].

The VZV vaccine is administered to two different target populations: children who

have not yet had a primary infection resulting in varicella (commonly called chicken pox) and then adults over 50 years of age that have been infected with VZV as children and are at risk of herpes zoster (shingles) [78, 79]. The VZV vaccine administered to children is a monovalent, live attenuated strain, and since 2005 has been added to the traditional Measles, Mumps, Rubella (MMR) vaccine series [78]. For adults, the vaccine differs only in that it contains fourteen times the amount of antigen to account for potential reduced immune responses in the target senior population [78]. In 2017, the herpes zoster vaccine was reengineered by producing a more immunogenic gE protein. This modified vaccine is a 2-dose series and confers 7-8 years of protection at an efficacy rate of 85-90% [78, 79]. There could be the potential for the adult VZV vaccine to fall out of use: as individuals vaccinated as children age they will not be at risk for developing herpes zoster since they will not have a latent VZV infection, and therefore only the childhood vaccine may be given in the future.

For PRV, the first vaccine was the live attenuated Bartha strain [80]. With its deletions of gE-gI-US9, PRV Bartha has reduced virulence in swine and other non-primate mammals [2, 80, 81]. Subsequent attenuated strains of PRV have also been used as a vaccine, including the Norden strain [80]. However, in China recent PRV outbreaks in swine have occurred because of vaccine escape by emerging PRV strains. These novel strains are due to antigen drift in vaccinated swine populations. As a result, additional vaccine strains that account for this antigen drift are going to be necessary in the coming years to avoid additional livestock losses [82–84]. Furthermore, with the reported cases of PRV infecting humans in China [7], it remains uncertain whether these cases are caused by the same vaccine escape strains also currently emerging. The potential for a PRV strain that is more infectious in humans and can

also escape existing vaccines is certainly a cause for concern and should drive next generation vaccines for PRV in livestock mammals.

As of 2020, there have been sixteen vaccine candidates for HSV that have all failed at the preclinical through clinical phases of trials [77]. Attempts at vaccine production for HSV have focused primarily on HSV-2 rather than HSV-1 because of the increased risk of HIV infection occurring in individuals positive for HSV-2, the prevalence and stigma of genital ulcers, viral transmission to neonates from mothers during birth, and the severity of neonatal herpes [77, 85, 86]. While HSV-1 can cause genital herpes, it is primarily associated with herpes labialis (cold sores) and therefore does not carry the social stigma of HSV-2. Additionally, since the viruses are highly orthologous, there is hope that a vaccine for HSV-2 would result in cross immunity for HSV-1. For these reasons, there is a reduced interest in developing an HSV-1 vaccine in comparison to that of one for HSV-2.

Vaccine candidates for both types of HSV have been prophylactic to prevent initial infection and therapeutic to reduce recurrence of lesion outbreaks in infected individuals [77]. The primary target of the vaccine is the gD protein, with some formulations using gE, gB, or both to complement the immunogenicity of gD. A new vaccine candidate that is DNA-based is currently being developed since other subunit, replication incompetent, and live attenuated platforms have all failed [76, 77]. Five viral proteins (gD, gB, ICP0, ICP4, and UL39) that have classically produced the strongest immune responses in previous studies will be encoded by the DNA to be delivered by intramuscular injection [77].

There is also interest in using alpha herpesviruses as vectors for other vaccines. Specifically, PRV has been engineered to express transgenes from other viruses and

used successfully to vaccinate swine and other livestock for swine influenza, classical swine fever, and foot-and-mouth disease [80].

1.7 Alpha Herpesvirus Vectors

Alpha herpesviruses are excellent candidates for viral vector systems because they infect a multitude of cell types and have large carrying capacity for transgenes [87–89]. Since alpha herpesviruses can infect the nervous system, spreading from neuron to neuron, and undergo axonal transport, they are particularly attractive as vectors to these otherwise inaccessible tissues [89].

HSV-1 amplicon vectors are specifically designed to deliver transgenes to cells. These vectors resemble an HSV-1 virus particle in all aspects but the genome. Instead of the HSV genome, the capsids are packaged with head-to-tail concatemers of plasmid DNA. The proteins encoded by the plasmid DNA are expressed by host cells after they are infected with the amplicon vector [87, 90]. Amplicon vectors are produced by transfecting cells with a plasmid carrying the transgene of interest, an origin of replication, and a viral packaging signal [87]. Then the cells are infected with an HSV-1 helper virus as the amplicon plasmid does not express the viral genes necessary to produce HSV-1 particles [87]. These amplicon vectors result in higher rates of transgene expression as they deliver multiple copies of the gene and can easily be engineered to express a variety of proteins of interest. Since they require a helper virus, a strain of interest can be used for this purpose [87, 90].

We have developed several HSV-1 amplicon vectors that express a variety of host factors that are of interest to our lab, and demonstrate their use in the studies presented in Chapter 4 [90]. Amplicon vectors can be powerful tools for researching host cell

biology and virus-host interactions, but they do result in active helper virus infection. Needless to say, this severely limits the types of studies that can be performed with this system unless active infection is a desired parameter.

Alpha herpesvirus vectors are being explored for *in vivo* studies as gene therapy treatments. Proof-of-concept studies have been performed with HSV-1 expressing GFP and mCherry reporter genes. These engineered vectors also had the immediate early genes deleted to reduce the host's immune response to the vector [91, 92]. Non-neuronal cells showed consistent and stable expression of the fluorescent proteins in addition to low inflammatory responses and cell toxicity *in vitro* [91]. Subsequent *in vivo* studies showed the same results in rat hippocampal neurons for six months [92].

Other HSV vector strategies are in the field of oncolytic viruses. The first oncolytic viruses to be FDA approved is an HSV-1 vector called T-VEC that treats melanoma in humans [93, 94]. T-VEC has been engineered to preferentially infect melanoma tumor cells, and therefore it only replicates in these cells. Tumor cell death is a direct result of infection, and the human granulocyte-macrophage colony stimulating factor expressed by the vector induces a host immune response against the tumor itself. Currently, T-VEC is administered via direct injection into the tumor site as part of melanoma treatment [93, 94].

Glioblastoma is a human brain cancer that is often inoperable and difficult to treat via radiation. It is also very aggressive, growing rapidly, and is always fatal. Since the traditional first line cancer treatments of surgery and radiation are either impossible or highly ineffective due to tumor location, there exists a need for alternative approaches [95]. HSV may fill this gap as it is capable of reaching glioblastoma tumor beds due to its existing neuroinvasive properties. Potential HSV oncolytic vectors for glioblastoma are engineered to express tumor-cell specific receptors so that, like T-VEC, they target

only tumor cells and not healthy ones [95, 96]. They are also being engineered to express genes that aide in the efficacy of chemotherapies. By increasing the sensitivity of the tumor to chemotherapy, inducing tumor cell death by infection, and prompting a host immune response against the tumor, these vectors may present a revolution in glioblastoma treatment [95, 96].

1.8 Open Alpha Herpesvirus Research Directions

While many studies have identified some of the interactions between host factors and alpha herpesviruses during viral egress, multiple questions still remain. Many studies have addressed only one virus in the sub-family, such as PRV or HSV-1, or only in specific cell types without broader connections between different host cells. Specifically, the identification of alpha herpesviruses egressing via Rab secretory vesicles was done with PRV and PK15 cells [68, 69]. As of yet, there have been no studies documenting Rab6 secretory vesicles serving a role in HSV-1 egress. Studies of HSV-1 egress from non-neuronal cells is another under-studied area in the field, particularly as it relates to potential host factor and viral interactions during this final step of viral infection.

In order to address some of these questions, we engineered a novel recombinant strain of HSV-1 to express a reporter fluorescent protein that allowed for detection of exocytosis in live cells. Then we examined the interaction between HSV-1 and potential host factor Rab6a during viral trafficking from the TGN to exocytosis at the plasma membrane. These experiments were conducted in a variety of cell types, with transformed epithelial cell lines and primary fibroblasts, in order to compare any potential differences between cell types and understand how underlying host

cell biology affects viral egress. Additionally, we investigated the potential effects of gE-gI-US9 proteins on viral egress and cell-cell spread as they may have broader implications for viral vector design.

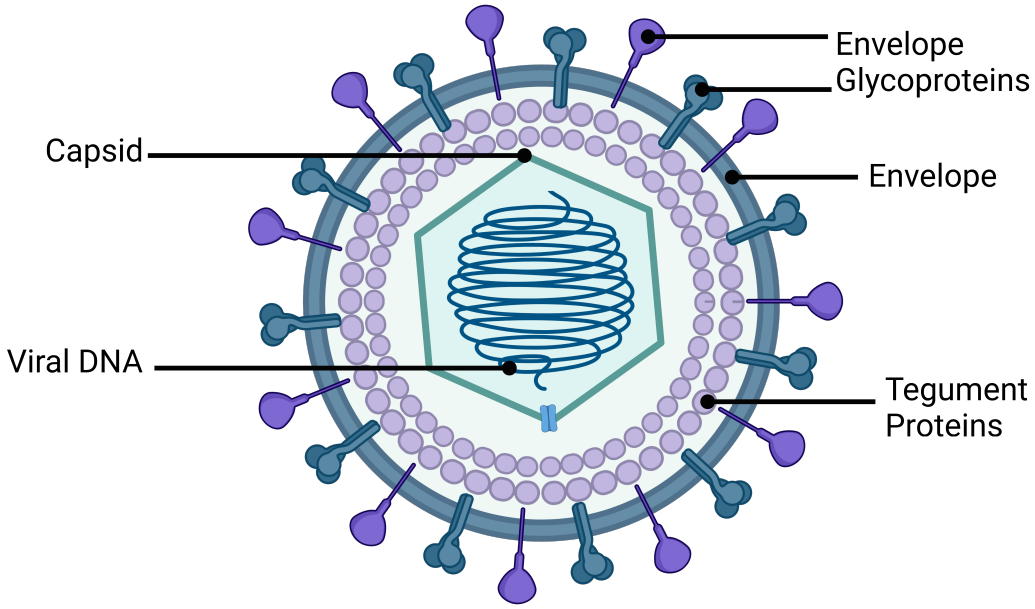

Figure 1.1. HSV-1 Virion

HSV-1 virus particle with envelope proteins, lipid envelope, tegument proteins, capsid, and DNA. Created in BioRender.com

Figure 1.2. Linear HSV-1 Genome

The HSV-1 genome is ∼150 kilobases. The unique long and short regions are flanked by terminal repeat and internal repeat sections. Created in BioRender.com.

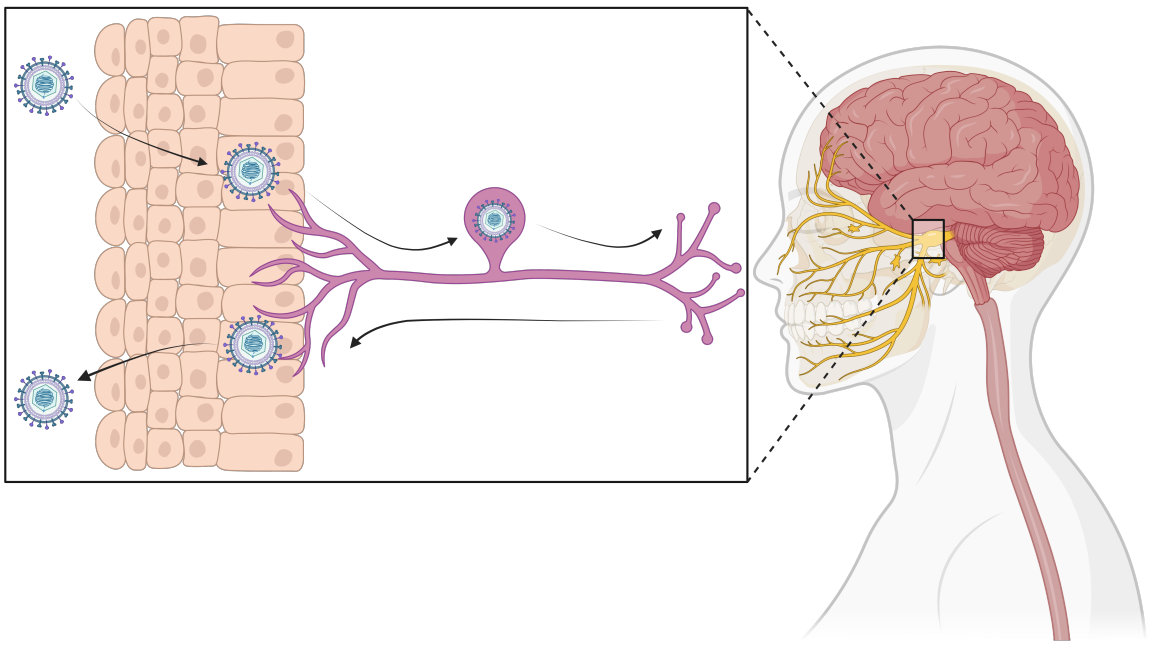

Figure 1.3. HSV-1 Infection Cycle Inside Human Host

HSV-1 enters a human host at oral mucosal membranes and enters the peripheral nervous system by sensory neurons. The virus then travels to subsequent neurons in the superior cervical ganglia, where it establishes latency for the person's lifetime. Reactivation of the virus results in the virus trafficking back to the mucosal tissues and producing lesions which shed virus particles that can infect another person. Created in BioRender.com.

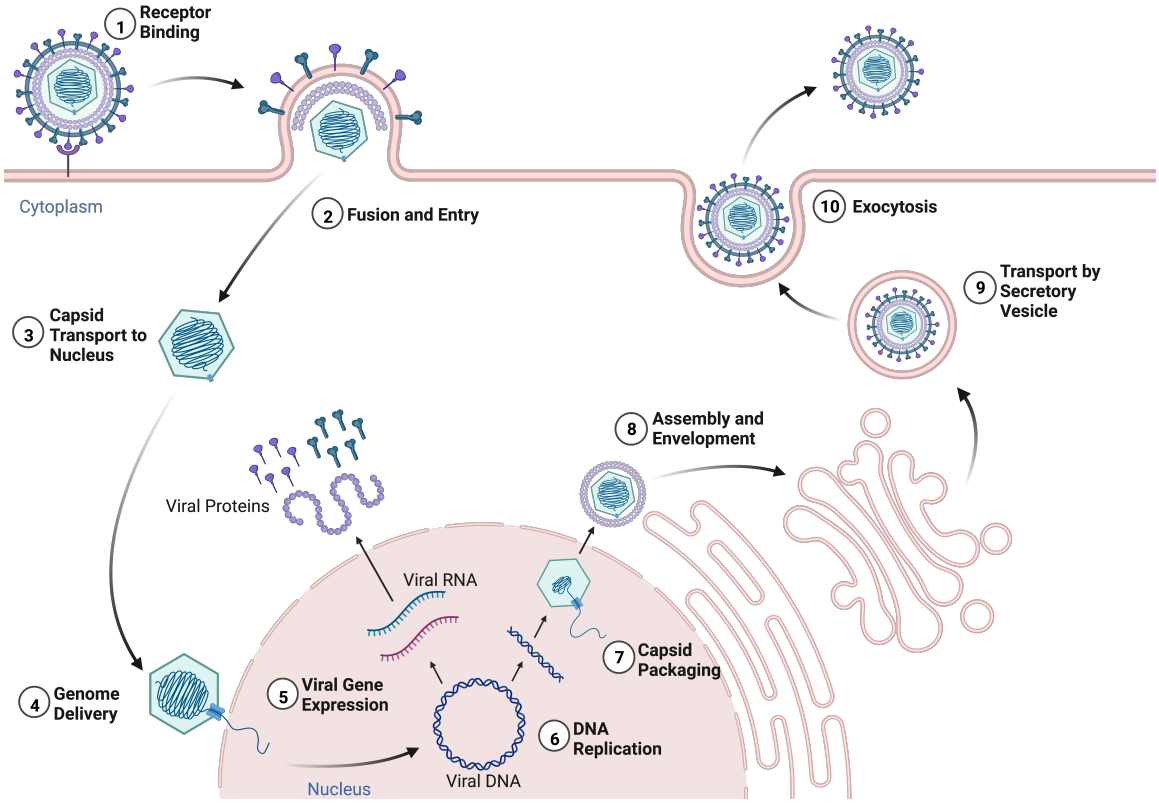

Figure 1.4. HSV-1 Replication Cycle

HSV-1 binds and enters through receptor-mediated endocytosis. The capsid delivers the genome to the cell nucleus for RNA and DNA synthesis and subsequent protein expression. Capsids are assembled, packaged with DNA, and exported to the Golgi and *trans*-Golgi network for envelopment. Virions are trafficked to the plasma membrane where they undergo exocytosis. Created in BioRender.com.

Chapter 2

VISUALIZING VIRAL INFECTION: FLUORESCENT ALPHA HERPESVIRUS RESEARCH

2.1 Fluorescent Proteins: A New Spotlight on Microscopy

In 1961, the first fluorescent protein was identified in the *Aequorea victoria* jellyfish. Other bioluminescence had been observed in various ecosystems, such as phosphorescent algal blooms, luciferase in bacterial species, and even the fluoresence of scorpions [97–99]. Luciferase became a powerful screening tool for bacteriology studies and then as a reporter in eukaryotic cell biology studies [100, 101]. Most bioluminescent reactions produce photons as byproducts of enzymatic reactions and have rate limiting steps that restrict the production of photons based on the availability of the substrates for those reactions. Unlike other bioluminescent molecules, green fluorescent protein (GFP) repeatedly emits photons for the time that is exposed to the excitation wavelength since the substrate for photon emission is the excitation source itself [102].

With the discovery of GFP, new possibilities for imaging studies opened up as researchers found that it could readily be expressed by mammalian cells and fused with mammalian proteins [103–105]. Additional colors of fluorescent proteins soon followed: DsRed was isolated from coral in 1999, mutations in the gene for GFP produced fluorescent proteins in additional spectra, and other modifications produced fluorescent proteins that are conditional reporters [106–109]. Protein-protein interactions could be determined, and the trafficking of intracellular cargo could be observed in both fixed and live cells with the use of multiple colors [110]. The Brainbow cassette was designed

to exhibit color change upon recombination, which can be used to visualize neural development, neural gene expression, and other aspects of neurobiology amongst a variety of organisms ranging from mice to zebrafish to *Drosophila*. [111].

2.2 Viral Imaging

With fluorescent proteins being used to study molecular, cellular, and neurobiology, it was not long before these areas merged with virology. Rabies virus (RABV), which infects mammals and is always terminal once symptoms appear, was engineered to express EGFP and a red fluorescent fusion to the RABV G protein transmembrane domain. With this dual-colored virus, axonal transport in virus particles was observed [112]. Axonal transport of RABV was also detected in DRG neurons using explanted embryonic rat DRGs cultured in a microfluidics chamber [113]. The near-infrared fluorescent protein iRFP720 expressed by RABV traced the pathway the virus traveled from inoculation site in the leg to the CNS to the brainstem in mice [114].

More recently, and of great current relevance to global health, coronaviruses have also been used to express fluorescent proteins. Mouse hepatitis virus (MHV) has been used as an analog for the highly infectious SARS coronavirus, and the cell-cell spread of MHV has been studied with a strain expressing GFP [115]. Specifically, the MHV infection of the CNS in mice was detected with this virus [115]. With the emergence and resulting pandemic of SARS-CoV-2, the neuroinvasive properties of coronaviruses has once again come into the spotlight. SARS-CoV-2 can enter the human nervous system via the olfactory route or the lungs, and can also cross the blood-brain barrier in cases of high viremia [116, 117]. While RABV, MHV, and SARS-CoV-2 certainly

have importance as human and veterinary pathogens, the use of fluorescent proteins has become an essential component of alpha herpesvirus research.

2.3 Fluorescent PRV Research Approaches

A major breakthrough in alpha herpesvirus research came when GFP was successfully inserted into PRV and used for *in vivo* studies of viral infection [118]. Smith et al inserted GFP into the attenuated vaccine Bartha strain of PRV to produce PRV 152 [119]. PRV Bartha was used as the parental strain of choice to produce PRV 152 because it contains a deletion of gE-gI-US9. These three proteins are essential for anterograde axonal transport, and deletion of these three genes renders the virus incapable of spreading anterograde in a synaptic circuit—i.e. from a presynaptic neuron to a postsynaptic neuron [81]. Thus, the mutant virus can only spread in the retrograde direction, from postsynaptic neuron to presynaptic neuron [120–123]. Despite this limitation in neurons, the mutant virus is replication competent and readily exits and spreads between non-neuronal cells. This allows for viral infection at the host's peripheral tissues and subsequent tracking of the virus as it spreads. Specifically, neurons that are linked to the infection site can be identified in the CNS and brain [2, 124]. For example, hamsters were inoculated in the nose with PRV 152 and tissues were harvested, fixed, and examined by fluorescence microscopy for the presence of PRV 152 [119].

This proof-of-concept, that neural networks could be identified by neurotracing viruses, led to the construction of additional fluorescent strains of PRV that would be extensively used in the growing field of neurotracing studies. PRV Bartha2001 (PRV Ba2001) exhibits conditional replication and fluorescent protein expression in the

nervous system, in the presence of Cre recombinase. This virus was used to study the network of feeding centers in the rat hypothalamus [125]. Additional studies with PRV Ba2001 followed: identification of neurons in the olfactory system that are involved in regulating reproduction and mating in mice [126] and the innervation of pancreatic islet cells leading to the brainstem and hypothalamus in rats [127]. However, studies with PRV Ba2001 are limited by very low GFP expression in neurons, leading to false positive results (misidentification of background as fluorescence) or false negatives (misidentification of low fluorescence as no fluorescence) [128].

Additional fluorescent strains of PRV were designed to overcome the low expression and subsequent dim fluorescence limitations of PRV Ba2001. Neuron to neuron viral transmission was tracked with PRV 263, which carries a Brainbow cassette of dTomato (red), EYFP (yellow), and mCerulean (cyan). In cells expressing Cre recombinase, the virus will undergo a color change as the fluorescence protein expression changes from dTomato to EYFP or mCerulean upon Cre recombination [129]. Similarly to Ba2001, PRV-Introvert exhibits Cre-dependent replication and fluorescent protein expression, but was additionally engineered to better control leaky gene expression in the absence of Cre recombinase. To achieve Cre-dependent replication in the nervous system, PRV Ba2001 and PRV-Introvert contain a viral thymidine kinase (TK) gene that is modified to prevent expression prior to Cre-mediated recombination. The TK gene is dispensable in rapidly dividing non-neuronal cells, but is required for efficient viral replication in non-dividing cells, like neurons. Cre-dependent recombination restores TK expression (and fluorescent protein expression), and the resulting virus replicates and spreads in the nervous system. Characterization of PRV-Introvert showed that it maintained appropriate replication under the Cre system and suitable GFP expression

[6]. Nectow et al. used PRV-Introvert to study the neural circuitry linked to feeding habits in mice [130, 131].

Another breakthrough came with the development of fluorescent protein fusions to viral structural proteins, used for *in vitro* live cell imaging studies. In one of the first such studies, GFP was inserted into the PRV Becker genome at the UL35 locus, which encodes the small capsid protein, VP26. Dorsal root ganglia from chicken embryos were harvested, cultured and infected with the recombinant PRV Becker strain. Images were captured of individual virus particles moving through the neuronal axon – one of the first times that intracellular transport of virus particles could be imaged in real time, in living cells, by fluorescent microscopy [132]. This opened the way for additional analyses of PRV biology in cell culture, particularly in live cell studies.

To better understand viral egress, Hogue et al. fused a pH-sensitive fluorescent protein to gM [68, 69]. pHluorin is a green fluorescent protein with several mutations near the fluorophore that cause its fluorescence excitation and emission to be sensitive to pH. When the protein is exposed to an acidic environment, it is quenched and does not emit light in the green 510 nm spectrum, since it cannot absorb incoming energy from the 488 nm excitation light. Upon exposure to a neutral pH environment, pHluorin is no longer quenched, resulting in absorption and subsequent emission of the proper spectra [133]. Hogue et al. fused pHluorin into the first extravirion loop of PRV gM to make PRV 486 [68, 69]. The secretory vesicles that transport alpha herpesviruses to the plasma membrane for exocytosis have a luminal pH of 5.2-5.7, compared to the cytoplasmic pH of 7.2-7.4 [134, 135]. With pHluorin expressed on an extravirion portion of the viral envelope, it is exposed to the acidic environment of the secretory vesicle lumen. Upon release from the cell, into the neutral extracellular

pH, pHluorin will undergo a detectable change from no fluorescence to fluorescence that appears as a spot of green on the infected cell [68, 69].

PRV 483 and 486 both express gM-pHluorin, and PRV 483 also has red mRFP on small capsid protein VP26. Using Total Internal Reflection Fluorescence (TIRF) microscopy, the exocytosis of PRV particles was imaged in live PK15 cells. In addition to studying PRV exocytosis in PK15 cells and primary rat embryonic neurons, PRV 486 was used to identify potential host factors that play a role in viral egress, particularly members of the Rab protein family [68, 69]. By transducing cells to express fluorescent Rab6a, it was shown that PRV exocytosis occurs from Rab6a secretory vesicles. In addition, Rab8 and Rab were also identified during viral egress [68, 69].

2.4 Case Study of Using Fluorescent PRV to Infer Host-Virus Interactions

While mutations in the alpha herpesvirus gE-gI-US9 proteins have well-documented phenotypes in neurons, there has been much less study of the function of these proteins in non-neuronal cells [81, 121–123, 136]. Specifically, it was unclear how these viral proteins function during viral egress in non-neuronal cells. Animal studies have shown that epithelial cells are readily infected with PRV Bartha, despite the lack of gE-gI-US9 proteins, and that the virus can spread to the peripheral and central nervous systems via retrograde circuits [6, 81, 119, 125]. The virus must be able to complete assembly, intracellular transport, and exocytosis in order to spread from cell to cell, but it remains an open question whether mutant gE-gI-US9 null viruses use the same host machinery and molecular interactions as wild type ones.

In order to address this question, a novel PRV strain was generated that carries the Bartha deletion (removing gE-gI-US9) and expresses gM-pHluorin in order to detect

exocytosis as described above. Alpha herpesviruses are highly recombinogenic, [15, 16, 137], so co-infecting cells with two parental strains to obtain a desired recombinant can be highly successful. PK15 cells were infected with two parental strains: one with the desired Bartha deletion and the other with gM-pHluorin and mRFP-VP26 fluorescent protein fusions. The fluorescent parental strain was also ΔUL25; UL25-null viruses do not package or retain viral DNA in capsids, and therefore cannot complete their replication cycles [38]. The novel recombinant PRV strain had to undergo multiple recombination events: rescuing UL25, inserting the Bartha deletion, and inserting the two fluorescent proteins.

After coinfection, the PK15 cells were maintained with DMEM (Gibco) supplemented with 2% fetal bovine serum (FBS) (Gibco) and 1%penicillin-streptomycin (Gibco) for 48 hpi at 37°C in a 5% CO_2 incubator to allow for viral replication and recombination. At 48 hpi, the supernatant was harvested for a plaque assay to isolate potential recombinants. Multiple recombinants were screened based on the presence of red and green fluorescence and a reduced plaque size phenotype. The successful recombinant was propagated on PK15 cells and named PRV 001.

Western blot analyses confirmed the deletion of gE, gI, and US9 proteins (Figure 2.1). PK15 cells were infected and incubated overnight with PRV 001, PRV BaBe (PRV Bartha deletion in the Becker genetic background), PRV Becker, or PRV 483. Cell lysates were harvested, prepped, and separated on SDS-PAGE gel. Proteins were then transferred onto PVDF membrane, blocked with 5% non-fat dry milk solution, and then probed with monoclonal antibodies for gE, gI, or US9 kindly provided by Lynn Enquist (Princeton University) [138, 139]. Blots for each protein were run in parallel for this experiment. PRV BaBe and PRV 001 produced no bands corresponding to gE, gI, and US9 proteins. Meanwhile, control strains PRV Becker

and PRV 483 both expressed gE, gI, and US9. Due to the differences in glycosylation at the time of sample preparation, protein bands can appear clustered or smeared beyond the predominant band (Figure 2.1).

In order to characterize the newly generated PRV 001, we conducted a single-step growth curve to analyze its replication kinetics in comparison to non-fluorescent PRV BaBe and PRV 483, which contains both gM-pHluorin and mRFP-VP26 [68, 69]. PRV 001 had a ∼1-log reduction in titer at 24 hpi compared to PRV BaBe; however, PRV 483 showed the same titer at 24hpi, indicating that the reduction in viral replication is likely due to fluorescent protein expression and not the Bartha deletion and is within standard titer reductions for fluorescent PRV strains (Figure 2.2A). Measurements of plaque diameters were also taken in this experiment, and both PRV 001 and PRV BaBe had comparable plaque sizes that were smaller than PRV 483 (Figure 2.2B). The reduced replication of PRV 001 and PRV 483 indicate that exogenous protein expression does delay viral replication. However, the smaller plaque sizes indicate that the gE-gI-US9 might impact cell-cell spread, accounting for the reduced plaque diameters seen in PRV 001 and PRV BaBe.

Next, we investigated viral egress by imaging viral exocytosis in live cells to determine if egress rates were slower and possibly accounting for slower cell-cell spread. Imaging was done on an inverted Nikon Ti2 Eclipse microscope in the ASU Biodesign Imaging Core facility, with 488 and 561 nm lasers used for TIRF microscopy in order to visualize viral exocytosis at the plasma membrane. After cells were infected with PRV 001 or PRV 483, they were imaged with TIRF at ∼5 hpi. Exocytosis events were confirmed by plotting mean fluorescence over time with Fiji software [140] (Figure 2.3A). Before the moment of exocytosis, the velocity of the virus particles was

calculated with MTrackJ [141] and then the mean velocity of all measured particles of PRV 001 or PRV 483 was determined.

Surprisingly, PRV 001 had a statistically significant higher mean velocity than the PRV 483 control (Figure 2.3B). We anticipated that since PRV 001 had smaller plaque sizes, from potential delays in viral egress, it would have a lower mean velocity compared to PRV 483. We inferred that since the gE-gI-US9 protein complex is responsible for recruiting kinesin motors that transport virus particles during egress [142–146], the mutant PRV 001 is likely recruiting kinesin motors through other means in order to complete viral egress. Further experiments are needed to determine which kinesin motors may be involved and what viral proteins are fulfilling the role of the missing gE-gI-US9 protein complex.

2.5 Use of Fluorescent HSV-1 Viruses

The first fluorescent strain of HSV-1 was also the first fluorescent alpha herpesvirus. EGFP was fused to VP22 in order to track this tegument protein during viral attachment and entry [147]. A different fusion of EGFP on glycoprotein K (gK) enabled researchers to further study HSV-1 attachment and entry processes [148]. A third variety of EGFP-tagged HSV-1, with the fluorescent protein on VP26, was used to image capsid proteins during assembly in the cell nucleus [149].

Fluorescent protein fusions to gM in PRV have proven to be stable and reliable, with high levels of expression [109], and the evidence that this strategy would hold for HSV-1 came with the first GFP fusion to HSV-1 gM [150]. HSV-1 VP26, orthologous to PRV VP26 protein, is also a consistently reliable choice for fluorescent protein fusions as the virus maintains replication and infection competency with the incorporation of

the exogenous protein into its capsid. Due to the fact that up to 900 individual VP26 proteins can be incorporated into a single capsid, large numbers of fluorescent proteins will be part of the virus particle when they are fused to VP26 [109]. In addition to the EGFP-VP26 described above, an mRFP-VP26 fusion produced the red fluorescent strain OK14 [151].

Since there has been less research on how HSV-1 egresses and completes exocytosis from infected cells, we have produced novel HSV-1 strains using these approaches. These strains of HSV-1 express gM-pHluorin in order to observe exocytosis in live cells with TIRF microscopy. Studies with these viruses that address questions about HSV-1 egress pathways and their associated host factors are described in depth below.

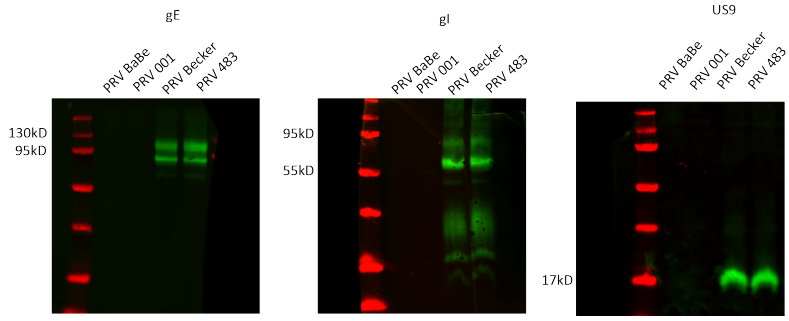

Figure 2.1. gE, gI, and US9 Expression in PRV Recombinants

Western blot of PRV 001, PRV BaBe, PRV Becker, PRV 483 expression of gE (∼100kD), gI (∼60kD), US9 (∼17kD). Bartha deletion strains PRV 001 and BaBe lack gE, gI, US9. Control strains PRV Becker and 483 express gE, gI, and US9.

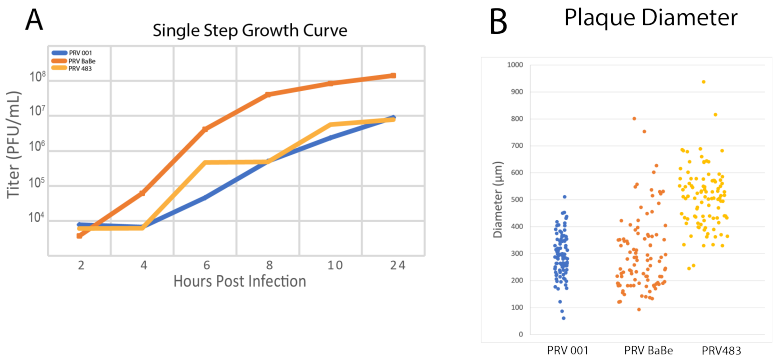

Figure 2.2. Growth Kinetics and Plaque Sizes of PRV Recombinants

A. Single step replication kinetics of PRV 001, PRV 483, and PRV BaBe shows modest ∼-log reduction in fluorescent PRV 001 and 483 titer. **B**. Plaque diameter measurements show reduced plaque sizes for PRV 001 and PRV BaBe (n=98), with compounded decrease in size for multiple fluorescent protein expression by the virus.

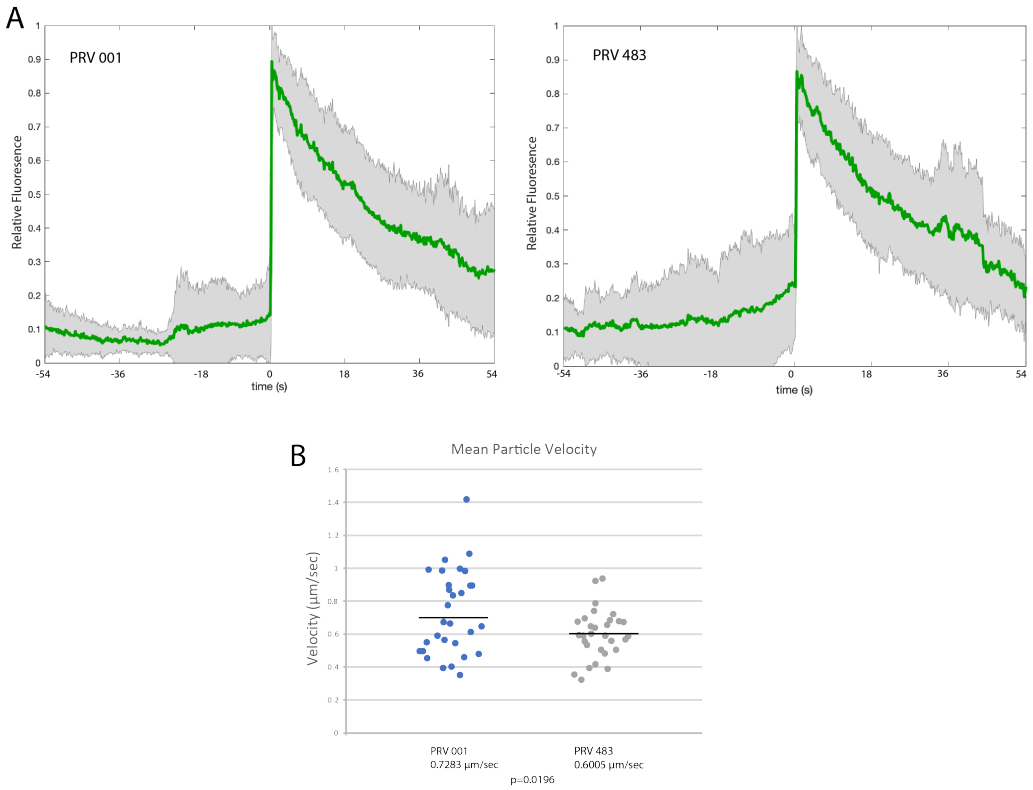

Figure 2.3. Recombinant PRV Exocytosis and Particle Velocity

A. Mean fluorescence over time of PRV 001 (n=31) and PRV 483 (n=31). Time=0 is the moment of exocytosis with the corresponding peak in fluorescence that fades over time. **B**. Mean velocity of virus particles before exocytosis. PRV 001 had an increased mean velocity over control strain PRV 483 (n=30).

Chapter 3

LIVE-CELL FLUORESCENCE MICROSCOPY OF HSV-1 CELLULAR EGRESS BY EXOCYTOSIS

Melissa H. Bergeman, Michaella Q. Hernandez, Jenna Diefenderfer, Jake A. Drewes, Kimberly Velarde, Wesley M. Tierney, Ian B. Hogue

Biodesign Center for Immunotherapy, Vaccines, and Virotherapy & School of Life Sciences, Arizona State University, Tempe, Arizona, United States

3.1 Abstract

The human pathogen Herpes Simplex Virus 1 (HSV-1) produces a lifelong infection in the majority of the world's population. While the generalities of alpha herpesvirus assembly and egress pathways are known, the precise molecular and spatiotemporal details remain unclear. In order to study this aspect of HSV-1 infection, we engineered a recombinant HSV-1 strain expressing a pH-sensitive reporter, gM-pHluorin. Using a variety of fluorescent microscopy modalities, we can detect individual virus particles undergoing intracellular transport and exocytosis at the plasma membrane. We show that particles exit from epithelial cells individually, not bulk release of many particles at once, as has been reported for other viruses. In multiple cell types, HSV-1 particles accumulate in clusters at the corners, edges, and cell-cell contacts. We show that this clustering effect is the result of individual particles undergoing exocytosis at preferential sites. We also show that the viral membrane proteins gE, gI, and US9, which have important functions in intracellular transport in neurons, have a subtle

effect on preferential egress and clustering in non-neuronal cells. Importantly, by comparing HSV-1 to a related alpha herpesvirus, pseudorabies virus, we show that this preferential exocytosis and clustering effect is cell type-dependent, not virus dependent.

Importance. Alpha herpesviruses produce lifelong infections of their human and animal hosts. The majority of people in the world are infected with Herpes Simplex Virus 1 (HSV-1), which typically causes recurrent oral or genital lesions. However, HSV-1 can also spread to the central nervous system, causing severe encephalitis, and might also contribute to the development of neurodegenerative diseases. Many of the steps of how these viruses infect and replicate inside host cells are known in depth, but the final step, exiting from the infected cell, is not fully understood. In this study, we engineered a novel variant of HSV-1 that allows us to visualize how individual virus particles exit from infected cells.

3.2 Introduction

The human pathogen Herpes Simplex Virus type 1 (HSV-1) is a member of the alpha herpesvirus sub-family, which includes several endemic human pathogens, economically-important veterinary pathogens, and zoonotic pathogens that can be severely neuroinvasive. The generalities of alpha herpesvirus assembly and egress pathways are known, but the spatiotemporal details remain unclear. Viral DNA replication and packaging occurs in the nucleus, nuclear egress occurs by transient envelopment/de-envelopment at the nuclear membranes [1–3], and secondary envelopment occurs on intracellular membranes derived from the secretory and endocytic pathways [4–11]. Following secondary envelopment, the secretory organelle containing

the enveloped virion traffics to the plasma membrane, predominantly using microtubule motors, where it is released by exocytosis [12–17]. However, the precise molecular details, virus-host interactions, and dynamics of this process are not well understood.

While fluorescence microscopy has been widely used to determine the relationships between viral proteins and cellular markers, it lacks the spatial resolution to determine the precise assembly state of the virion. Electron microscopy has also provided many insightful results, but this technique is confounded by difficulties in sample preparation, small sample sizes, and the fact that samples are fixed and static [18–21]. This last constraint is of particular concern as it does not offer insights into the dynamic aspects of the viral replication cycle in infected cells. To overcome some of these limitations, we previously developed a live-cell fluorescence microscopy method to study exocytosis of the important veterinary and zoonotic virus, Pseudorabies Virus (PRV; suid alphaherpesvirus 1) [16, 17]. In these studies, we showed that PRV particles exit from infected cells by exocytosis using cellular secretory mechanisms, are mainly released as single particles from individual secretory vesicles, and the spatial distribution viral exocytosis is largely uniform across the adherent cell surface (in PK15 cells, a non-polarized porcine kidney epithelial cell line). However, other studies focusing on HSV-1 showed that viral proteins and particles accumulate at preferential locations, which the authors inferred was the result of viral exocytosis at preferential "hot spots" in Vero cells, a non-polarized African green monkey kidney epithelial cell line [22–25].

In other viruses, a variety of egress modes have been observed: The beta herpesvirus human cytomegalovirus (HCMV) was shown to exit by bulk release – exocytosis of many particles from a larger organelle – in human foreskin fibroblast (HFF-1) cells [26]. Both flaviviruses and coronaviruses have been observed by electron microscopy to

accumulate large numbers of virus particles in large intracellular organelles, but it is unclear whether these large organelles mediate bulk release or if there are subsequent intracellular sorting steps to release single virions from individual exocytosis events [27, 28]. In retroviruses, HIV-1 has been observed to assemble and exit preferentially at the trailing uropod of polarized T cells [29, 30], and human T-lymphotropic virus (HTLV) forms large accumulations of virions and extracellular matrix (termed "viral biofilms") on the cell surface that may promote more efficient cell-cell spread [31–34]. Thus, the relationship between exocytosis (single particles in individual secretory vesicles, versus bulk release of many particles from a larger organelle) and accumulation at preferential locations on the cell surface following exocytosis varies according to the particular virus and cell type, but is likely important for subsequent cell-cell spread.

In the present study, we have extended our previous work on PRV to visualize the exocytosis of HSV-1 particles via Total Internal Reflection Fluorescence (TIRF) microscopy. We engineered a recombinant strain of HSV-1 which expresses the fluorescent protein superecliptic pHluorin on an extravirion loop of the multipass transmembrane glycoprotein M (gM). A variant of GFP, pHluorin was developed as a means to image secretory vesicle exocytosis in a variety of cell types, including neurons [35, 36]. Following secondary envelopment, pHluorin is quenched in the acidic lumen of secretory vesicles (pH of 5.2-5.7) [36, 37]. When the secretory vesicle fuses with the plasma membrane to release the virus particle to the extracellular medium (pH $\sim$7.5), pHluorin is dequenched and becomes brightly fluorescent, allowing the unambiguous identification of individual viral exocytosis events [16, 17, 37, 38] (Figure 3.1A). Using this technique, we show that HSV-1 exits from infected cells by exocytosis of individual virus particles, not bulk release of many virions at once. In some cell types, viral exocytosis occurs at preferential plasma membrane sites, leading

to the gradual accumulation of large clusters of virus particles, but we show that this phenomenon is cell-type dependent. Consistent with previous reports [22], mutations in viral membrane proteins gE, gI, and US9 had modest effects, but were not essential for preferential viral egress and accumulation into clusters.

3.3 Results

Insertion of pHluorin into gM. To produce the recombinant strain HSV-1 IH01, we inserted the pHluorin coding sequence into the gM (UL10) gene in the HSV-1 genome by homologous recombination between a synthesized shuttle plasmid and purified HSV-1 DNA. The construct was designed to insert the pHluorin moiety into the first extravirion loop of gM (Figure 3.1B). A second recombinant, HSV-1 IH02, expressing gM-pHluorin and an mRFP-VP26 capsid tag, was produced by co-infecting Vero cells with HSV-1 IH01 and HSV-1 OK14 [39] and then purifying two-color plaques.

We confirmed the correct recombination occurred by PCR amplification and Sanger sequencing (Figure 3.2, Table 3.1). We also confirmed expression of gM-pHluorin by western blot of infected cell lysates, probing with anti-gM and anti-GFP antibodies simultaneously (Figure 3.3A). Viral membrane proteins frequently produce complex banding patterns due to differences in glycosylation and aggregation of these highly hydrophobic proteins during sample prep [40, 41]. Cells infected with parental strains HSV-1 17syn$^+$ and OK14 produced major gM-immunoreactive bands near the predicted 51 kDa of native gM, whereas cells infected with the recombinant HSV-1 IH01 and IH02 strains produced bands that are immunoreactive to both gM and GFP

antibodies, and shifted ∼30 kDa, consistent with the predicted gM-pHluorin fusion (Figure 3.3A).

gM-pHluorin Labels Virus Particles and Exhibits pH-Sensitive Fluorescence. To determine whether gM-pHluorin is incorporated into individual virus particles, we spotted ∼100μl of freshly-prepared infected cell supernatants onto a glass coverslip, and imaged by fluorescence microscopy (Figure 3.3B). To measure the pH sensitivity of the gM-pHluorin fluorescence, we added an excess of PBS buffer at pH ∼6 followed by an excess of PBS buffer at pH ∼7. gM-pHluorin incorporated into virus particles exhibited reversible pH-dependent green fluorescence, whereas the mRFP-VP26 capsid tag exhibited a non-pH-sensitive reduction in fluorescence due to photobleaching (Figure 3.3B).

Virus Replication. To determine whether the recombinant HSV-1 IH01 and IH02 strains replicate comparably to the parental viruses, we performed single-step growth curves (Figure 3.3C) and measured plaque size (Figure 3.3D) on Vero cell monolayers. Compared to the parental HSV-1 17syn$^+$ strain, HSV-1 OK14, IH01, and IH02 exhibited a modest delay in replication at 8 hpi. By 24 hpi, HSV-1 OK14 and IH01 caught up to 17syn$^+$, but HSV-1 IH02 exhibited a modest <1 log defect (Figure 3.3C). These data suggest that the gM-pHluorin and mRFP-VP26 fluorescent protein fusions result in a small reduction in viral replication, and these defects are additive in the HSV-1 IH02 recombinant that expresses both. Consistent with these results, plaque sizes of the HSV-1 OK14 and IH01 were also reduced, and these defects were additive in the HSV-1 IH02 recombinant (Figure 3.3D).

Live-Cell Fluorescence Microscopy of Virus Particle Exocytosis. To investigate virus particle exocytosis, we infected Vero cells with HSV-1 IH01 at a high multiplicity of infection (MOI) to roughly synchronize viral infection, and imaged by

live-cell fluorescence microscopy at approximately 5-6 hpi. This time point represents the earliest production of viral progeny, and prior to the onset of cytopathic effects. To compare to our previous studies of PRV [16], we also infected PK15 cells with PRV 483, which expresses orthologous gM-pHluorin and mRFP-VP26 fusions. We identified productively infected cells by imaging in widefield fluorescence mode to detect mRFP-VP26 red fluorescence in the nucleus and gM-pHluorin green fluorescence on the plasma membrane and in intracellular membranes. We then acquired timelapse movies in TIRF microscopy mode, which excludes out-of-focus fluorescence and emphasizes particle dynamics near the adherent cell surface (Figure 3.4A).

As previously reported with PRV, viral exocytosis events are characterized by the sudden (<90 ms) appearance of green gM-pHluorin fluorescence, which then remains punctate and mostly immobile during the time of imaging (>2-3 min) [16, 17]. To quantify this process over many exocytosis events, we measured the relative fluorescence intensity at exocytosis sites for 54 sec before and after each exocytosis event, aligned all data series to a common time=0, and calculated the ensemble average over many events (Figure 3.4B-C). Prior to exocytosis at time=0, the relative gM-pHluorin fluorescence remains low, consistent with pHluorin quenching in the acidic lumen of the viral secretory vesicle. At the moment of exocytosis, gM-pHluorin fluorescence increases suddenly due to dequenching at extracellular pH. Finally, the fluorescence decays gradually, which represents a combination of: 1. diffusion of gM-pHluorin that is incorporated into the vesicle membrane; 2. occasional movement of the cell or virus particle after exocytosis; 3. photobleaching. These data are consistent with our previous studies of PRV exocytosis [16, 17], validating that this approach works for HSV-1.

HSV-1 Particles Accumulate at Preferential Exocytosis Sites. Previous

studies showed that HSV-1 structural proteins and particles accumulate in large clusters at the adherent corners and edges of Vero cells, and cell-cell junctions in epithelial cells [22–25]. However, based on static fluorescence and electron microscopy images, it is unclear if virus particles gradually accumulate in these clusters due to preferential exocytosis at these sites, if large clusters are deposited at once due to bulk release (as recently observed with HCMV [26]), or if virus particles accumulate in clusters later in infection due to cell movement and rounding associated with cytopathic effects. Previously, we did not observe preferential exocytosis sites or large clusters of virus particles with PRV in PK15 cells [16, 17], so it was unclear whether this represents a difference between viruses or a cell-type difference.

To better understand how these large clusters of virus particles form, we infected Vero or PK15 cells with HSV-1 IH02, and imaged at 6-7 hpi. At this time point, HSV-1 IH02 particles were beginning to accumulate in clusters at the "corners" of Vero cells (Figure 3.5A). By tracking virus particles prior to exocytosis and observing the location of exocytosis, we found that viral exocytosis can occur outside of existing clusters, but that clusters appear to grow by individual particles undergoing exocytosis at or near these clusters (Figure 3.5A-B). Notably, the distribution of virion and L-particle exocytosis (as distinguished by the mRFP-VP26 capsid tag) was similar.

Because we previously reported no such accumulation of virus particles with PRV in PK15 cells [16, 17], we compared HSV-1 IH02 to PRV 483 in PK15 cells (Figure 3.5C-D). In contrast to Vero cells, there appears to be no large accumulations and no preferential sites of HSV-1 egress in PK15 cells (Figure 3.5C), similarly to PRV in PK15 cells (Figure 3.5D).

To determine whether this clustering occurs in a more biologically-relevant primary cell type, we prepared rat embryonic fibroblasts (REFs), and infected them with

HSV-1 IH02 or PRV 483. In these cells, we observed HSV-1 exocytosis events (Figure 3.6A-B), similarly to Vero and PK15 cells. It was difficult to assess whether virus particles clustered to the same degree as in Vero cells, because REFs exhibited cell rounding and cytopathic effects earlier than in the transformed cell lines; however, clusters of virus particles were visible in ∼50% of REF cells infected with HSV-1 IH02 and up to 90% of REF cells infected with PRV 483 (Figure 3.6A and 3.7A-B).

Altogether, these data show that the long-observed clustering of HSV-1 particles in Vero cells occurs due to preferential exocytosis of individual particles at these sites, rather than bulk release or post-exocytosis movements. Our prior observations, that this clustering does not occur with PRV in PK15 cells, is the result of cell type differences, not virus differences, as HSV-1 does not form clusters in PK15 cells (Figure 3.5C), and PRV does form clusters in REFs (Figure 3.7A-B).

Viral Membrane Proteins gE, gI, and US9 are Not Required for Clustered Egress in Vero and REF Cells. The three viral membrane proteins, gE, gI, and US9, have important functions in both HSV-1 and PRV egress. The clinical isolate HSV-1 MacIntyre and attenuated vaccine strain PRV Bartha, spread only in the retrograde direction and are incapable of anterograde spread in host nervous systems due mutations that disrupt the gE, gI, and US9 genes [42–47]. These proteins contribute to secondary envelopment, recruit microtubule motors for particle transport in multiple cell types [14, 48–50], and are required for axonal sorting and anterograde axonal spread in neurons [23, 42, 51–54]. However, it is not clear how mutations in gE, gI and US9 might affect egress in non-neuronal cells.

HSV-1 OK14, which is based on the 17syn$^+$ laboratory strain, expresses functional gE, gI, and US9 [39, 55]. HSV-1 425 is based on the HSV-1 MacIntyre strain, which contains mutations that disrupt gE/gI/US9 function [46, 47]. Both viruses express

an mRFP-VP26 capsid tag. At about 5 hpi, we manually categorized infected cells in random fields of view based on the presence of virus particle clusters at the cell periphery. Cells infected with HSV-1 425 demonstrated a roughly similar proportion of clustering compared to HSV-1 OK14 in Vero cells (Figure 3.7A). These results show that gE, gI, and US9 are not required for clustered egress of HSV-1.

To compare PRV to HSV-1, and further assess the function of gE, gI, and US9 in this clustering phenotype, we also infected cells with PRV recombinants. PRV 483 is based on the Becker laboratory strain, which expresses functional gE, gI, and US9 [56, 57] . We also constructed PRV 001, which is also based on PRV Becker, but contains the PRV Bartha deletion that removes the gE/gI/US9 genes. Both of these viruses express gM-pHluorin and mRFP-VP26. While PRV will infect and form plaques on Vero cells, we were unable to achieve sufficient levels of infection for our microscopy experiments — it is possible that the efficiency of plating of PRV in Vero cells is too low to achieve a high-MOI roughly synchronous infection in our experimental conditions. To overcome this limitation, we instead infected primary REF cells, which support robust infection of both viruses. HSV-1 and PRV exhibited clustering at the cell periphery, and gE, gI, and US9 proteins were not required for clustering. However, virus particle clustering appears to be slightly decreased in viruses that are deficient in gE, gI, and US9 (Figure 3.7A-B). These results further reinforce the idea that this clustering effect is common to both HSV-1 and PRV, and varies by cell type. However, the polarized trafficking that is mediated by gE/gI/US9 in neurons is not essential for clustered egress in these non-neuronal cells.

3.4 Discussion

By producing an HSV-1 recombinant virus that expresses the pH-sensitive fluorescent protein, pHluorin, we have developed a live-cell microscopy assay that allows us to visualize the process of viral egress from infected cells. pHluorin is genetically fused to the viral envelope glycoprotein gM, is incorporated into virus particles, is quenched in the lumen of cellular vesicles, but dequenches upon exocytosis, allowing detection of virus particle exocytosis. We are able to detect individual virus particles undergoing exocytosis, and while this approach had been successful in previous alpha herpesvirus studies [16, 17], this is the first time that this approach has been applied to the important human pathogen, HSV-1.

Individual HSV-1 particles undergo exocytosis, not bulk release that has been observed with other herpesviruses [26]. The fact that virus particles have been observed in large clusters in infected cells [22, 23] is the result of individual particles undergoing exocytosis at preferential sites at the corners and edges of adherent cells, leading to the gradual accumulation of virus particles as these hot spots. However, this clustering does not occur in all cell types: both HSV-1 and PRV form clusters in Vero and primary REF cells, but not in PK15 cells.

Differences in intracellular transport and secretory mechanisms may explain why the spatial distribution of viral egress varies across these cell types. We, and others, have previously shown that alpha herpesvirus particles use cellular secretory pathways, regulated by Rab family GTPases, and recruit kinesin microtubule motors for intracellular transport to the site of exocytosis. Different cell types have been noted to express different kinesin motors and different Rab GTPases to transport and secrete cellular cargoes. As an extreme example of polarized trafficking and secretory pathways, in

neurons, vesicles containing axonal cargoes can transport into the axon, but other vesicles are strongly excluded. The alpha herpesviruses appear to modulate axonal sorting and transport of viral secretory vesicles by recruiting additional kinesin motors via the viral gE, gI, and US9 proteins. However, in the present study, these viral factors are not required for transport to and exocytosis at preferential egress sites. It remains to be determined in future studies what cellular mechanisms are responsible for polarized transport and preferential exocytosis sites in these non-neuronal cells.

3.5 Materials and Methods

Cells. Vero cells (ATCC, CCL-81), PK15 cells (ATCC, CCL-33), and primary rat embryonic fibroblasts (REFs) were all maintained in Dulbecco's Modified Eagle's Media (DMEM, Cytiva) supplemented with 10% FBS (Omega Scientific) and 1% penicillin-streptomycin (Hyclone), and incubated in a 5% CO_2 incubator at 37°C.

REFs were collected from E16-17 Sprague-Dawley rat embryos (Charles River Laboratories), as follows: Animal work was performed in accordance with all applicable regulations and guidelines, and with the approval of the Institutional Animal Care and Use Committee (IACUC) at Arizona State University (protocol #20-1799R). The animal care and use program at Arizona State University has an assurance on file with the Office of Laboratory Animal Welfare (OLAW), is registered with the USDA, and is accredited by AAALAC International. Briefly, embryos were decapitated and internal organs removed. Remaining skin and connective tissue was trypsinized (Trypsin-EDTA, Gibco) at 37°C, pipetted vigorously in complete DMEM, and supernatants were plated onto 10cm cell culture dishes (Celltreat). REFs were passaged no more than 4 times before use in experiments [58].

Viruses. All HSV-1 or PRV strains were propagated and titered by plaque assay on Vero or PK15 cells, respectively, in DMEM supplemented with 2% FBS and 1% penicillin-streptomycin. HSV-1 17syn$^+$ and OK14 were obtained from the Lynn Enquist laboratory (Princeton University) and verified by whole genome sequencing. HSV-1 OK14, which expresses an mRFP-VP26 capsid tag, was previously described [39]. HSV-1 425, which is based on HSV-1 MacIntyre and expresses an mRFP-VP26 capsid tag, was a kind gift from Esteban Engel (Princeton University) [47]. PRV 483 and PRV 495, which express gM-pHluorin and an mRFP-VP26 capsid tag, were previously described [16]. PRV BaBe was obtained from the Lynn Enquist laboratory (Princeton University) [56, 57].

Construction of New HSV-1 Recombinants. Three confluent 10 cm dishes of Vero cells were infected with HSV 17syn$^+$ at MOI of 5 pfu/cell, and incubated overnight. Infected cells were rinsed with PBS, scraped from the dish, and lysed with an NP-40/Tris buffer (140mM NaCl, 2mM MgCl2, 0.5% Nonidet P-40, 200mM Tris). Nuclei were pelleted by centrifugation, and then lysed with 1% SDS in PBS. 100μg/mL proteinase K was added, and incubated at 50°C for 1 hour. DNA was then isolated by phenol-chloroform extraction and ethanol precipitation. To produce HSV-1 IH01, a shuttle plasmid containing the pHluorin coding sequence flanked by HSV-1 sequences homologous to the HSV-1 UL10/gM locus was synthesized (Genewiz). This construct was designed to insert pHluorin into the first extravirion loop of the gM protein. Vero cells were cotransfected with linearized shuttle plasmid and DNA isolated from HSV-1 17syn$^+$ infected cells using JetPrime transfection reagent (Polyplus). Following reconstitution of replicating virus, plaques were screened for expression of green fluorescence and plaque purified three times. To produce HSV-1 IH02, Vero cells were

co-infected with HSV-1 IH01 and OK14, and progeny were screened for red and green fluorescence, and plaque purified three times.

Construction of New PRV Recombinants. PRV 001 was constructed by co-infecting PK15 cells with PRV 495 and PRV BaBe. PRV 495 expresses gM-pHluorin and mRFP-VP26, but also contains a deletion in the essential UL25 gene and cannot replicate on its own. PRV BaBe contains a deletion in the US region encoding gE, gI, and US9 [56, 57]. Following co-infection, progeny plaques were screened for green and red fluorescence. Several clones were picked, plaque purified three times, and further screened for lack of gE, gI, and US9 expression via western blot (Chapter 2, Figure 2.1).

Fluorescence microscopy. Vero, PK15, or REF cells were seeded at subconfluent density ($\sim 10^5$ cells/dish) on glass-bottom 35mm dishes (Celltreat, Ibidi, and Mattek), incubated overnight, and then infected with HSV-1 or PRV at a relatively high MOI (>1 pfu/cell). To account for differences in the efficiency of plating between different viruses and cells, the amount of inoculum needed to synchronously infect most cells was determined empirically by fluorescence microscopy. HSV-1 infected cells were imaged beginning at 5-6 hpi, and PRV infected cells were imaged beginning at 4-5 hpi, unless otherwise stated. Fluorescence microscopy was performed using a Nikon Eclipse Ti2-E inverted microscope in the Biodesign Imaging Core facility at Arizona State University. This microscope is equipped with TIRF and widefield illuminators, a Photometrics Prime95B sCMOS camera, a 60X high-NA TIRF objective, and objective and stage warmers for 37°C live-cell microscopy. For widefield fluorescence, a Lumencor SpectraX LED lightsource provided 470/24nm and 550/15nm excitation for green and red fluorescent proteins, respectively.

For TIRF microscopy, 488nm and 561nm lasers were used to excite green and red

fluorescent proteins, respectively. Image analysis was performed using Fiji software [59]. Fluorescence microscopy images were prepared for publication using Adjust Brightness/Contrast, Reslice (to produce kymographs), and Plot Z-axis Profile (to measure fluorescence over time) functions in Fiji. Maximum difference projections were calculated as previously described [16], using the Duplicate, Stacks->Tools, Math->Subtract, and Z Project functions in Fiji. Maximum difference projection shows where fluorescence intensity increases most rapidly, which emphasizes exocytosis events and particle movement, and deemphasizes static features that do not change during the course of imaging. Ensemble averages of fluorescence intensity during exocytosis events (Figure 3.4B-C, Figure 3.6B) were calculated using Matlab (Mathworks).

Western Blot. Vero cells were infected with HSV-1 and PK15 cells were infected with PRV at high MOI and incubated overnight. Infected cells were lysed with an NP-40 lysis buffer (50mM Tris, 150mM NaCl, 1% Nonident P-40, diH2O) on ice for 3 minutes, nuclei were pelleted by centrifugation at 16000 rpm for 20 min, supernatants were mixed with 2X Laemmli sample buffer containing SDS and 2-mercaptoethanol, and heated to 95°C for 5 min. SDS-PAGE separation was run on Nu-Page precast gels (Invitrogen). Proteins were then transferred onto PVDF membrane (Immobilon-FL, Millipore) using a semi-dry transfer apparatus (BioRad). Membranes were blocked with a 5% nonfat dry milk solution, and probed with antibodies overnight. Mouse monoclonal anti-GFP antibody (Sigma) was used to detect pHluorin. Rabbit polyclonal antibodies targeting HSV-1 gM (PAS980), PRV gE, gI, and US9 were kindly provided by Lynn Enquist (Princeton University) [60, 61]. The next day, membranes were probed with fluorescent secondary antibodies (LI-COR) for one hour, washed, and imaged using a LI-COR Odyssey CLx scanner.

PCR of gM-pHluorin Insert. All PCR samples were prepared with Taq PCR

Master Mix Kit (Qiagen), 1.0 ng of DNA, and one primer pair (Table 1). All PCR reactions were performed using the following conditions: 94°C for 3 min (initial denaturation); 35 cycles of 94°C for 45s, 54°C for 45s, and 72°C for 1 min; followed by a final extension at 72°C for 10 minutes. Primers utilized are listed in Table 3.1. PCR products were then run on a 0.8% agarose gel for 1 hour at 100V and imaged using an ethidium bromide stain and UV excitation.

Particle Imaging and pHluorin Quenching. Vero cells in 35mm cell culture dishes were infected with HSV IH02 at high MOI. 24 hours post-infection, 100μL of supernatant was pipetted onto glass bottom 35mm dishes for imaging. After allowing virus particles in the supernatant to adhere non-specifically to the glass, excess media was aspirated off and HBSS (Gibco) was added to prevent drying. Virus particles were subjected to a pH change by adding 150μL PBS at pH 6. pH was then returned to neutral by adding an excess of PBS at pH 8. Imaging was performed using widefield LED illumination and 60X magnification to detect individual virus particles.

Single Step Growth Curve and Plaque Size Measurements. Vero cells were seeded to confluence in 35mm 6-well dishes and infected at MOI of 5 PFU/cell. The inoculated cells were incubated for 1 hour, washed with PBS three times, and incubated with viral medium at 37°C. At the specified time points, cells and supernatants were harvested. Mean titers were determined for each time point via serial dilution plaque assay in triplicate. Plaque sizes were measured in Fiji from brightfield and fluorescence microscopy images of 35mm wells of plaque assays from the single step growth curve.

Acknowledgements. Thank you to Joli Bastin for her work on producing the recombinant HSV IH01 and IH02 strains carrying gM-pHluorin.

Funding. This work was supported by NIH NIAID K22 AI123159 and NINDS R01 NS117513.

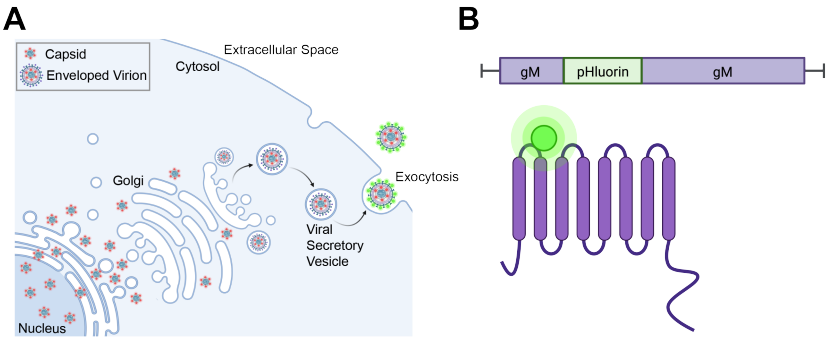

Figure 3.1. HSV-1 Egress and gM-pHluorin Insert

A. Schematic of HSV-1 egress from infected cells. Nonenveloped virus capsids (red) exit the nucleus and traffic to the site of secondary envelopment. Following secondary envelopment, virions are transported to the plasma membrane by acidic secretory organelles. pHluorin (green) dequenches upon exocytosis at the plasma membrane. **B.** Schematic of gM-pHluorin, with the pHluorin moiety (green) inserted into the first extravirion loop of gM (purple).

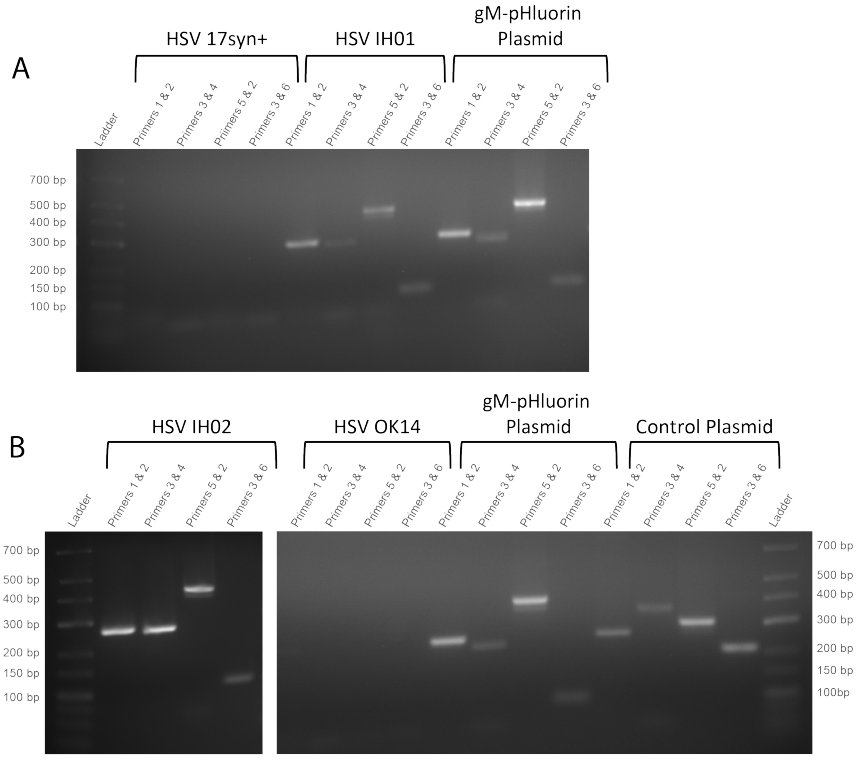

Figure 3.2. PCR of gM-pHluorin Insert

PCR of gM-pHluorin insert. **A-B.** Primer pairs (Table 1) produced PCR products spanning the insertion junctions: ∼300bp, ∼500bp, and ∼150bp for HSV-1 IH01, HSV-1 IH02, and the gM-pHluorin shuttle plasmid. HSV-1 17^{+} and OK14 did not produce products because they do not contain a pHluorin insert. A control plasmid that contains pHluorin inserted into a different location in the gM coding sequence produced a distinct set of PCR products: ∼250bp, ∼350bp, ∼300bp, ∼200bp.

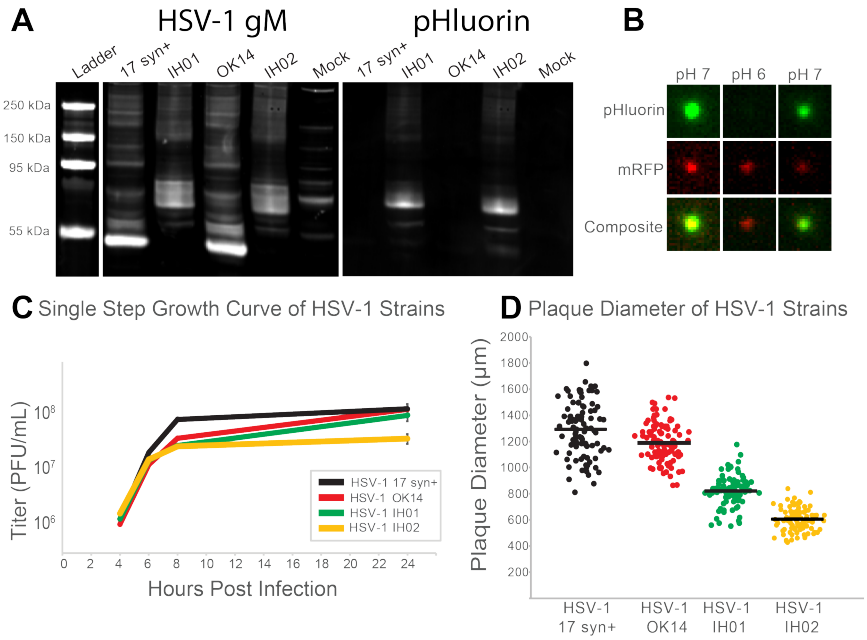

Figure 3.3. pHluorin Expression and Impact on Viral Replication

A. Western blot detecting HSV-1 gM and pHluorin. Vero cells were infected with HSV-1 17syn$^+$, IH01, OK14, and IH02, or mock infected. Blots were probed with primary antibodies detecting gM and pHluorin, and imaged using fluorescent secondary antibodies to detect HSV-1 gM and pHluorin simultaneously. **B.** gM-pHluorin is incorporated into virus particles, and exhibits reversibly pH-sensitive fluorescence. Freshly prepared supernatants from Vero cells infected with HSV-1 IH02 were spotted onto glass bottom dishes. Particles were imaged at pH ∼7, pH ∼6, and pH ∼7. A representative virus particle is shown with gM-pHluorin and mRFP-VP26. Images represent 3.6x3.6 μm. **C.** Single step growth curve. Vero cells were infected with HSV-1 17syn$^+$, OK14 , IH01, or IH02 in triplicate, and harvested at 4, 6, 8, and 24 hpi. Samples were titered by serial-dilution plaque assay. **D.** Plaque size measurements. At 4 days post-infection, virus plaques were imaged, and the zone of clearance diameter was measured in Fiji software and used to calculate mean plaque sizes (n=100).

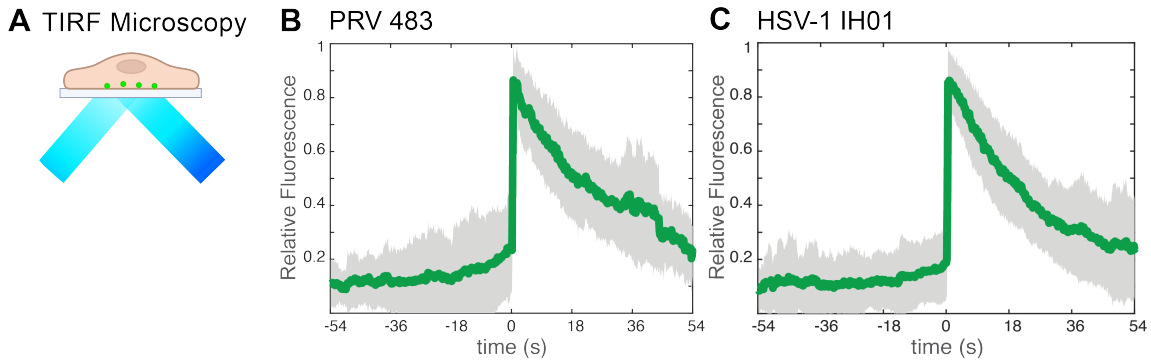

Figure 3.4. TIRF Microscopy of HSV-1 Exocytosis

A. Schematic of TIRF microscopy. The excitation laser excites fluorescent molecules near the coverslip, and excludes out-of-focus fluorescence from deeper in the cell. **B-C.** Relative fluorescence intensity of gM-pHluorin before, during, and after exocytosis of individual virus particles. Green line represents mean fluorescence and gray shading indicates standard deviation. **B.** PRV 483 exocytosis events in PK15 cells, at 4-5 hpi (n=31). **C.** HSV-1 IH01 exocytosis events in Vero cells, at 5-6 hpi (n=67).

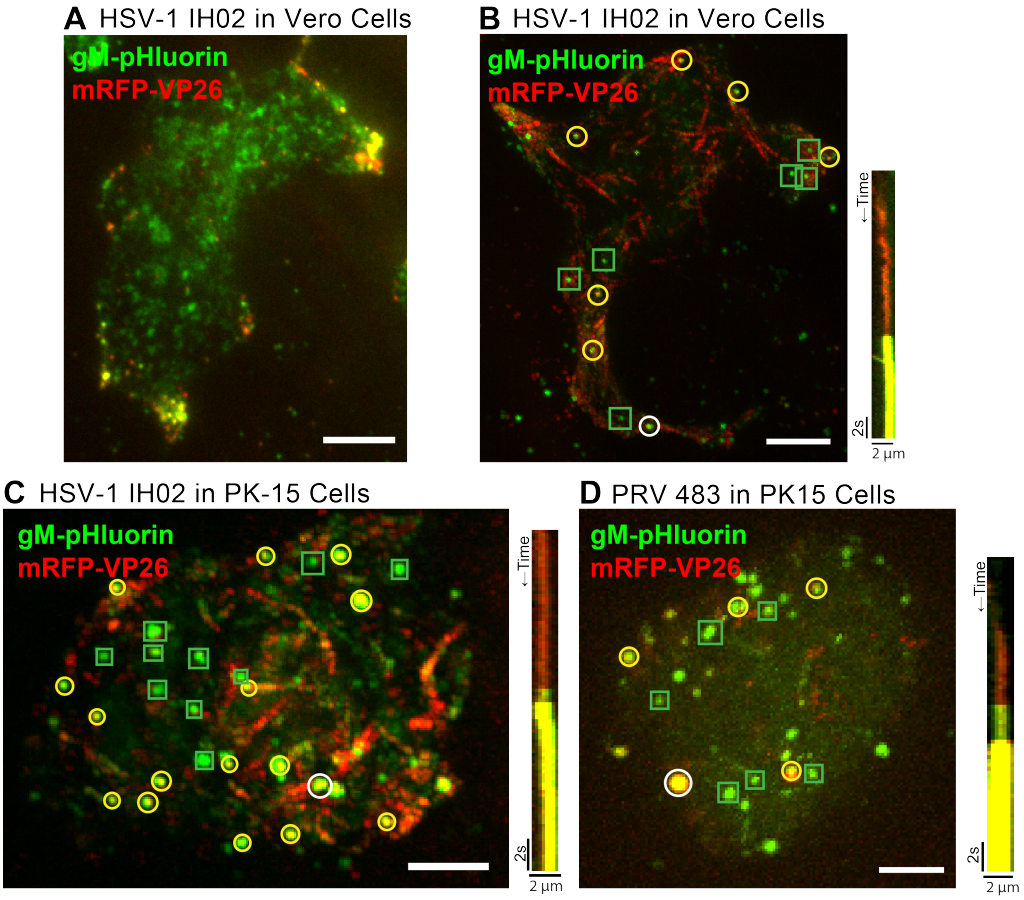

Figure 3.5. Single Virus Particle Exocytosis of HSV-1 and PRV

A. HSV-1 IH02 infection in Vero cells, imaged by TIRF microscopy. Virus capsids (red) and gM-pHluorin (green) accumulate in clusters at the cell periphery at 6-7 hpi. **B-D**. Maximum difference projections showing viral exocytosis events over time (left image) at exocytosis hot spots. Green squares indicate exocytosis events containing gM-pHluorin (L-particles), yellow circles indicate exocytosis events containing both gM-pHluorin and mRFP-VP26 (virions), and white circles indicate the exocytosis events shown in the accompanying kymographs (right image). **B**. HSV-1 IH02 in Vero cells. Projection image represents 4:01 min:sec of imaging time at 6-7 hpi. **C**. HSV-1 IH02 in PK15 cells. Projection image represents 3:56 min:sec of imaging time at 6-7 hpi. **D**. PRV 483 in PK15 cells. Projection image represents 1:45 min:sec of imaging time at 4-5 hpi. In all panels, scale bars represent 10μm.

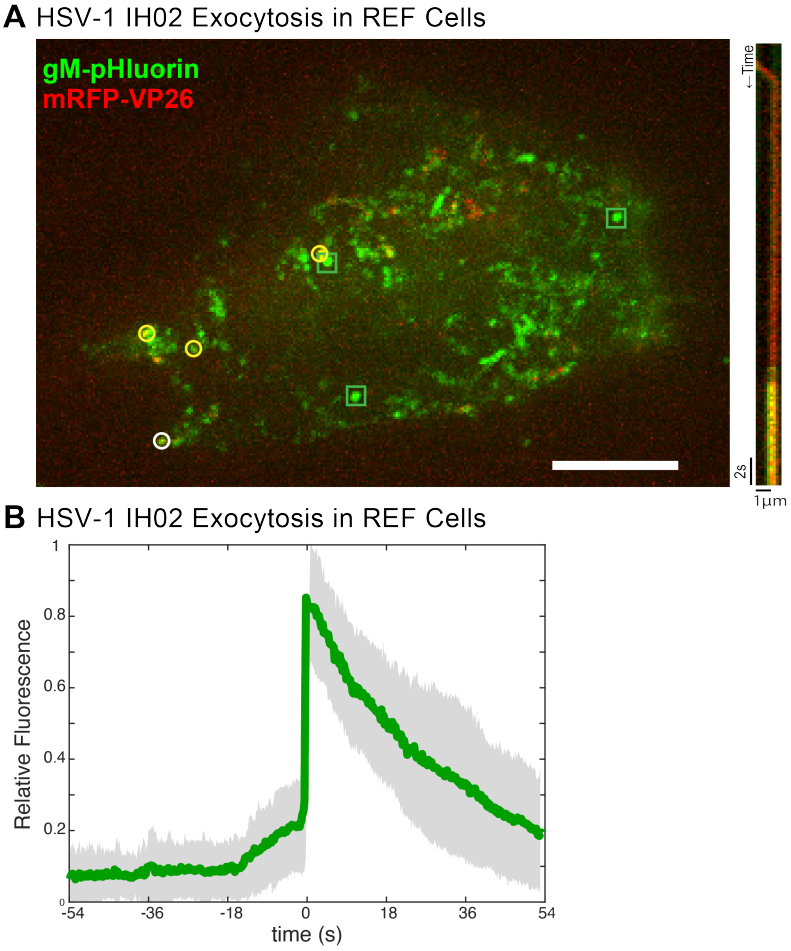

Figure 3.6. HSV-1 Exocytosis in Primary REF Cells

A. Maximum difference projections showing viral exocytosis events over time (top image) of HSV-1 IH02 in REF cells. Green squares indicate exocytosis events containing gM-pHluorin (L-particles), yellow circles indicate exocytosis events containing both gM-pHluorin and mRFP-VP26 (virions), and white circle indicates the exocytosis event shown in the accompanying kymograph (bottom image). **B**. Relative fluorescence intensity of gM-pHluorin before, during, and after exocytosis of individual virus particles of HSV-1 IH02 in REF cells. Green line represents mean fluorescence and gray shading indicates standard deviation (n=42).

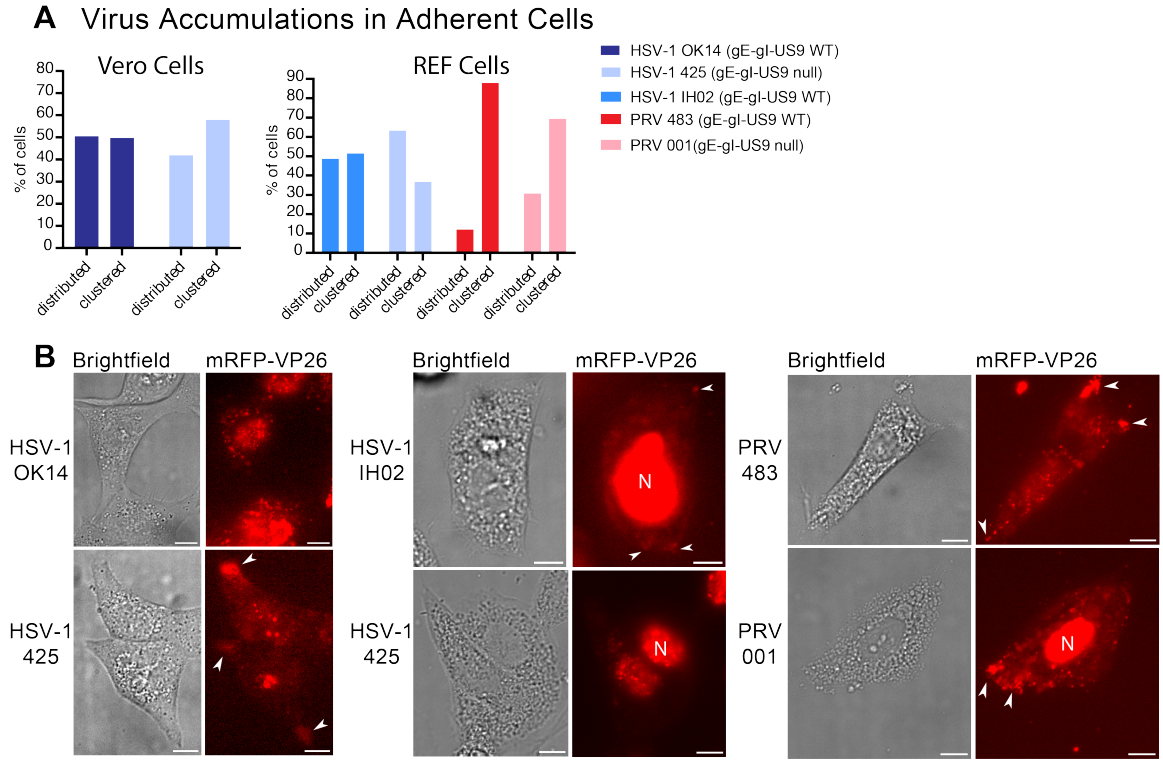

Figure 3.7. Accumulations of Progeny Virus Particles

Accumulation of virus particles into clusters at the periphery of infected cells at 6-7 hpi across three imaging experiments. **A.**The percentage of cells (n=100) with clustered capsids was scored from random fields of view. **B.** Representative fluorescence microscopy images of infected Vero cells (right panels) and REF cells (center and left panels) showing peripheral clusters (arrowheads), or lack of clusters (no arrowheads) are provided. Scale bars = 15μm.

Table 3.1. PCR Primer Sequences

Primer	Sequence
1	CGGTTTCCCTGCTTTTACGC
2	TGCCGGTGGTGCAGATAAAC
3	ACATGGTCCTGCTGGAGTTC
4	TGCAGCAACCAAGAGCAGAC
5	CCCAGAGGATCTCCCGACTC
6	TACATAAGTGCCCACAAGGCTC

List of primers used for PCR confirmation of pHluorin insertion. See Figure 3.2

BIBLIOGRAPHY

1. Batterson, W, Furlong, D & Roizman, B. Molecular genetics of herpes simplex virus. VIII. further characterization of a temperature-sensitive mutant defective in release of viral DNA and in other stages of the viral reproductive cycle. *Journal of Virology* **45,** 397–407 (1 1983).

2. Bigalke, J. M., Heuser, T., Nicastro, D. & Heldwein, E. E. Membrane deformation and scission by the HSV-1 nuclear egress complex. *Nature Communications* **5,** 4131 (1 2014).

3. Liu, Z. *et al.* Herpes Simplex Virus 1 UL47 Interacts with Viral Nuclear Egress Factors UL31, UL34, and Us3 and Regulates Viral Nuclear Egress. *Journal of Virology* **88,** 4657–4667 (9 2014).

4. Wloga, D., Joachimiak, E. & Fabczak, H. Tubulin Post-Translational Modifications and Microtubule Dynamics. *International Journal of Molecular Sciences* **18,** 2207 (10 2017).

5. Owen, D. J., Crump, C. M. & Graham, S. C. Tegument Assembly and Secondary Envelopment of Alphaherpesviruses. *Viruses* **7,** 5084–5114 (9 2015).

6. Miranda-Saksena, M. *et al.* Herpes simplex virus utilizes the large secretory vesicle pathway for anterograde transport of tegument and envelope proteins and for viral exocytosis from growth cones of human fetal axons. *Journal of virology* **83,** 3187–99 (7 2009).

7. Turcotte, S., Letellier, J. & Lippé, R. Herpes Simplex Virus Type 1 Capsids Transit by the trans-Golgi Network, Where Viral Glycoproteins Accumulate Independently of Capsid Egress. *Journal of Virology* **79,** 8847–8860 (14 2005).

8. Sugimoto, K. *et al.* Simultaneous Tracking of Capsid, Tegument, and Envelope Protein Localization in Living Cells Infected with Triply Fluorescent Herpes Simplex Virus 1. *Journal of Virology* **82,** 5198–5211 (11 2008).

9. Hollinshead, M. *et al.* Endocytic tubules regulated by Rab GTPases 5 and 11 are used for envelopment of herpes simplex virus. *The EMBO Journal* **31,** 4204–4220. https://onlinelibrary.wiley.com/doi/full/10.1038/emboj.2012.262https://onlinelibrary.wiley.com/doi/abs/10.1038/emboj.2012.262https://www.embopress.org/doi/10.1038/emboj.2012.262 (21 Nov. 2012).

10. Albecka, A., Laine, R. F., Janssen, A. F. J., Kaminski, C. F. & Crump, C. M. HSV-1 Glycoproteins Are Delivered to Virus Assembly Sites Through Dynamin-Dependent Endocytosis. *Traffic* **17,** 21–39 (1 2016).

11. Russell, T. *et al.* Novel role for escrt-iii component chmp4c in the integrity of the endocytic network utilized for herpes simplex virus envelopment. *mBio* **12.** https://journals.asm.org/doi/10.1128/mBio.02183-20 (3 2021).

12. Lee, G. E., Murray, J. W., Wolkoff, A. W. & Wilson, D. W. Reconstitution of Herpes Simplex Virus Microtubule-Dependent Trafficking In Vitro†. *Journal of Virology* **80,** 4264–4275 (9 2006).

13. Shanda, S. K. & Wilson, D. W. UL36p Is Required for Efficient Transport of Membrane-Associated Herpes Simplex Virus Type 1 along Microtubules. *Journal of Virology* **82,** 7388–7394 (15 2008).

14. Diefenbach, R. J. *et al.* The Basic Domain of Herpes Simplex Virus 1 pUS9 Recruits Kinesin-1 To Facilitate Egress from Neurons. *Journal of Virology* **90,** 2102–2111 (4 2016).

15. Huang, H., Koyuncu, O. O. & Enquist, L. W. Pseudorabies Virus Infection Accelerates Degradation of the Kinesin-3 Motor KIF1A. *Journal of Virology* **94** (9 2020).

16. Hogue, I. B., Bosse, J. B., Hu, J.-R., Thiberge, S. Y. & Enquist, L. W. Cellular Mechanisms of Alpha Herpesvirus Egress: Live Cell Fluorescence Microscopy of Pseudorabies Virus Exocytosis. *PLoS Pathogens* **10,** e1004535 (12 2014).

17. Hogue, I. B., Scherer, J. & Enquist, L. W. Exocytosis of Alphaherpesvirus Virions, Light Particles, and Glycoproteins Uses Constitutive Secretory Mechanisms. *mBio* **7,** e00820–16 (3 2016).

18. Granzow, H. *et al.* Egress of Alphaherpesviruses: Comparative Ultrastructural Study. *Journal of Virology* **75,** 3675–3684. https://journals.asm.org/doi/10.1128/JVI.75.8.3675-3684.2001 (8 Apr. 2001).

19. Leuzinger, H. *et al.* Herpes Simplex Virus 1 Envelopment Follows Two Diverse Pathways. *Journal of Virology* **79,** 13047–13059. https://journals.asm.org/doi/10.1128/JVI.79.20.13047-13059.2005 (20 Oct. 2005).

20. Mettenleiter, T. C. & Minson, T. Egress of Alphaherpesviruses. *Journal of Virology* **80,** 1610–1612. https://journals.asm.org/doi/10.1128/JVI.80.3.1610-1612.2006 (3 Feb. 2006).

21. Huang, J., Lazear, H. M. & Friedman, H. M. Completely assembled virus particles detected by transmission electron microscopy in proximal and mid-axons of neurons infected with herpes simplex virus type 1, herpes simplex virus type 2 and pseudorabies virus. *Virology* **409,** 12–16 (1 Jan. 2011).

22. Mingo, R. M., Han, J., Newcomb, W. W. & Brown, J. C. Replication of herpes simplex virus: egress of progeny virus at specialized cell membrane sites. *Journal of virology* **86,** 7084–97 (13 2012).

23. Johnson, D. C., Webb, M., Wisner, T. W. & Brunetti, C. Herpes Simplex Virus gE/gI Sorts Nascent Virions to Epithelial Cell Junctions, Promoting Virus Spread. *Journal of Virology* **75,** 821–833 (2 2001).

24. McMillan, T. N. & Johnson, D. C. Cytoplasmic Domain of Herpes Simplex Virus gE Causes Accumulation in the trans -Golgi Network, a Site of Virus Envelopment and Sorting of Virions to Cell Junctions. *Journal of Virology* **75,** 1928–1940 (4 2001).

25. Norrild, B., Virtanen, I., Lehto, V. P. & Pedersen, B. Accumulation of herpes simplex virus type 1 glycoprotein D in adhesion areas of infected cells. *Journal of General Virology* **64,** 2499–2503. https://www.microbiologyresearch.org/content/journal/jgv/10.1099/0022-1317-64-11-2499 (11 Nov. 1983).

26. Flomm, F. J. *et al.* Intermittent bulk release of human cytomegalovirus. *PLOS Pathogens* **18,** e1010575. https://journals.plos.org/plospathogens/article?id=10.1371/journal.ppat.1010575 (8 Aug. 2022).

27. Romero-Brey, I. & Bartenschlager, R. Membranous Replication Factories Induced by Plus-Strand RNA Viruses. *Viruses 2014, Vol. 6, Pages 2826-2857* **6,** 2826–2857. https://www.mdpi.com/1999-4915/6/7/2826/htmhttps://www.mdpi.com/1999-4915/6/7/2826 (7 July 2014).

28. Ghosh, S. *et al.* β-Coronaviruses Use Lysosomes for Egress Instead of the Biosynthetic Secretory Pathway. *Cell* **183,** 1520–1535.e14 (6 Dec. 2020).

29. Llewellyn, G. N., Hogue, I. B., Grover, J. R. & Ono, A. Nucleocapsid Promotes Localization of HIV-1 Gag to Uropods That Participate in Virological Synapses between T Cells. *PLOS Pathogens* **6,** e1001167. https://journals.plos.org/plospathogens/article?id=10.1371/journal.ppat.1001167 (10 Oct. 2010).

30. Llewellyn, G. N., Grover, J. R., Olety, B. & Ono, A. HIV-1 Gag Associates with Specific Uropod-Directed Microdomains in a Manner Dependent on Its MA Highly Basic Region. *Journal of Virology* **87,** 6441–6454. https://journals.asm.org/doi/10.1128/JVI.00040-13 (11 June 2013).

31. Pais-Correia, A. M. *et al.* Biofilm-like extracellular viral assemblies mediate HTLV-1 cell-to-cell transmission at virological synapses. *Nature Medicine 2009 16:1* **16,** 83–89. https://www.nature.com/articles/nm.2065 (1 Dec. 2009).

32. Tarasevich, A., Filatov, A., Pichugin, A. & Mazurov, D. Monoclonal antibody profiling of cell surface proteins associated with the viral biofilms on HTLV-1

transformed cells. *Acta Virologica* **59,** 247–256. https://europepmc.org/article/med/26435148 (3 Sept. 2015).

33. Millen, S. *et al.* Collagen iv (Col4a1, col4a2), a component of the viral biofilm, is induced by the htlv-1 oncoprotein tax and impacts virus transmission. *Frontiers in Microbiology* **10,** 2439 (OCT Oct. 2019).

34. Nakamura, H. *et al.* Initial human T-cell leukemia virus type 1 infection of the salivary gland epithelial cells requires a biofilm-like structure. *Virus Research* **269,** 197643 (Aug. 2019).

35. Miesenböck, G., Angelis, D. A. D. & Rothman, J. E. Visualizing secretion and synaptic transmission with pH-sensitive green fluorescent proteins. *Nature* **394,** 192–195 (6689 1998).

36. Sankaranarayanan, S., Angelis, D. D., Rothman, J. E. & Ryan, T. A. The Use of pHluorins for Optical Measurements of Presynaptic Activity. *Biophysical Journal* **79,** 2199–2208 (4 2000).

37. Paroutis, P., Touret, N. & Grinstein, S. The pH of the Secretory Pathway: Measurement, Determinants, and Regulation. *Physiology* **19,** 207–215 (4 2004).

38. Llopis, J., McCaffery, J. M., Miyawaki, A., Farquhar, M. G. & Tsien, R. Y. Measurement of cytosolic, mitochondrial, and Golgi pH in single living cells with green fluorescent proteins. *Proceedings of the National Academy of Sciences* **95,** 6803–6808 (12 1998).

39. Song, R. *et al.* Two Modes of the Axonal Interferon Response Limit Alphaherpesvirus Neuroinvasion. *mBio* **7,** e02145–15 (1 2016).

40. Kasmi, I. E. & Lippé, R. Herpes Simplex Virus 1 gN Partners with gM To Modulate the Viral Fusion Machinery. *Journal of Virology* **89,** 2313–2323. https://journals.asm.org/doi/10.1128/JVI.03041-14 (4 Feb. 2015).

41. Kasmi, I. E. *et al.* Extended Synaptotagmin 1 Interacts with Herpes Simplex Virus 1 Glycoprotein M and Negatively Modulates Virus-Induced Membrane Fusion. *Journal of Virology* **92.** https://journals.asm.org/doi/10.1128/JVI.01281-17 (1 Jan. 2018).

42. Yang, M., Card, J. P., Tirabassi, R. S., Miselis, R. R. & Enquist, L. W. Retrograde, Transneuronal Spread of Pseudorabies Virus in Defined Neuronal Circuitry of the Rat Brain Is Facilitated by gE Mutations That Reduce Virulence. *Journal of Virology* **73,** 4350–4359. https://journals.asm.org/doi/10.1128/JVI.73.5.4350-4359.1999 (5 May 1999).

43. Jacobs, L. Glycoprotein E of pseudorabies virus and homologous proteins in other alphaherpesvirinae. *Archives of Virology* **137,** 209–228. https://link.springer.com/article/10.1007/BF01309470 (3-4 Sept. 1994).

44. Enquist, L. W., Husak, P. J., Banfield, B. W. & Smith, G. A. Infection and Spread of Alphaherpesviruses in the Nervous System. *Advances in virus research* **51,** 237–347 (Jan. 1998).

45. Lomniczi, B., Watanabe, S., Ben-Porat, T. & Kaplan, A. S. Genetic basis of the neurovirulence of pseudorabies virus. *Journal of Virology* **52,** 198–205. https://journals.asm.org/doi/10.1128/jvi.52.1.198-205.1984 (1 Oct. 1984).

46. Szpara, M. L. *et al.* Genome Sequence of the Anterograde-Spread-Defective Herpes Simplex Virus 1 Strain MacIntyre. *Genome Announcements* **2** (6 Nov. 2014).

47. Tierney, W. M. *et al.* Methods and Applications of Campenot Trichamber Neuronal Cultures for the Study of Neuroinvasive Viruses. *Methods in Molecular Biology* **2431,** 181–206. https://link.springer.com/protocol/10.1007/978-1-0716-1990-2_9 (2022).

48. Kratchmarov, R. *et al.* Glycoproteins gE and gI Are Required for Efficient KIF1A-Dependent Anterograde Axonal Transport of Alphaherpesvirus Particles in Neurons. *Journal of Virology* **87,** 9431–9440 (17 2013).

49. Kramer, T. *et al.* Kinesin-3 Mediates Axonal Sorting and Directional Transport of Alphaherpesvirus Particles in Neurons. *Cell Host Microbe* **12** (6 2012).

50. Scherer, J. *et al.* A kinesin-3 recruitment complex facilitates axonal sorting of enveloped alpha herpesvirus capsids. *PLOS Pathogens* **16,** e1007985 (1 2020).

51. DuRaine, G., Wisner, T. W., Howard, P., Williams, M. & Johnson, D. C. Herpes Simplex Virus gE/gI and US9 Promote both Envelopment and Sorting of Virus Particles in the Cytoplasm of Neurons, Two Processes That Precede Anterograde Transport in Axons. *Journal of Virology* **91,** e00050–17 (11 2017).

52. Farnsworth, A., Wisner, T. W. & Johnson, D. C. Cytoplasmic Residues of Herpes Simplex Virus Glycoprotein gE Required for Secondary Envelopment and Binding of Tegument Proteins VP22 and UL11 to gE and gD. *Journal of Virology* **81,** 319–331 (1 2007).

53. Enquist, L. W., Tomishima, M. J., Gross, S & Smith, G. A. Directional spread of an α-herpesvirus in the nervous system. *Veterinary Microbiology* **86,** 5–16 (1-2 2002).

54. Tomishima, M. J. & Enquist, L. W. A conserved α-herpesvirus protein necessary for axonal localization of viral membrane proteins. *The Journal of Cell Biology* **154,** 741–752 (4 2001).

55. Enk, J. *et al.* HSV1 MicroRNA Modulation of GPI Anchoring and Downstream Immune Evasion. *Cell Reports* **17,** 949–956 (4 2016).

56. Tirabassi, R. S., Townley, R. A., Eldridge, M. G. & Enquist, L. W. Molecular Mechanisms of Neurotropic Herpesvirus Invasion and Spread in the CNS. *Neuroscience Biobehavioral Reviews* **22,** 709–720 (6 1998).

57. Card, J. P., Levitt, P. & Enquist, L. W. Different Patterns of Neuronal Infection after Intracerebral Injection of Two Strains of Pseudorabies Virus. *Journal of Virology* **72,** 4434–4441 (5 May 1998).

58. Xu, J. Current Protocols in Molecular Biology. *Current protocols in molecular biology / edited by Frederick M. Ausubel ... [et al.]* **Chapter 28,** 28.1.1–28.1.8 (2005).

59. Schindelin, J. *et al.* Fiji: an open-source platform for biological-image analysis. *Nature Methods* **9,** 676–682 (7 2012).

60. Tirabassi, R. S. & Enquist, L. W. Role of Envelope Protein gE Endocytosis in the Pseudorabies Virus Life Cycle. *Journal of Virology* **72,** 4571–4579. https://journals.asm.org/doi/10.1128/JVI.72.6.4571-4579.1998 (6 June 1998).

61. Brideau, A. D., Banfield, B. W. & Enquist, L. W. The Us9 Gene Product of Pseudorabies Virus, an Alphaherpesvirus, Is a Phosphorylated, Tail-Anchored Type II Membrane Protein. *Journal of Virology* **72,** 4560–4570. https://journals.asm.org/doi/10.1128/JVI.72.6.4560-4570.1998 (6 June 1998).

Chapter 4

HERPES SIMPLEX VIRUS 1 (HSV-1) USES THE RAB6 POST-GOLGI SECRETORY PATHWAY FOR VIRAL EGRESS

Authors: Melissa H. Bergeman, Kimberly Velarde, Honor L. Glenn, Ian B. Hogue

Biodesign Center for Immunotherapy, Vaccines, and Virotherapy & School of Life Sciences, Arizona State University, Tempe, Arizona, United States

4.1 Abstract

Herpes Simplex Virus 1 (HSV-1) is an alpha herpesvirus that infects a majority of the world population. The mechanisms and cellular host factors involved in the intracellular transport and exocytosis of HSV-1 particles are not fully understood. To elucidate these late steps in the replication cycle, we developed a live-cell fluorescence microscopy assay of HSV-1 virion intracellular trafficking and exocytosis. This method allows us to track individual virus particles, and identify the precise moment and location of particle exocytosis using a pH-sensitive reporter. We show that HSV-1 uses the host Rab6 post-Golgi secretory pathway during egress. The small GTPase Rab6 binds to nascent secretory vesicles at the *trans*-Golgi network and regulates vesicle trafficking and exocytosis at the plasma membrane. Here we show that HSV-1 particles colocalize with Rab6a in the region of the Golgi, cotraffic with Rab6a to the cell periphery, and undergo exocytosis from Rab6a vesicles. Consistent with previous reports in the HSV-1 literature, we find that HSV-1 particles accumulate at particular egress "hotspots" in Vero cells. We show that Rab6a secretory vesicles

mediate this preferential/polarized egress, since Rab6a vesicles accumulate near the plasma membrane similarly in uninfected cells. These data suggest that, following particle envelopment, HSV-1 egress follows a pre-existing cellular secretory pathway to exit infected cells rather than novel, virus-induced mechanisms.

Importance. HSV-1 infects a majority of people. It establishes a life-long latent infection, and occasionally reactivates, typically causing characteristic oral or genital lesions. Rarely in healthy natural hosts, but more commonly in zoonotic infections and in elderly, newborn, or immunocompromised patients, HSV-1 can cause severe herpes encephalitis. The precise cellular mechanisms used by HSV-1 remain an important area of research. In particular, the egress pathways that newly-assembled virus particles use to exit from infected cells are unclear. In this study, we used fluorescence microscopy to visualize individual virus particles exiting from cells, and found that HSV-1 particles use the pre-existing cellular secretory pathway, regulated by the cellular protein Rab6.

4.2 Introduction

During the late stages of viral replication, HSV-1 particles traffic to the plasma membrane to undergo exocytosis and complete the infectious cycle. The details of this process, including which host factors are associated, and whether HSV-1 uses pre-existing cellular pathways or induces novel virus-induced pathways, are little understood. Here we describe how HSV-1 particles use the Rab6a secretory pathway to traffic from the region of the Golgi to the plasma membrane for viral egress by exocytosis.

Rab6a, a member of the Ras GTPase superfamily, is a highly conserved protein

across eukaryotic organisms [1]. As molecular switches, Rab proteins alternate between an active form that binds GTP and an inactive form that binds GDP. Rab proteins localize to particular intracellular membranes, and function to recruit a wide variety of effector proteins that determine organelle identity and direct vesicular traffic between organelles [1]. Rab6a localizes strongly to the Golgi and is involved in ER-Golgi and intra-Golgi vesicular traffic. Importantly, Rab6a is present on nascent secretory vesicles that bud from the Trans-Golgi Network (TGN), and directs their intracellular transport and exocytosis at the plasma membrane [2–5].

In terms of viral infection, Rab6a has been identified as an important host factor for replication and intracellular transport/egress of several types of viruses. Parvovirus capsids have been shown to associate with Rab6a secretory vesicles [6], and genetic screens have shown that HIV requires Rab6a for infection [7]. The beta herpesvirus human cytomegalovirus (HCMV) requires Rab6a for viral protein trafficking to the viral assembly compartment [8, 9]. Alpha herpesviruses Varicella Zoster Virus (VZV) and Pseudorabies Virus (PRV) are associated with Rab6a, and PRV undergoes exocytosis from Rab6a secretory vesicles [10–12]. In HSV-1, Rab6 contributes to proper intracellular trafficking of viral membrane proteins prior to secondary envelopment [13, 14], but the role of Rab6 in post-assembly trafficking and egress is not known.

Using a combination of immunofluorescence, and live-cell oblique and Total Internal Reflection Fluorescence (TIRF) microscopy, we show that HSV-1 progeny virus particles colocalize with Rab6a, cotransport with Rab6a from the Golgi region to the cell periphery, and complete exocytosis from Rab6a secretory vesicles. In addition, we show that Rab6a preferentially accumulates at particular locations at the adherent corners, cell extensions, and cell-cell junctions, in both infected and uninfected Vero

cells. Our data suggest that HSV-1 egress uses pre-existing cellular pathways, rather than inducing novel viral-specific trafficking routes.

4.3 Results

Rab6a Secretory Vesicles Accumulate at Particular "Hot Spots". To assess the intracellular localization and trafficking of HSV-1 and Rab6a, we transduced Vero (African green monkey kidney) cells with an HSV-1-based amplicon vector that expresses an EmGFP-Rab6a transgene. The amplicon vector consists of a bacterial plasmid, transgene expression cassette, and origin of replication and packaging signal sequences from the HSV-1 genome. In the presence of a helper virus, the amplicon vector is replicated and packaged into HSV-1 particles, producing a mixed virus stock containing both amplicon and helper virus genomes. We used HSV-1 OK14 [15], based on the 17syn$^+$ laboratory strain, as the helper virus because it expresses an mRFP-VP26 capsid tag to image virus particles in infected cells (Figure 4.1A).

Oblique microscopy (sometimes called HiLo or "dirty TIRF") is similar to TIRF microscopy, except that the excitation laser is projected into a light sheet that selectively illuminates a thin section of the cell (Figure 4.1A). Using this method, we observed that EmGFP-Rab6a strongly localizes to juxtanuclear organelles (Figure 4.1B-C), consistent with the well-established role of Rab6a as a Golgi marker [2, 3, 5]. In cells singly infected with the EmGFP-Rab6a amplicon (without detectable mRFP-VP26 capsid protein expression), Rab6a also accumulates in clusters at the cell periphery (Figure 4.1B).

In cells that were doubly infected with both the EmGFP-Rab6a amplicon and HSV-1 OK14, large amounts of mRFP-VP26 capsids accumulate in the nucleus, a

few particles colocalize with EmGFP-Rab6a in the juxtanuclear Golgi region, and particles begin to appear at sites of EmGFP-Rab6a clustering at the cell periphery by 6 hours post-infection (hpi) (Figure 4.1C). Importantly, virus particles and Rab6a vesicles appear to form clusters in similar locations in singly and coinfected cells, indicating HSV-1 particles and Rab6a share similar trafficking routes and intracellular localization mechanisms.

HSV-1 Particles and Rab6a Vesicles CoTraffic from the Golgi to the Plasma Membrane. After exiting the nucleus, HSV-1 capsids transport to the cellular membranes where secondary envelopment occurs. While the organelles that contribute to HSV-1 secondary envelopment are not entirely clear, viral membrane proteins do traffic through the TGN, colocalize with viral tegument proteins and capsids, and therefore the TGN or TGN-derived secretory organelles are likely where secondary envelopment occurs [16–20].

To assess whether virus particles cotraffic with Rab6a, we coinfected Vero cells with HSV-1 OK14 and EmGFP-Rab6a amplicon, and imaged by live-cell oblique microscopy. Again, capsids were found in the juxtanuclear Golgi region, including colocalizing with discrete EmGFP-Rab6a puncta (Figure 4.2A). Over the course of several minutes, we observed EmGFP-Rab6a vesicles and mRFP-VP26 capsids also traffic together towards the cell periphery, as shown using maximum difference projections and kymographs (Figure 4.2B-C) of the same infected cell shown in Figure 4.2A. Maximum difference projections highlight areas where fluorescence increases rapidly, while suppressing background fluorescence from structures that are not moving or changing over time. Kymographs show particle movement along a path on the X-axis, over time on the Y-axis. Multiple particles cotrafficking with EmGFP-Rab6a moved along parallel paths converging at the tip of cell extensions, as can be seen in

the lower portion of Figure 4.2B. Altogether, these data are consistent with HSV-1 particles trafficking from the Golgi region to the cell periphery in EmGFP-Rab6a secretory vesicles.

Endogenous Rab6a Colocalizes with Exogenous Rab6a. To ensure that the Rab6a vesicle clustering was not an artifact of exogenous EmGFP-Rab6a expression, we also infected cells without exogenous Rab6a expression, or with a non-replicating adenovirus vector expressing mCherry-Rab6a. Cells were fixed and immunostained to detect endogenous Rab6a, and imaged by confocal microscopy. Endogenous Rab6a was found in the juxtanuclear Golgi area, and with some accumulation at the cell periphery (Figure 4.3A), similarly to EmGFP-Rab6a. Exogenous mCherry-Rab6a expressed from the adenovirus vector also colocalized with the endogenous Rab6a (Figure 4.3B). These results show that the colocalization and clustering effects described with EmGFP-Rab6a above are not due to viral vector transduction and overexpression of fluorescent protein-tagged variants.

Endogenous Rab6a Colocalizes with HSV-1 Envelope Proteins. Since HSV-1 capsids cotraffic with Rab6a secretory vesicles, it follows that HSV-1 glycoproteins might also colocalize and cotraffic with Rab6a (Figure 4.3A). Previously, we constructed a recombinant virus, HSV-1 IH01 expressing a pH-sensitive variant of GFP fused to the extravirion loop of glycoprotein M (gM-pHluorin) [21]. In fixed and immunostained cells, pH equilibrates to that of the extracellular buffer, so gM-pHluorin exhibits consistent green fluorescence. In Vero cells infected with HSV-1 IH01, gM-pHluorin appears in the juxtanuclear Golgi region, and colocalizes with endogenous Rab6a (Figure 4.3A) and exogenous mCherry-Rab6a (Figure 4.3A-B). We also observed clustering of gM-pHluorin at the cell periphery, similarly to the clustering of capsids (Figure 4.1-4.2). Together, these results show that HSV-1 cap-

sids, glycoproteins, and Rab6a vesicles colocalize at the juxtanuclear Golgi region, consistent with this being the site of secondary envelopment, and cluster at the cell periphery, consistent with this being sites of preferential viral exocytosis.

HSV-1 Particles Undergo Exocytosis from Rab6a Vesicles. Since HSV-1 particles cotraffic with Rab6a to the plasma membrane, we next wanted to determine if these intracellular trafficking events culminate in virus particle exocytosis from these Rab6a vesicles. Previously, we showed that PRV particles undergo exocytosis from Rab6a vesicles in non-neuronal cells [11, 12] and from the cell body of primary neurons [22]. To visualize HSV-1 exocytosis, we infected Vero cells with HSV-1 IH01, which expresses gM-pHluorin. We previously showed that gM-pHluorin is incorporated into virus particles, and exhibits pH-dependent green fluorescence [21]. In live cells, the lumen of secretory vesicles is acidic (pH of 5.2-5.7) [23, 24], which quenches the green fluorescence of gM-pHluorin (Figure 4.4A). At the moment of exocytosis, the pHluorin moiety is exposed to the extracellular pH and its fluorescence is dequenched [11, 12, 21, 23], allowing us to identify virus particle exocytosis events using TIRF microscopy (Figure4.4A).

Vero cells were transduced with a non-replicating adenovirus vector expressing mCherry-Rab6a, coinfected with HSV-1 IH01, and imaged by live-cell TIRF microscopy beginning at 6 hpi. Consistent with previous results (Figures 4.1-4.3), in singly transduced cells (without detectable gM-pHluorin expression), mCherry-Rab6a vesicles accumulated in clusters at the cell periphery, and in singly infected cells (without detectable mCherry-Rab6a expression), gM-pHluorin appeared in clusters at the cell periphery (Figure 4.4B).

In doubly transduced and coinfected cells, we observed individual virus particles undergoing exocytosis from Rab6a vesicles (Figure 4.4C). After exocytosis, virus

particles remained attached to the cell surface and largely immobile, resulting in the accumulation of large clusters of particles. Clusters of mCherry-Rab6a most likely represent secretory vesicles that have not yet fused, and clusters of dequenched, fluorescent gM-pHluorin puncta represent a combination of virions and L-particles. Because we also observed similar clustering of mRFP-VP26 capsids (Figure 4.1-4.2), and clusters of colocalized gM-pHluorin and mRFP-VP26 capsids (Chapter 3), a subset of these clustered particles represent complete mature virions.

In Vero cells, identifying exocytosis of virus particles from individual Rab6a vesicles was difficult against the high background fluorescence from these large clusters of previously released particles — individual vesicles were no longer distinguishable in a large cluster. To overcome this problem, we transduced and infected PK15 (porcine kidney epithelial) cells, which were previously used to investigate egress of PRV [11, 12]. We have shown that HSV-1 productively infects PK15 cells, but unlike in Vero cells, HSV-1 and PRV exocytosis events are uniformly distributed across the adherent cell surface, with much less accumulation of large clusters (Chapter 3).

Over the course of several minutes, we observed individual virus particles undergoing exocytosis from mCherry-Rab6a vesicles, which were easily distinguishable without the formation of large clusters. A representative exocytosis event is shown using maximum difference projection and a kymograph (Figure 4.5A). Here, maximum difference projections highlight areas where fluorescence increases rapidly due to gM-pHluorin dequenching, and kymographs show the change in particle fluorescence over time on the Y-axis. To quantify gM-pHluorin and mCherry-Rab6a fluorescence over many individual exocytosis events, we calculated the average relative fluorescence intensity over time. Individual exocytosis events were measured, and time series data were aligned to a common time=0 based on the peak of gM-pHluorin fluorescence

intensity. Average green fluorescence exhibits a sharp increase, representing rapid dequenching of gM-pHluorin upon exocytosis, followed by a slow exponential decay due to photobleaching. For a majority of exocytosis events (n=27/44, 61%), red fluorescence gradually increased prior to exocytosis, representing the arrival of a mCherry-Rab6a positive vesicle to the site of exocytosis. Immediately after exocytosis, the red signal rapidly decays, representing a combination of mCherry-Rab6a molecules diffusing away from the site of exocytosis and photobleaching (Figure 4.5B). However, some exocytosis events (n=17/44, 39%) did not appear to be associated with a strong mCherry-Rab6a signal (Figure 4.5B). This may be a result of low mCherry-Rab6a expression, high fluorescence background, or a minority of HSV-1 particles may use alternative secretory mechanisms. Using Imaris software, we produced 3D renderings of a selected Rab6a vesicle and the HSV-1 virus particle cargo in order to conceptualize how the virus particle is carried to the site of exocytosis by the Rab6a vesicle. The vesicle travels towards the edge of the cell, near the plasma membrane, in a long, tubular shape. At time=0 sec, at which exocytosis occurs, the secretory vesicle has contracted to a round shape and begins to release the virus particle. As the virus particle is released to the extracellular space, the Rab6a vesicle dissipates and is no longer detectable while the virus particle still remains.

Endocytic Rab5a is Not Associated with HSV-1 Egress. As a negative control, we also tested Rab5a, which localizes to early endosomes. Cell surface receptors can trigger endocytosis pathways by activating Rab5a [25]. In the context of viral infection, Newcastle Disease Virus uses Rab5a endocytic vesicles for viral entry [26]. Endocytic axonal transport in neurons is dependent on Rab5 [27, 28]. Previously the Elliott lab showed that viral glycoproteins traffic via the endocytic pathway, including Rab5 early endosomes, prior to secondary envelopment [13, 14].

However, Rab5 early endosomes typically undertake further sorting steps to deliver cargoes to late endosomes/lysosomes, retrograde trafficking to the Golgi, or recycling back to the plasma membrane. These results show that, while Rab5a likely plays important roles in membrane trafficking upstream of secondary envelopment and egress, our experiments are not observing these upstream steps, and thus Rab5a serves as a negative control to show that overexpression of other Rab GTPases does not result in artefactual associations with viral exocytosis.

We transduced Vero cells with an adenovirus vector expressing mCherry-Rab5a, coinfected with HSV-1 IH01, and imaged by live-cell oblique and TIRF microscopy at 6 hpi. While gM-pHluorin exhibited clustering at the cell periphery and cell-cell contacts, as observed above, mCherry-Rab5a localized to distinct punctae. We observed no colocalization between gM-pHluorin and mCherry-Rab5a (Figure 4.6A). In average fluorescence intensity curves, mCherry-Rab5a exhibited no association with gM-pHluorin exocytosis (Figure 4.6B). Thus, it appears that interactions between HSV-1 and Rab GTPases are specific, and overexpression of other Rab GTPases does not result in spurious associations.

4.4 Discussion

Viral egress is a highly involved process: after assembly, virus particles must be sorted and delivered to the appropriate site of exocytosis, and must be released from the infected cell by exocytosis. It has been shown via knockdown and knockout studies that Rab6a is important for HSV-1 replication. We have also previously shown that Rab6a secretory vesicles are involved in egress of the related alpha herpesvirus, PRV [11, 12, 20, 22]. By using live cell fluorescence microscopy, we found that Rab6a is

associated with the final stages of HSV-1 replication. Rab6a and HSV-1 progeny particles colocalize in the region of the Golgi (Figure 4.1-4.2), where they cotraffic to the plasma membrane (Figure 4.2B-C). At the plasma membrane, virus particles undergo exocytosis from Rab6a secretory vesicles (Figure 4.4-4.5).

However, Rab6a is likely not the sole Rab GTPase that plays a role in HSV-1 egress and exocytosis. PRV particles undergo exocytosis from secretory vesicles that are also labeled with Rab8a and Rab11a [11, 12], and the same might be the case for HSV-1. Rab6a is also not the only effector for microtubule transport and cargo trafficking, and it interacts with Rab8 and Rab11 [3, 29]. Since we found that some viral exocytosis events were not associated with detectable Rab6a, it may be that these viral egress events were associated with other Rab proteins.

Furthermore, alpha herpesviruses have evolved to carry out their replication cycles in a broad range of host cells, including neurons with highly specialized cell biology. Thus, these viruses have to overcome differences of host cell biology from one cell type to another. With HSV-1 specifically, it can be expected that there is some overlap between host factors involved with egress across cell types, as humans express several dozen different types of Rab GTPases [1]. Rab6a is expressed in neurons, along with a Rab6b isoform that is neuron-specific [30]. It is possible that both isoforms of Rab6 may contribute to HSV-1 transport and egress in neuronal cells.

In addition to HSV-1 egress from Rab6a vesicles, we also observed that HSV-1 particles and Rab6a accumulated in clusters together at the cell periphery. This clustering has been previously reported by others [31–33], including as far back as some of the earliest indirect immunofluorescence studies with HSV-1 [34]. In the cell biological literature, it has been shown that Rab6a coordinates the delivery of secretory vesicles near focal adhesions [5]. The coclustering of HSV-1 particles and

Rab6a may be explained by this function of Rab6a targeting exocytosis to particular sites in the cell. Further studies will be needed to determine what connections may exist between Rab6, other Rab GTPases that may function combinatorially, and their effector molecules that govern trafficking and exocytosis.

4.5 Materials and Methods

Cell lines and cell culture. Vero (African green monkey), human embryonic kidney 293 (HEK 293A), and PK15 cells were obtained from ATCC, and maintained in DMEM medium (Cytiva) supplemented with 10% fetal bovine serum (Gibco) and 1% penicillin-streptomycin (Gibco), in a 5% CO_2 incubator at 37℃.

HSV-1 Viruses. HSV-1 IH01 was constructed and propagated as previously described [21]. HSV-1 OK14 was obtained from Lynn Enquist (Princeton University) [15] from whole-genome sequenced archival stocks.

HSV-1 Amplicon Vector Construction and Propagation. The amplicon vector plasmid pCPD-HSV-N-EmGFP-DEST was constructed by the DNASU Plasmid Repository (Biodesign Institute, Arizona State University), as follows: The plasmid HSV-DYN-hM4Di was a gift from John Neumaier (Addgene plasmid # 53327) [35]. Unnecessary promoter and transgene sequences were removed by digestion with HindIII and religating, to produce pCPD-HSV. This plasmid contains the HSV-1 packaging signal and OriS origin of replication. The plasmid pcDNA6.2/N-EmGFP-DEST was obtained from Invitrogen (ThermoFisher). The CMV promoter, Emerald GFP coding region, Gateway recombination cassette (attR1, CmR selection marker, ccdB counterselection marker, attR2), and HSV-1 TK polyadenylation signal were PCR amplified and ligated into the HindIII site on pCPD-HSV, to produce pCPD-HSV-N-

EmGFP-DEST. The human Rab6a coding sequence (DNASU Plasmid Repository, #HsCD00296778, NCBI Nucleotide reference BC096818) was inserted by Gateway recombination (Invitrogen) to make an in-frame EmGFP-Rab6a fusion.

To propagate the EmGFP-Rab6a amplicon vector, 3.5 x 10^5 HEK 293A cells were seeded into each well of a 6-well plate (Celltreat), incubated overnight, and then transfected with 3μg of amplicon plasmid using Lipofectamine 2000 (Invitrogen). 24 hours after transfection, cells were infected with 10^5 infectious units of HSV-1 OK14. Cells were incubated for another 24 hours, and then cells and supernatants were harvested. The amplicon stock was passaged at high MOI three times on Vero cells, cells and supernatants were harvested, and stored at -80℃.

Adenovirus Vectors. Non-replicating E1/E3-deleted adenovirus vectors expressing mCherry-Rab6a or mCherry-Rab5a were previously described [11, 12], and propagated on HEK 293A cells.

Live Cell Oblique and TIRF Microscopy. Cultures were prepared for TIRF and oblique microscopy by seeding cells at a low density on glass-bottom 35mm dishes (Celltreat, Ibidi, or MatTek), and incubated overnight before viral transduction and infection. Cells were infected with HSV-1, amplicon vectors, and/or adenovirus vectors, and imaged beginning at 6 hpi. The HSV-1, amplicon vector, and adenovirus vector inoculum amounts were determined empirically to synchronously infect/transduce a majority of cells as observed by fluorescence microscopy. Fluorescence microscopy was performed using a Nikon Eclipse Ti2-E inverted microscope in the Biodesign Imaging Core facility (Arizona State University, Tempe, AZ). This microscope is equipped with TIRF and widefield illuminators, a Photometrics Prime95B sCMOS camera, a 60X high-NA TIRF objective, and objective and stage warmers for 37°C live-cell

microscopy. 488nm and 561nm lasers were used to excite green and red fluorescent proteins, respectively.

Immunofluorescence and Confocal Microscopy. Vero cells were seeded into 8-well Ibidi dishes and cultured overnight. Cells were infected with HSV-1 IH01, mCherry-Rab6a adenovirus vector, or cotransduced/infected, as described above. At 7 hpi, cells were fixed for 10 minutes with 4% freshly-prepared paraformaldehyde in PBS, permeabilized with 0.5% Triton X-100 for 90 seconds, then fixed again for 2 minutes. After fixation, samples were rinsed three times with PBS, then blocked with 5% goat serum in PBS for 30 minutes at room temperature. Primary rabbit polyclonal antibody against Rab6a (Abcam ab95954) was used at a 1:200 dilution in antibody diluent (0.05% Tween 20, 1% goat serum, in PBS). Cells were incubated in primary antibody overnight in the dark at 4°C, then rinsed 3 times in wash buffer (0.05% Tween 20, in PBS). Secondary antibody, anti-rabbit AlexaFluor 633 (ThermoFisher A21071) was diluted 1:1000 in antibody diluent and incubated on samples for 2 hr at room temperature with gentle rocking. Cells well rinsed 3 times with wash buffer, and once with PBS. Nuclei were labeled with 0.1 μg/mL DAPI in PBS. Samples were imaged on a Nikon AX R laser scanning confocal microscope in the Biodesign Imaging Core facility (Arizona State University, Tempe, AZ) using a 60X 1.42 NA objective. The DAPI channel was excited at 405nm, pHluorin at 488nm, mCherry at 568nm, and AlexaFluor 633 at 640nm. Emissions for these channels were collected in the blue, green, red, and far red spectral ranges respectively.

Image Analysis. Image analysis to identify exocytosis events and HSV colocalization with Rab6a vesicles was conducted in Fiji software [36]. Fluorescence microscopy images were prepared for publication using Adjust Brightness/Contrast, Reslice (to produce kymographs), and Plot Z-axis Profile (to measure fluorescence over

time) functions in Fiji. Maximum difference projections were calculated as previously described [11], using the Duplicate, Stacks->Tools, Math->Subtract, and Z Project functions in Fiji. Maximum difference projection shows where fluorescence intensity increases most rapidly, which emphasizes exocytosis events and particle movement, and deemphasizes static features that do not change during the course of imaging. Plots of average fluorescence intensity during exocytosis events were calculated using Matlab (Mathworks). Imgage segmentation and 3D rendering of HSV-1 virus particle undergoing exocytosis from Rab6a vesicle was done in Imaris (Oxford Instruments) by constructing spots and surfaces for the objects at respective image slices.

Acknowledgements. Thank you to Joli Bastin for her work on producing the recombinant HSV IH01 and IH02 strains carrying gM-pHluorin. Access to the Imaris software was kindly provided by Drs. M. Foster Olive and Jessica Verpeut (Dept. of Psychology, Arizona State University).

Conflict of Interest. The authors declare no conflict of interest.

Funding. This work was supported by NIH NIAID K22 AI123159 and NINDS R01 NS117513.

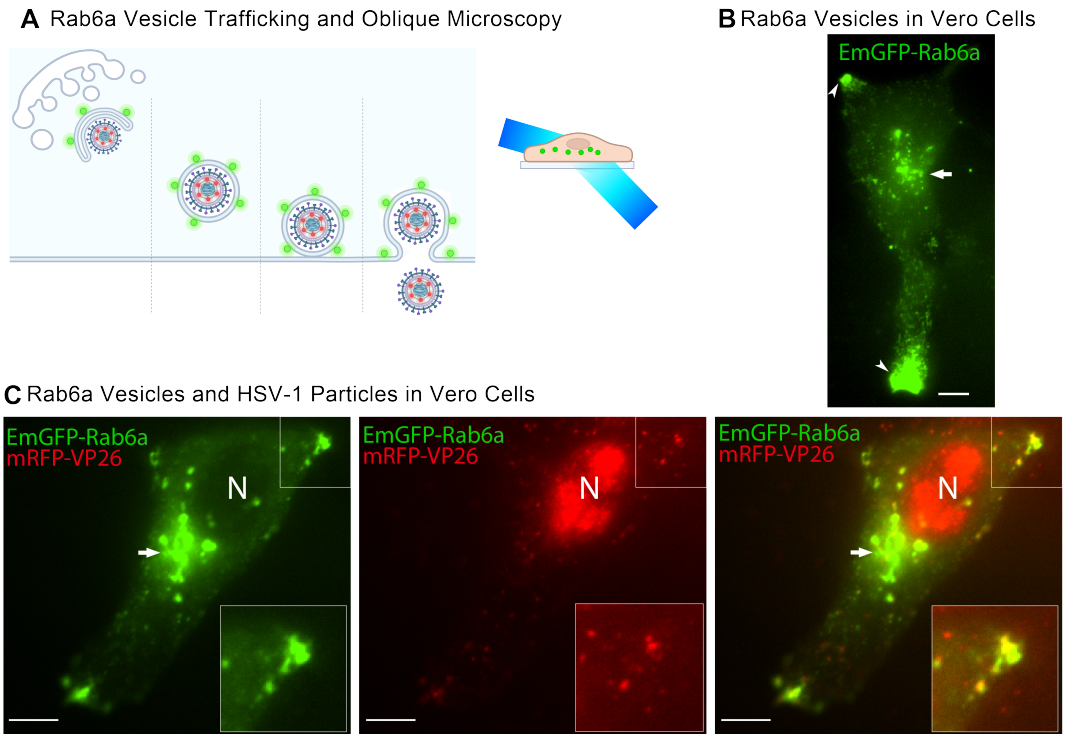

Figure 4.1. Rab6a Secretory Pathway

A. Schematic of viral egress and fluorescent reporters. Secretory vesicles marked with Rab6a (green) transport virus particles marked with mRFP-VP26 (red) to the plasma membrane. Oblique microscopy projects a light sheet that excites fluorescent molecules within a thin section of the cell volume. **B.** Vero cells transduced with an HSV-1 amplicon vector expressing EmGFP-Rab6a. Rab6a, a Golgi marker, localizes to the juxtanuclear Golgi region, and accumulates forming clusters at the cell periphery at 6 hpi. **C.** EmGFP-Rab6a (green) and HSV-1 capsids (red) colocalize in clusters at the cell periphery in Vero cells 6 hpi. Scale bars represent 10μm.

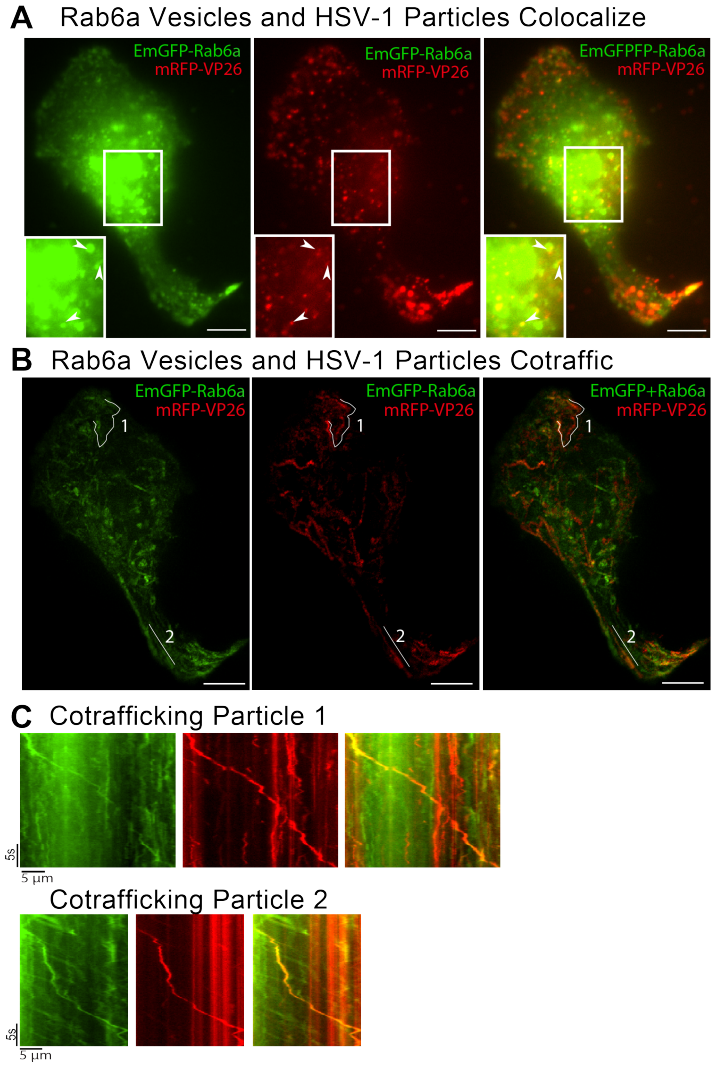

Figure 4.2. Rab6a and HSV-1 Cotrafficking

HSV-1 particles colocalize and cotraffic with Rab6a towards the cell periphery. Vero cells transduced with an HSV-1 amplicon vector expressing EmGFP-Rab6a, coinfected with HSV-1 OK14, and imaged by live-cell oblique microscopy at 6 hpi. Scale bars = 10μm. **A.** HSV-1 capsids and EmGFP-Rab6a colocalize in distinct punctae in the Golgi region **B.** Rab6a and HSV-1 capsids cotraffic towards the cell periphery. **C.** Kymographs showing movement of Rab6a and HSV-1 capsid cotrafficking. Kymographs represent particle tracks 1 and 2 indicated in panel B.

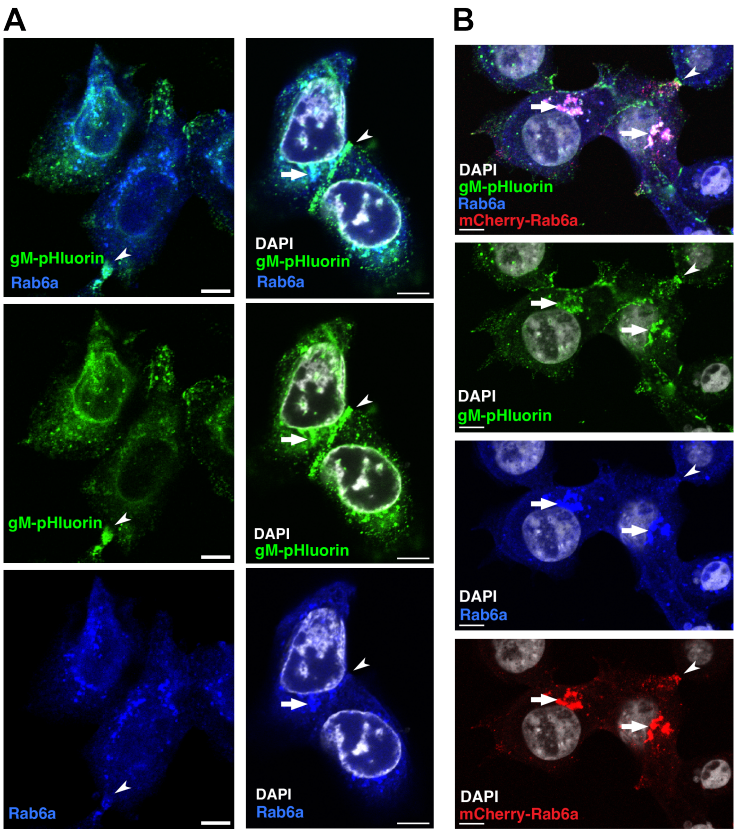

Figure 4.3. Endogenous and Exogeous Rab6a with HSV-1 Infection

Confocal microscopy of fixed and immunostained cells detecting endogenous and exogenous Rab6a, with HSV-1 infection, in Vero cells at 7 hpi. Scale bars = 10μm. **A.** Endogenous Rab6a (blue) and HSV-1 gM-pHluorin protein (green) colocalizes to the juxtanuclear space and cell periphery in Vero cells that are not transduced to express exogenous Rab6a. **B.** Endogenous Rab6a (blue), exogenous Rab6a (red), and HSV-1 gM protein (green) colocalize in Vero cells transduced to express exogenous Rab6a.

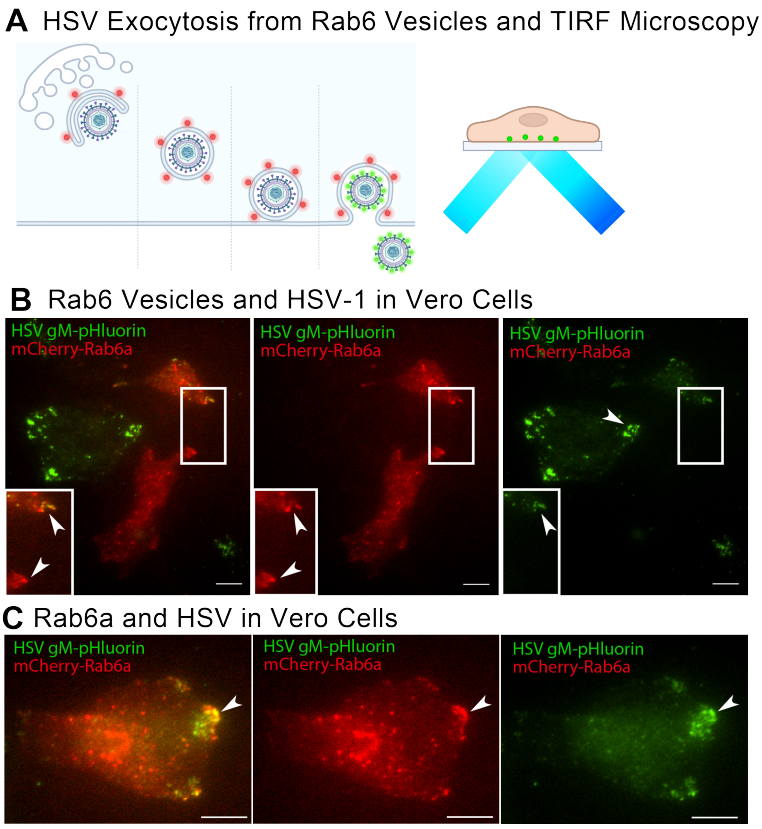

Figure 4.4. Rab6a and HSV-1 Accumulate at Exocytosis Sites

TIRF microscopy at 6 hpi of Vero cells transduced with mCherry-Rab6a adenovirus vector (red) and infected with HSV-1 IH01 expressing gM-pHluorin (green). Scale bars = 10μm. **A.** Schematic of mCherry-Rab6a secretory vesicles transport virus particles to the plasma membrane. gM-pHluorin becomes fluorescent with the pH change at the moment of exocytosis. TIRF microscopy excites fluorescent molecules at the plasma membrane. **B.** HSV-1 gM accumulates in the cell periphery in cells that are transduced and not transduced. Rab6a accumulates in the cell periphery in cells that are transduced and not transduced. **C.** HSV-1 particles undergo exocytosis from Rab6a secretory vesicles at the cell periphery, and HSV-1 and Rab6a accumulate at these locations in the infected cell.

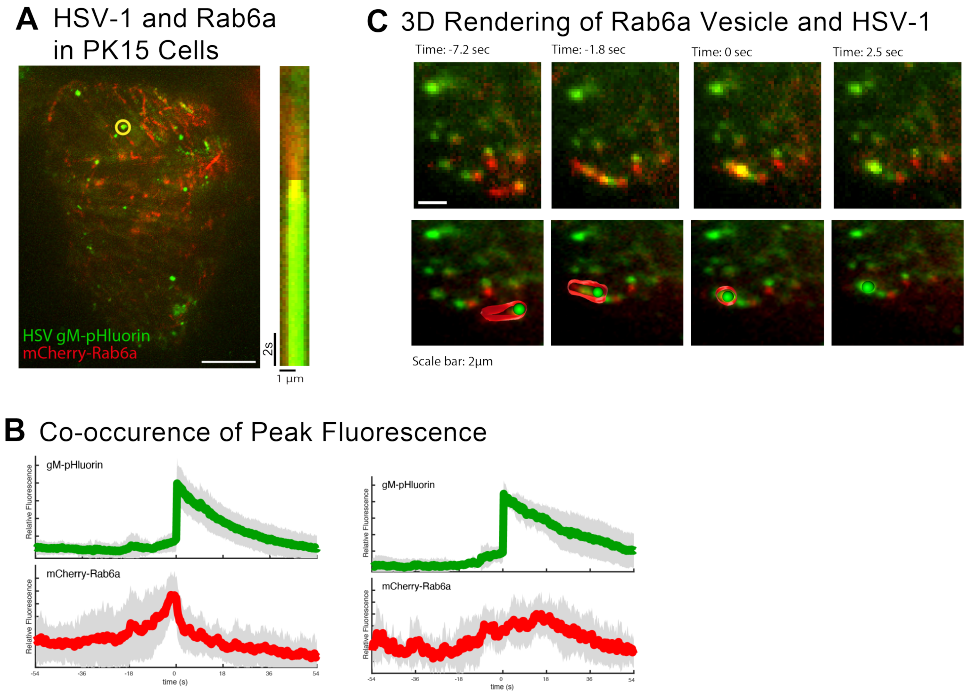

Figure 4.5. HSV-1 Undergoes Exocytosis from Rab6a Secretory Vesicles

TIRF microscopy at 6 hpi of PK-15 cells transduced with mCherry-Rab6a adenovirus vector and infected with HSV-1 IH01. Scale bar = 10μm. **A.** Maximum difference projection of coinfected cell over 3:38sec of imaging. Kymograph of particle (yellow circle) movement and fluorescence over time showing HSV-1 exocytosis from a Rab6a vesicle. **B.** Plot of mean fluorescence over time at exocytosis event (time = 0). mCherry-Rab6a fluorescence (red) peaks before HSV-1 gM-pHluorin (green) as the secretory vesicle arrives and the plasma membrane and the virus particle is released to the extracellular space. Shading is standard deviation (n=44). **C**. Top row panels are TIRF microscpy images at the indicated time point before, at (Time=0sec), and after viral exocytosis from Rab6a vesicle. Bottom row panels show 3D model of the veiscle and virus particle at the same time points, as compiled in Imaris (Oxford Instruments).

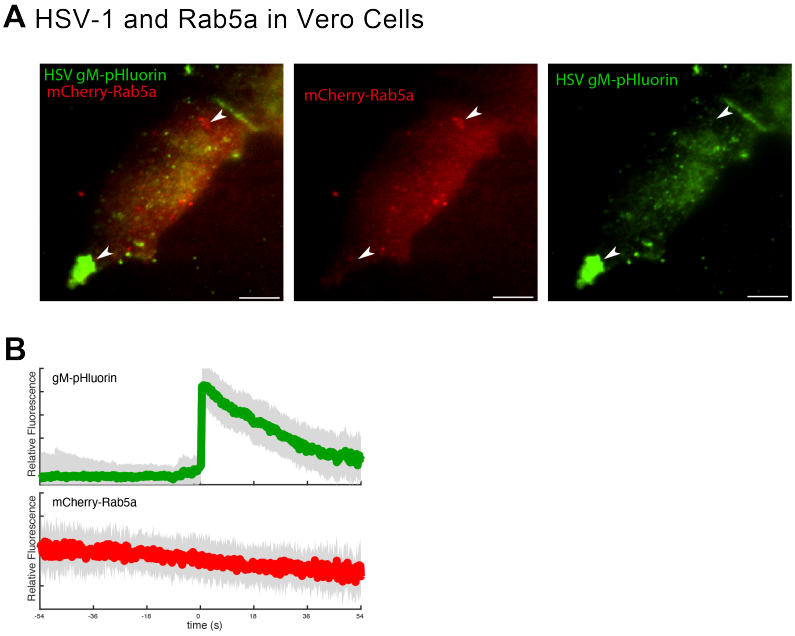

Figure 4.6. HSV-1 Does Not Undergo Exocytosis from Rab5a Vesicles

HSV-1 does not undergo exocytosis from mCherry-Rab5a vesicles in Vero cells. Scale bar = 10μm. **A.** HSV-1 gM-pHluorin accumulates in hotspots and cell junctions. Rab5a does not accumulate with HSV-1 progeny or envelope proteins. **B.** Plot of HSV-1 gM-pHluorin and mCherry-Rab5a mean fluorescence aligned at the exocytosis event (time=0). gM-pHluorin peaks at exocytosis, and mCherry-Rab5a has no corresponding peak. Shading is standard deviation (n=63).

BIBLIOGRAPHY

1. Stenmark, H. Rab GTPases as coordinators of vesicle traffic. *Nature Reviews Molecular Cell Biology* **10,** 513–525 (8 2009).

2. Goud, B., Zahraoui, A., Tavitian, A. & Saraste, J. Small GTP-binding protein associated with Golgi cisternae. *Nature* **345,** 553–556 (6275 1990).

3. Grigoriev, I. *et al.* Rab6 Regulates Transport and Targeting of Exocytotic Carriers. *Developmental Cell* **13,** 305–314 (2 Aug. 2007).

4. Jordens, I., Marsman, M., Kuijl, C. & Neefjes, J. Rab proteins, connecting transport and vesicle fusion. *Traffic* **6,** 1070–1077 (12 Dec. 2005).

5. Fourriere, L. *et al.* RAB6 and microtubules restrict protein secretion to focal adhesions. *Journal of Cell Biology* **218,** 2215–2231 (7 2019).

6. Bär, S., Daeffler, L., Rommelaere, J. & Nüesch, J. P. Vesicular Egress of Non-Enveloped Lytic Parvoviruses Depends on Gelsolin Functioning. *PLOS Pathogens* **4,** e1000126. https://journals.plos.org/plospathogens/article?id=10.1371/journal.ppat.1000126 (8 Aug. 2008).

7. Brass, A. L. *et al.* Identification of host proteins required for HIV infection through a functional genomic screen. *Science* **319,** 921–926. https://www.science.org/doi/10.1126/science.1152725 (5865 Feb. 2008).

8. Indran, S. V., Ballestas, M. E. & Britt, W. J. Bicaudal D1-Dependent Trafficking of Human Cytomegalovirus Tegument Protein pp150 in Virus-Infected Cells.

Journal of Virology **84,** 3162–3177. https://journals.asm.org/doi/10.1128/JVI.01776-09 (7 Apr. 2010).

9. Indran, S. V. & Britt, W. J. A Role for the Small GTPase Rab6 in Assembly of Human Cytomegalovirus. *Journal of Virology* **85,** 5213–5219. https://journals.asm.org/doi/10.1128/JVI.02605-10 (10 May 2011).

10. Girsch, J. H. *et al.* Exocytosis of Progeny Infectious Varicella-Zoster Virus Particles via a Mannose-6-Phosphate Receptor Pathway without Xenophagy following Secondary Envelopment. *Journal of Virology* **94.** https://journals.asm.org/doi/10.1128/JVI.00800-20 (16 July 2020).

11. Hogue, I. B., Bosse, J. B., Hu, J.-R., Thiberge, S. Y. & Enquist, L. W. Cellular Mechanisms of Alpha Herpesvirus Egress: Live Cell Fluorescence Microscopy of Pseudorabies Virus Exocytosis. *PLoS Pathogens* **10,** e1004535 (12 2014).

12. Hogue, I. B., Scherer, J. & Enquist, L. W. Exocytosis of Alphaherpesvirus Virions, Light Particles, and Glycoproteins Uses Constitutive Secretory Mechanisms. *mBio* **7,** e00820–16 (3 2016).

13. Johns, H. L., Gonzalez-Lopez, C., Sayers, C. L., Hollinshead, M. & Elliott, G. Rab6 Dependent Post-Golgi Trafficking of HSV1 Envelope Proteins to Sites of Virus Envelopment. *Traffic (Copenhagen, Denmark)* **15,** 157–178 (2 2014).

14. Hollinshead, M. *et al.* Endocytic tubules regulated by Rab GTPases 5 and 11 are used for envelopment of herpes simplex virus. *The EMBO Journal* **31,** 4204–4220. https://onlinelibrary.wiley.com/doi/full/10.1038/emboj.2012.

262https://onlinelibrary.wiley.com/doi/abs/10.1038/emboj.2012.262https://www.embopress.org/doi/10.1038/emboj.2012.262 (21 Nov. 2012).

15. Song, R. *et al.* Two Modes of the Axonal Interferon Response Limit Alphaherpesvirus Neuroinvasion. *mBio* **7,** e02145–15 (1 2016).

16. Turcotte, S., Letellier, J. & Lippé, R. Herpes Simplex Virus Type 1 Capsids Transit by the trans-Golgi Network, Where Viral Glycoproteins Accumulate Independently of Capsid Egress. *Journal of Virology* **79,** 8847–8860 (14 2005).

17. Sugimoto, K. *et al.* Simultaneous Tracking of Capsid, Tegument, and Envelope Protein Localization in Living Cells Infected with Triply Fluorescent Herpes Simplex Virus 1. *Journal of Virology* **82,** 5198–5211 (11 2008).

18. White, S., Kawano, H., Harata, N. C. & Roller, R. J. Herpes Simplex Virus Organizes Cytoplasmic Membranes To Form a Viral Assembly Center in Neuronal Cells. *Journal of Virology* **94.** https://journals.asm.org/doi/10.1128/JVI.00900-20 (19 Sept. 2020).

19. Miranda-Saksena, M. *et al.* Herpes simplex virus utilizes the large secretory vesicle pathway for anterograde transport of tegument and envelope proteins and for viral exocytosis from growth cones of human fetal axons. *Journal of virology* **83,** 3187–99 (7 2009).

20. Raza, S. *et al.* Role of Rab GTPases in HSV-1 infection: Molecular understanding of viral maturation and egress. *Microbial Pathogenesis* **118,** 146–153 (2018).

21. Bergeman, M. H. *et al.* Live-cell Fluorescence Microscopy of HSV-1 Cellular Egress by Exocytosis. *bioRxiv,* 2023.02.27.530373. https://www.biorxiv.org/

content/10.1101/2023.02.27.530373v1https://www.biorxiv.org/content/10.1101/2023.02.27.530373v1.abstract (Feb. 2023).

22. Ambrosini, A. E., Deshmukh, N., Berry, M. J., Enquist, L. W. & Hogue, I. B. Alpha Herpesvirus Egress and Spread from Neurons Uses Constitutive Secretory Mechanisms Independent of Neuronal Firing Activity. *bioRxiv,* 729830. https://www.biorxiv.org/content/10.1101/729830v1https://www.biorxiv.org/content/10.1101/729830v1.abstract (Aug. 2019).

23. Sankaranarayanan, S., Angelis, D. D., Rothman, J. E. & Ryan, T. A. The Use of pHluorins for Optical Measurements of Presynaptic Activity. *Biophysical Journal* **79,** 2199–2208 (4 2000).

24. Paroutis, P., Touret, N. & Grinstein, S. The pH of the Secretory Pathway: Measurement, Determinants, and Regulation. *Physiology* **19,** 207–215 (4 2004).

25. Barbieri, M. A. *et al.* Epidermal Growth Factor and Membrane TraffickingEgf Receptor Activation of Endocytosis Requires Rab5a. *Journal of Cell Biology* **151,** 539–550. http://www.jcb.org/cgi/content/full/151/3/539 (3 Oct. 2000).

26. Tan, L. *et al.* Newcastle disease virus employs macropinocytosis and Rab5a-dependent intracellular trafficking to infect DF-1 cells. *Oncotarget* **7,** 86117. /pmc/articles/PMC5349901//pmc/articles/PMC5349901/?report=abstracthttps://www.ncbi.nlm.nih.gov/pmc/articles/PMC5349901/ (52 Dec. 2016).

27. De Hoop, M. J. *et al.* The involvement of the small GTP-binding protein Rab5a in neuronal endocytosis. *Neuron* **13,** 11–22 (1 July 1994).

28. Deinhardt, K. *et al.* Rab5 and Rab7 Control Endocytic Sorting along the Axonal Retrograde Transport Pathway. *Neuron* **52,** 293–305 (2 Oct. 2006).

29. Miserey-Lenkei, S. *et al.* Rab6-interacting Protein 1 Links Rab6 and Rab11 Function. *Traffic* **8,** 1385–1403. https://onlinelibrary.wiley.com/doi/full/10.1111/j.1600-0854.2007.00612.xhttps://onlinelibrary.wiley.com/doi/abs/10.1111/j.1600-0854.2007.00612.xhttps://onlinelibrary.wiley.com/doi/10.1111/j.1600-0854.2007.00612.x (10 Oct. 2007).

30. Opdam, F. J. *et al.* The small GTPase Rab6B, a novel Rab6 subfamily member, is cell-type specifically expressed and localised to the Golgi apparatus. *Journal of Cell Science* **113,** 2725–2735. https://journals.biologists.com/jcs/article/113/15/2725/26177/The-small-GTPase-Rab6B-a-novel-Rab6-subfamily (15 Aug. 2000).

31. Mingo, R. M., Han, J., Newcomb, W. W. & Brown, J. C. Replication of herpes simplex virus: egress of progeny virus at specialized cell membrane sites. *Journal of virology* **86,** 7084–97 (13 2012).

32. Johnson, D. C., Webb, M., Wisner, T. W. & Brunetti, C. Herpes Simplex Virus gE/gI Sorts Nascent Virions to Epithelial Cell Junctions, Promoting Virus Spread. *Journal of Virology* **75,** 821–833 (2 2001).

33. McMillan, T. N. & Johnson, D. C. Cytoplasmic Domain of Herpes Simplex Virus gE Causes Accumulation in the trans -Golgi Network, a Site of Virus Envelopment and Sorting of Virions to Cell Junctions. *Journal of Virology* **75,** 1928–1940 (4 2001).

34. Norrild, B., Virtanen, I., Lehto, V. P. & Pedersen, B. Accumulation of herpes simplex virus type 1 glycoprotein D in adhesion areas of infected cells. *Journal of General Virology* **64,** 2499–2503. https://www.microbiologyresearch.org/content/journal/jgv/10.1099/0022-1317-64-11-2499 (11 Nov. 1983).

35. Ferguson, S. M. *et al.* Transient neuronal inhibition reveals opposing roles of indirect and direct pathways in sensitization. *Nature Neuroscience 2010 14:1* **14,** 22–24. https://www.nature.com/articles/nn.2703 (1 Dec. 2010).

36. Schindelin, J. *et al.* Fiji: an open-source platform for biological-image analysis. *Nature Methods* **9,** 676–682 (7 2012).

Chapter 5

DISCUSSION

5.1 Summary of Results

In order to ascertain some of the means by which HSV-1 particles emerge from infected cells, we generated a recombinant strain of HSV-1 that allows us to visualize virus particles as they traffic and undergo exocytosis. With a combination of fluorescent microscopy techniques and viral vector transduction, we were able to identify one pathway of HSV-1 egress.

HSV-1 particles complete exocytosis on an individual basis: single virus particles are released at the plasma membrane. Virus particles do not exit in bulk, as has been observed with beta herpesviruses and retroviruses [152–158].

Previous studies with PRV showed that this member of the alpha herpesvirus subfamily also exits infected cells as individual particles [68, 69]; however, other studies with HSV-1 showed accumulated clusters of virus particles late in infection [72, 142, 159, 160]. The differences in these observations appears to be accounted for by differences in cell biology rather than those of viral biology. While we observed PRV and HSV-1 virus particles exiting individually in a non-clustered pattern in PK15 cells, we found that PRV and HSV-1 exited at preferential hot spots in Vero and primary REF cells. The clustered phenotype is the result of many virus particles completing exocytosis at the same location over a period of time, rather than bulk release or particle movement after egress. We did observe that some cases of viral exocytosis from Rab6a vesicles had a holding period or pause between the vesicle

arriving at the exocytosis site and the release of the virion. This may be because the vesicle membrane merges with the plasma membrane, and then the Rab6a proteins dissipate from the exocytosis site. In addition, interactions between the vesicles and other target proteins, such as ERC1 discussed below, may also be responsible for the holding period.

Furthermore, the three proteins gE-gI-US9, which are orthologous between PRV and HSV-1 and form a tripartite complex in the viral envelope, have been extensively studied as they are integral in the process of intracellular transport in neurons and non-neuronal cells [61, 81, 121, 142–144, 161–164]. Our studies indicate that PRV and HSV-1 strains that are gE-gI-US9 null have a decreased rate of clustering at the cell periphery late in infection, which aligns with studies in neurons that have shown that they are essential for axonal sorting and transport. PRV had a higher mean particle velocity in a gE-gI-US9 null strain than a wild type strain, indicating that virus particles lacking these proteins still undergo exocytosis and complete the infectious cycle, but perhaps do so by recruiting alternative microtubule motors. These alternative motors, despite having higher velocities, may target viral intracellular transport to different subcellular locations, altering the observed egress and cell-cell spread phenotype. Since alpha herpesviruses infect a broad range of cell types, it would follow that viral proteins that play a role in one process in one cell type would do so in another. While alpha herpesviruses are larger in terms of virus particle size and in genome capacity, strict limitations do exist on the size of both due to physical limitations on spatial geometry and packaging capacity. Essentially: better for the virus to express a smaller number of proteins that are sufficient in activity across a broad range of cell types, enabling the completion of the replication cycle, than

relying on a superfluous number of proteins that are more specific in activity and could introduce more failure points into the replication cycle.

We also demonstrated that HSV-1 trafficks with and undergoes exocytosis from cells via Rab6a secretory vesicles, similar to PRV [68, 69]. Virus particles are transported from the TGN region to the plasma membrane by Rab6a secretory vesicles. These vesicles then accumulate in clusters at the plasma membrane, where they release their HSV-1 cargo for exocytosis. However, the studies presented here were limited to non-neuronal epithelial cells – whether Rab6a is involved in HSV-1 egress in neurons is still an open question.

5.2 Future Directions: Rab6 in Neurons

Like epithelial cells that express Rab6 as part of the secretion pathways for soluble and membrane cargo [165, 166], neurons also express Rab6 proteins. In neurons, Rab6 localizes at nerve terminals in presynaptic neurons [166], presumably at the conclusion of vesicle transport through the axon. Some studies have shown correlations between increased Rab6 expression and endoplasmic reticulum stress in Alzheimer's disease [167], and possible links between HSV-1 infection and Alzheimer's as well [168–170]. If Rab6 proteins are involved in HSV-1 egress in neurons, it may be one potential factor in the link between these two diseases. Furthermore, neurons are the only cell type that express Rab6b protein [171]. Studies of Rab6b and HSV-1 egress are lacking, and Rab6b may well be part of the HSV-1 egress pathway. In addition to Alzheimer's Disease, the interplay between Rab proteins and alpha herpesvirus egress may prove to be important in future alpha herpesvirus vector design of vaccines and therapeutics.

5.3 Future Directions: Rab6 and Other Rab Protein Interactions

Many Rab proteins have been found to interact in concert with other Rabs and similar small GTPases. Rab5 and Rab7 interact together during retrograde axonal transport of cargo towards the cell body after endocytosis [172]. During anterograde axonal transport away from the cell body, Rab6 and Rab8 interact, and Rab8 is dependent on Rab6 during vesicular transport [173]. Rab6, Rab8, and Rab10 share many interacting partners [174]. Rab6 interacting protein (Rab6IP) binds both Rab6 and Rab11 so that Rab6 and Rab11 interact [175]. Both Rab8 and Rab11 have been shown to be associated with PRV exocytosis [68, 69], and several RNA viruses have been shown to interact with Rab11 [176].

Thus it is possible that these additional Rab proteins are also associated with HSV-1 egress. Studies with Rab8 and Rab11 have focused on PRV and not HSV-1 thus far. Since Rab proteins can also interact with each other, follow up studies should examine Rab8, Rab10, and Rab11. HSV-1 may undergo exocytosis from vesicles with multiple Rab proteins and may require the presence of more than one Rab protein for optimal trafficking and exocytosis. Since these proteins work to recruit the motors that actively transport the secretory vesicles, and also coordinate the end destination at the conclusion of transport, Rab proteins acting in concert with each other may be the reason that we observed the egress hot spots and also account for not all exocytosis events being strongly associated with Rab6a. With the ability to express fluorescent host factors and HSV-1, similar techniques to assess the colocalization and trafficking as presented here could be used to address these questions in neurons and non-neuronal cells alike.

5.4 Future Directions: Rab and ERC1

ERC1 (ELKS1) protein is found at the cell periphery, associated with the plasma membrane. It assists in directing vesicles to exocytosis sites and synaptic proteins to active zones at the synapses in neurons [166, 177]. ERC1 binds Rab6, and thus may help sort Rab6a vesicles to the sites where they release their cargo [166]. Furthermore, ERC1 and LL5β bind to each other [173], and Hogue et al. found colocalization between LL5β and PRV during PRV exocytosis [68].

The role of ERC1 in HSV-1 egress is unclear, especially within the context of Rab and ERC1 interactions. Since ERC1 directs secretory vesicles to exocytosis sites, it may be that the clusters of Rab6a vesicles, and the corresponding HSV-1 cargo, we observed are a result of ERC1 function. If Rab6 binds to ERC1, these vesicles may be targeted towards sites in the cell that are rich in ERC1 expression to ensure proper cargo delivery and distribution. Future studies should examine whether or not ERC1 and HSV-1 clustering are correlated, and if HSV-1 undergoes exocytosis near ERC1 more frequently than not in non-neuronal cells and neurons both. Our lab is currently interested in the hypothesis that HSV-1 undergoes exocytosis at synapses between neurons as the primary means of neuron-neuron spread, and so the correlation between ERC1 and HSV-1 egress, if it does exist, may be part of the mechanism behind this supposition.

5.5 Motor Transport

Kinesin-3 motors directly transport alpha herpesvirus progeny through axons, particularly KIF1A [145, 178]. PRV infection depletes KIF1A, as does HSV-1 infection

[144, 145]. In both viruses, these motors are recruited by gE-gI-US9 proteins, and defective expression of these proteins results in ineffective axonal transport of virus cargo and even a complete inability for virus particles to undergo anterograde transport [61, 81, 121, 142–145, 161, 163, 164, 179]. As stated above, the differences in motor recruitment by these viral proteins may account for some of the clustering effects between null and wild type strains.

Studies can be done that examine the differences in motor recruitment between null and wild type viruses in neurons, but more particularly, in non-neuronal cells as most of the studies mentioned have focused on neurons. With HSV-1 infection initially occurring at epithelial cells, in order for the virus to gain entry to the nervous system, understanding the mechanisms of motor recruitment and transport in these cell types may provide a groundwork for future research applications to vector vaccines and therapies.

5.6 Concluding Remarks

Viral infection comprises a complex interplay between virus and host cell, virus proteins and host proteins. As viruses are completely reliant on host cells for replication, many have evolved very specific host-pathogen relationships. Alpha herpesviruses are unique among other pathogenic viruses because they infect two vastly different types of tissues: neurons and non-neuronal cells in the mammalian host. Neurons are highly specialized and present a specific set of challenges for viruses to overcome. In addition, alpha herpesviruses can produce lifelong infections, where reactivation produces new viral progeny and can also stimulate renewed immune responses to the

infection. Therefore these viruses must be able to thrive in the neuron, but not be so restrictively specialized that they cannot replicate in other host cell types.

The need for this balance may be why HSV-1 demonstrates a crossover in host factor reliance and interactions between cell types during replication. As demonstrated above, Rab6a is expressed in the Vero cells used in these experiments, but also in neurons [166, 167, 171]. While we demonstrated that Rab6a is a component of the egress pathway of HSV-1, Rab6a has connections to other elements of intracellular transport. It interacts with other Rab proteins, binds to cellular proteins found at the interface between microtubules and the plasma membrane, and recruits microtubule motors for vesicle transport. gE-gI-US9 proteins may direct Rab protein recruitment, which in turn may affect kinesin motor recruitment during transport. Multiple Rab proteins may be necessary during transport, and Rab6a may interact with other Rabs as vesicles are transported. At the conclusion of transport, Rab proteins may serve as the link that directs the vesicles to their destination sites by ERC1.

The interplay between these various host factors during HSV-1 infection remain to be explored, and the specific viral proteins by which HSV-1 mediates these interactions also need to be addressed. Furthermore, alterations to these viral-host protein interactions may result in alternative egress pathways, and thus open their own respective directions of inquiry.

The understanding of cell-cell spread, and specifically how alpha herpesviruses egress from infected cells, is essential if strides are to be made in the area of viral vector development. From use as vaccine platforms to gene therapy to cancer treatments, it is essential to understand how these viruses undergo intracellular trafficking in order to manipulate and design vectors that are more targeted and effective. On the other hand, where it is desirable to control or limit HSV infection, alternative treatments

are necessary. Current antivirals are limited in usability, effectiveness, and availability. Knowledge of intracellular transport and the mechanisms of viral egress may prove to be potential targets for future therapeutics.

REFERENCES

1. Tirabassi, R. S., Townley, R. A., Eldridge, M. G. & Enquist, L. W. Molecular Mechanisms of Neurotropic Herpesvirus Invasion and Spread in the CNS. *Neuroscience Biobehavioral Reviews* **22,** 709–720 (6 1998).

2. Pomeranz, L. E., Reynolds, A. E. & Hengartner, C. J. Molecular Biology of Pseudorabies Virus: Impact on Neurovirology and Veterinary Medicine. *Microbiology and Molecular Biology Reviews* **69,** 462–500 (3 2005).

3. Davison, A. J. Herpesvirus systematics. *Veterinary Microbiology* **143,** 52–69 (1 June 2010).

4. Whitley, R. J. & Roizman, B. Herpes simplex virus infections. *The Lancet* **357,** 1513–1518 (9267 2001).

5. Koyuncu, O. O., Hogue, I. B. & Enquist, L. W. Virus Infections in the Nervous System. *Cell Host Microbe* **13,** 379–393 (4 2013).

6. Pomeranz, L. E. *et al.* Gene Expression Profiling with Cre-Conditional Pseudorabies Virus Reveals a Subset of Midbrain Neurons That Participate in Reward Circuitry. *The Journal of neuroscience : the official journal of the Society for Neuroscience* **37,** 4128–4144 (15 2017).

7. Guo, Z., Chen, X.-X. & Zhang, G. Human PRV Infection in China: An Alarm to Accelerate Eradication of PRV in Domestic Pigs. *Virologica Sinica,* 1–6 (2021).

8. Jainkittivong, A. & Langlais, R. P. Herpes B virus infection. *Oral Surgery, Oral Medicine, Oral Pathology, Oral Radiology, and Endodontology* **85,** 399–403 (4 1998).

9. Rice, S. A. Release of HSV-1 Cell-Free Virions: Mechanisms, Regulation, and Likely Role in Human-Human Transmission. *Viruses* **13,** 2395 (12 2021).

10. James, C. *et al.* Herpes simplex virus: Global infection prevalence and incidence estimates, 2016. *Bulletin of the World Health Organization* **98,** 315–329 (5 May 2020).

11. Gnann, J. W. & Whitley, R. J. Herpes Simplex Encephalitis: an Update. *Current infectious disease reports* **19,** 13 (3 2017).

12. Lv, Y., Zhou, S., Gao, S. & Deng, H. Remodeling of host membranes during herpesvirus assembly and egress. *Protein Cell* **10,** 315–326 (5 2019).

13. Booy, F. P. *et al.* Liquid-crystalline, phage-like packing of encapsidated DNA in herpes simplex virus. *Cell* **64,** 1007–1015 (5 Mar. 1991).

14. Grünewald, K. *et al.* Three-Dimensional Structure of Herpes Simplex Virus from Cryo-Electron Tomography. *Science* **302,** 1396–1398 (5649 Nov. 2003).

15. McGeoch, D. J., Rixon, F. J. & Davison, A. J. Topics in herpesvirus genomics and evolution. *Virus Research* **117,** 90–104 (1 2006).

16. Bowden, R., Sakaoka, H., Donnelly, P. & Ward, R. High recombination rate in herpes simplex virus type 1 natural populations suggests significant co-infection. *Infection, Genetics and Evolution* **4,** 115–123 (2 2004).

17. Boehmer, P. E. & Lehman, I. R. HERPES SIMPLEX VIRUS DNA REPLICATION. *Annu. Rev. Biochem* **66,** 347–84. www.annualreviews.org (1997).

18. Card, J. P. & Enquist, L. W. Transneuronal Circuit Analysis with Pseudorabies Viruses. *Current Protocols in Neuroscience* **68,** 1.5.1–39 (1 2014).

19. Laval, K. & Enquist, L. W. The Neuropathic Itch Caused by Pseudorabies Virus. *Pathogens* **9,** 254 (4 2020).

20. Hilterbrand, A. T. & Heldwein, E. E. Go go gadget glycoprotein!: HSV-1 draws on its sizeable glycoprotein tool kit to customize its diverse entry routes. *PLoS Pathogens* **15** (5 May 2019).

21. Heldwein, E. E. & Krummenacher, C. Entry of herpesviruses into mammalian cells. *Cellular and Molecular Life Sciences* **65,** 1653–1668 (11 2008).

22. Kwon, H. *et al.* Soluble V Domain of Nectin-1/HveC Enables Entry of Herpes Simplex Virus Type 1 (HSV-1) into HSV-Resistant Cells by Binding to Viral Glycoprotein D. *Journal of Virology* **80,** 138–148 (1 2006).

23. Smith, G. Herpesvirus Transport to the Nervous System and Back Again. *Microbiology* **66,** 153–176 (1 2012).

24. Atanasiu, D. *et al.* Regulation of Herpes Simplex Virus gB-Induced Cell-Cell Fusion by Mutant Forms of gH/gL in the Absence of gD and Cellular Receptors. *mBio* **4,** e00046–13 (2 2013).

25. Atanasiu, D., Saw, W. T., Cohen, G. H. & Eisenberg, R. J. Cascade of Events Governing Cell-Cell Fusion Induced by Herpes Simplex Virus Glycoproteins gD, gH/gL, and gB. *Journal of Virology* **84,** 12292–12299. https://journals.asm.org/doi/10.1128/JVI.01700-10 (23 Dec. 2010).

26. Sodeik, B., Ebersold, M. W. & Helenius, A. Microtubule-mediated Transport of Incoming Herpes Simplex Virus 1 Capsids to the Nucleus. *Journal of Cell Biology* **136,** 1007–1021. http://rupress.org/jcb/article-pdf/136/5/1007/1270058/14462.pdf (5 Mar. 1997).

27. Batterson, W, Furlong, D & Roizman, B. Molecular genetics of herpes simplex virus. VIII. further characterization of a temperature-sensitive mutant defective in release of viral DNA and in other stages of the viral reproductive cycle. *Journal of Virology* **45,** 397–407 (1 1983).

28. Huffman, J. B. *et al.* The C Terminus of the Herpes Simplex Virus UL25 Protein Is Required for Release of Viral Genomes from Capsids Bound to Nuclear Pores. *Journal of Virology* **91.** https://journals.asm.org/doi/10.1128/JVI.00641-17 (15 Aug. 2017).

29. Villanueva-Valencia, J. R., Tsimtsirakis, E. & Evilevitch, A. Role of HSV-1 Capsid Vertex-Specific Component (CVSC) and Viral Terminal DNA in Capsid Docking at the Nuclear Pore. *Viruses* **13,** 2515 (12 2021).

30. Jovasevic, V., Liang, L. & Roizman, B. Proteolytic Cleavage of VP1-2 Is Required for Release of Herpes Simplex Virus 1 DNA into the Nucleus. *Journal of Virology* **82,** 3311–3319 (7 2008).

31. Honess, R. W. & Roizman, B. Regulation of Herpesvirus Macromolecular Synthesis I. Cascade Regulation of the Synthesis of Three Groups of Viral Proteins. *Journal of Virology* **14,** 8–19. https://journals.asm.org/doi/10.1128/jvi.14.1.8-19.1974 (1 July 1974).

32. Honess, R. W. & Roizman, B. Regulation of herpesvirus macromolecular synthesis: sequential transition of polypeptide synthesis requires functional viral polypeptides. *Proceedings of the National Academy of Sciences* **72,** 1276–1280. https://www.pnas.org/doi/abs/10.1073/pnas.72.4.1276 (4 Apr. 1975).

33. Kobiler, O, Brodersen, P, Taylor, M. P., Ludmir, E. B. & Enquist, L. W. Herpesvirus Replication Compartments Originate with Single Incoming Viral Genomes. *mBio* **2,** e00278–11 (6 2011).

34. Packard, J. E. & Dembowski, J. A. HSV-1 DNA Replication—Coordinated Regulation by Viral and Cellular Factors. *Viruses 2021, Vol. 13, Page 2015* **13,** 2015. https://www.mdpi.com/1999-4915/13/10/2015/htmhttps://www.mdpi.com/1999-4915/13/10/2015 (10 Oct. 2021).

35. Al-Kobaisi, M. F., Rixon, F. J., McDougall, I. & Preston, V. G. The herpes simplex virus UL33 gene product is required for the assembly of full capsids. *Virology* **180,** 380–388 (1 1991).

36. Skaliter, R. & Lehman, I. R. Rolling circle DNA replication in vitro by a complex of herpes simplex virus type 1-encoded enzymes. *Proceedings of the National Academy of Sciences* **91,** 10665–10669. https://www.pnas.org/doi/abs/10.1073/pnas.91.22.10665 (22 Oct. 1994).

37. Skaliter, R., Makhov, A. M., Griffith, J. D. & Lehman, I. R. Rolling circle DNA replication by extracts of herpes simplex virus type 1-infected human cells. *Journal of Virology* **70,** 1132–1136. https://journals.asm.org/doi/10.1128/jvi.70.2.1132-1136.1996 (2 Feb. 1996).

38. Ogasawara, M., Suzutani, T., Yoshida, I. & Azuma, M. Role of the UL25 Gene Product in Packaging DNA into the Herpes Simplex Virus Capsid: Location of UL25 Product in the Capsid and Demonstration that It Binds DNA. *Journal of Virology* **75,** 1427–1436 (3 2001).

39. Newcomb, W. W. *et al.* The UL6 Gene Product Forms the Portal for Entry of DNA into the Herpes Simplex Virus Capsid. *Journal of Virology* **75,** 10923–10932 (22 2001).

40. Snijder, J. *et al.* Vertex-Specific Proteins pUL17 and pUL25 Mechanically Reinforce Herpes Simplex Virus Capsids. *Journal of Virology* **91.** https://journals.asm.org/doi/10.1128/JVI.00123-17 (12 June 2017).

41. Freeman, K. G., Huffman, J. B., Homa, F. L. & Evilevitch, A. UL25 Capsid Binding Facilitates Mechanical Maturation of the Herpesvirus Capsid and Allows Retention of Pressurized DNA. *Journal of Virology* **95,** 755–776. https://journals.asm.org/doi/10.1128/JVI.00755-21 (20 Sept. 2021).

42. Bigalke, J. M., Heuser, T., Nicastro, D. & Heldwein, E. E. Membrane deformation and scission by the HSV-1 nuclear egress complex. *Nature Communications* **5,** 4131 (1 2014).

43. Draganova, E., Zhang, J., Zhou, H. & Heldwein, E. Structural Basis for Capsid Recruitment and Coat Formation during HSV-1 Nuclear Egress. *Viruses 2020—Novel Concepts in Virology,* 101 (2020).

44. Liu, Z. *et al.* Herpes Simplex Virus 1 UL47 Interacts with Viral Nuclear Egress Factors UL31, UL34, and Us3 and Regulates Viral Nuclear Egress. *Journal of Virology* **88,** 4657–4667 (9 2014).

45. Ahmad, I. & Wilson, D. W. HSV-1 Cytoplasmic Envelopment and Egress. *International Journal of Molecular Sciences* **21,** 5969 (17 2020).

46. Owen, D. J., Crump, C. M. & Graham, S. C. Tegument Assembly and Secondary Envelopment of Alphaherpesviruses. *Viruses* **7,** 5084–5114 (9 2015).

47. Vittone, V. *et al.* Determination of Interactions between Tegument Proteins of Herpes Simplex Virus Type 1. *Journal of Virology* **79,** 9566–9571 (15 2005).

48. Svobodova, S., Bell, S. & Crump, C. M. Analysis of the Interaction between the Essential Herpes Simplex Virus 1 Tegument Proteins VP16 and VP1/2. *Journal of Virology* **86,** 473–483 (1 2012).

49. Kamen, D. E., Gross, S. T., Girvin, M. E. & Wilson, D. W. Structural Basis for the Physiological Temperature Dependence of the Association of VP16 with the Cytoplasmic Tail of Herpes Simplex Virus Glycoprotein H. *Journal of Virology* **79,** 6134–6141 (10 2005).

50. Fossum, E. *et al.* Evolutionarily Conserved Herpesviral Protein Interaction Networks. *PLoS Pathogens* **5,** e1000570 (9 2009).

51. Gross, S. T., Harley, C. A. & Wilson, D. W. The cytoplasmic tail of Herpes simplex virus glycoprotein H binds to the tegument protein VP16 in vitro and in vivo. *Virology* **317,** 1–12 (1 Dec. 2003).

52. Szilagyi, J. F. & Cunningham, C. Identification and characterization of a novel non-infectious herpes simplex virus-related particle. *Journal of General Virology* **72,** 661–668. https://www.microbiologyresearch.org/content/journal/jgv/10.1099/0022-1317-72-3-661 (3 Mar. 1991).

53. Heilingloh, C. S. & Krawczyk, A. Role of L-particles during herpes simplex virus infection. *Frontiers in Microbiology* **8,** 2565 (DEC Dec. 2017).

54. Naghavi, M. H., Gundersen, G. G. & Walsh, D. Plus-end tracking proteins, CLASPs, and a viral Akt mimic regulate herpesvirus-induced stable microtubule formation and virus spread. *Proceedings of the National Academy of Sciences* **110,** 18268–18273 (45 2013).

55. Albecka, A. *et al.* Dual Function of the pUL7-pUL51 Tegument Protein Complex in Herpes Simplex Virus 1 Infection. *Journal of Virology* **91,** e02196–16 (2 2017).

56. Pasdeloup, D., Labetoulle, M. & Rixon, F. J. Differing Effects of Herpes Simplex Virus 1 and Pseudorabies Virus Infections on Centrosomal Function. *Journal of Virology* **87,** 7102–7112 (12 2013).

57. Austefjord, M. W., Gerdes, H.-H. & Wang, X. Tunneling nanotubes. *Communicative Integrative Biology* **7,** e27934 (1 2014).

58. Rustom, A., Saffrich, R., Markovic, I., Walther, P. & Gerdes, H.-H. Nanotubular Highways for Intercellular Organelle Transport. *Science* **303,** 1007–1010 (5660 2004).

59. Kotsakis, A., Pomeranz, L. E., Blouin, A. & Blaho, J. A. Microtubule Reorganization during Herpes Simplex Virus Type 1 Infection Facilitates the Nuclear Localization of VP22, a Major Virion Tegument Protein. *Journal of Virology* **75,** 8697–8711 (18 2001).

60. Elliott, G. & O'Hare, P. Herpes Simplex Virus Type 1 Tegument Protein VP22 Induces the Stabilization and Hyperacetylation of Microtubules. *Journal of Virology* **72,** 6448–6455 (8 1998).

61. Farnsworth, A., Wisner, T. W. & Johnson, D. C. Cytoplasmic Residues of Herpes Simplex Virus Glycoprotein gE Required for Secondary Envelopment and Binding of Tegument Proteins VP22 and UL11 to gE and gD. *Journal of Virology* **81,** 319–331 (1 2007).

62. Harley, C. A., Dasgupta, A. & Wilson, D. W. Characterization of Herpes Simplex Virus-Containing Organelles by Subcellular Fractionation: Role for Organelle Acidification in Assembly of Infectious Particles. *Journal of Virology* **75,** 1236–1251 (3 2001).

63. Hutagalung, A. H. & Novick, P. J. Role of Rab GTPases in Membrane Traffic and Cell Physiology. *Physiological Reviews* **91,** 119–149 (1 2011).

64. Desai, P., Sexton, G. L., Huang, E. & Person, S. Localization of Herpes Simplex Virus Type 1 UL37 in the Golgi Complex Requires UL36 but Not Capsid Structures. *Journal of Virology* **82,** 11354–11361 (22 2008).

65. Hogue, I. B. Tegument Assembly, Secondary Envelopment and Exocytosis. *Current Issues in Molecular Biology* **42,** 551–604 (2022).

66. Pasdeloup, D. *et al.* Inner tegument protein pUL37 of herpes simplex virus type 1 is involved in directing capsids to the trans-Golgi network for envelopment. *Journal of General Virology* **91,** 2145–2151 (9 2010).

67. Johnson, D. C. & Baines, J. D. Herpesviruses remodel host membranes for virus egress. *Nature Reviews Microbiology* **9,** 382–394 (5 2011).

68. Hogue, I. B., Bosse, J. B., Hu, J.-R., Thiberge, S. Y. & Enquist, L. W. Cellular Mechanisms of Alpha Herpesvirus Egress: Live Cell Fluorescence Microscopy of Pseudorabies Virus Exocytosis. *PLoS Pathogens* **10,** e1004535 (12 2014).

69. Hogue, I. B., Scherer, J. & Enquist, L. W. Exocytosis of Alphaherpesvirus Virions, Light Particles, and Glycoproteins Uses Constitutive Secretory Mechanisms. *mBio* **7,** e00820–16 (3 2016).

70. Stenmark, H. Rab GTPases as coordinators of vesicle traffic. *Nature Reviews Molecular Cell Biology* **10,** 513–525 (8 2009).

71. Johns, H. L., Gonzalez-Lopez, C., Sayers, C. L., Hollinshead, M. & Elliott, G. Rab6 Dependent Post-Golgi Trafficking of HSV1 Envelope Proteins to Sites of Virus Envelopment. *Traffic (Copenhagen, Denmark)* **15,** 157–178 (2 2014).

72. Mingo, R. M., Han, J., Newcomb, W. W. & Brown, J. C. Replication of herpes simplex virus: egress of progeny virus at specialized cell membrane sites. *Journal of virology* **86,** 7084–97 (13 2012).

73. Saksena, M. M. *et al.* Herpes Simplex Virus Type 1 Accumulation, Envelopment, and Exit in Growth Cones and Varicosities in Mid-Distal Regions of Axons. *Journal of Virology* **80,** 3592–3606 (7 2006).

74. Miranda-Saksena, M. *et al.* Herpes simplex virus utilizes the large secretory vesicle pathway for anterograde transport of tegument and envelope proteins and for viral exocytosis from growth cones of human fetal axons. *Journal of virology* **83,** 3187–99 (7 2009).

75. Birkmann, A. & Zimmermann, H. HSV antivirals – current and future treatment options. *Current Opinion in Virology* **18,** 9–13 (June 2016).

76. Koelle, D. M. & Corey, L. Recent Progress in Herpes Simplex Virus Immunobiology and Vaccine Research. *Clinical Microbiology Reviews* **16,** 96–113. https://journals.asm.org/doi/10.1128/CMR.16.1.96-113.2003 (1 Jan. 2003).

77. Ike, A. C., Onu, C. J., Ononugbo, C. M., Reward, E. E. & Muo, S. O. Immune Response to Herpes Simplex Virus Infection and Vaccine Development. *Vaccines 2020, Vol. 8, Page 302* **8,** 302. https://www.mdpi.com/2076-393X/8/2/302/htmhttps://www.mdpi.com/2076-393X/8/2/302 (2 June 2020).

78. Gabutti, G., Bolognesi, N., Sandri, F., Florescu, C. & Stefanati, A. Varicella zoster virus vaccines: an update . *ImmunoTargets and Therapy* **Volume 8,** 15–28. https://www.tandfonline.com/action/journalInformation?journalCode=ditt20 (Aug. 2019).

79. Levin, M. J. & Weinberg, A. Immune Responses to Varicella-Zoster Virus Vaccines. *Current Topics in Microbiology and Immunology* **438,** 223–246. https://link.springer.com/chapter/10.1007/82_2021_245 (2023).

80. Freuling, C. M., Müller, T. F. & Mettenleiter, T. C. Vaccines against pseudorabies virus (PrV). *Veterinary Microbiology* **206,** 3–9 (July 2017).

81. Enquist, L. W., Tomishima, M. J., Gross, S & Smith, G. A. Directional spread of an α-herpesvirus in the nervous system. *Veterinary Microbiology* **86,** 5–16 (1-2 2002).

82. Yu, X. *et al.* Pathogenic Pseudorabies Virus, China, 2012 - Volume 20, Number 1—January 2014 - Emerging Infectious Diseases journal - CDC. *Emerging Infectious Diseases* **20,** 102–104. https://wwwnc.cdc.gov/eid/article/20/1/13-0531_article (1 2014).

83. Wu, R., Bai, C., Sun, J., Chang, S. & Zhang, X. Emergence of virulent pseudorabies virus infection in Northern China. *Journal of Veterinary Science* **14,** 363–365. https://synapse.koreamed.org/articles/1041246 (3 Sept. 2013).

84. Gu, Z. *et al.* A novel inactivated gE/gI deleted pseudorabies virus (PRV) vaccine completely protects pigs from an emerged variant PRV challenge. *Virus Research* **195,** 57–63 (Jan. 2015).

85. Schiffer, J. T. & Gottlieb, S. L. Biologic interactions between HSV-2 and HIV-1 and possible implications for HSV vaccine development. *Vaccine* **37,** 7363–7371 (50 Nov. 2019).

86. Gottlieb, S. L. *et al.* Modelling efforts needed to advance herpes simplex virus (HSV) vaccine development: Key findings from the World Health Organization Consultation on HSV Vaccine Impact Modelling. *Vaccine* **37,** 7336–7345 (50 Nov. 2019).

87. Marconi, P., Argnani, R., Berto, E., Epstein, A. L. & Manservigi, R. HSV as a vector in vaccine development and gene therapy. *Human Vaccines* **4,** 91–105. https://www.tandfonline.com/doi/abs/10.4161/hv.4.2.6212 (2 2008).

88. Sena-Esteves, M., Saeki, Y., Fraefel, C. & Breakefield, X. O. HSV-1 Amplicon Vectors—Simplicity and Versatility. *Molecular Therapy* **2,** 9–15. http://www.cell.com/article/S1525001600900960/fulltexthttp://www.cell.com/article/S1525001600900960/abstracthttps://www.cell.com/molecular-therapy-family/molecular-therapy/abstract/S1525-0016(00)90096-0 (1 July 2000).

89. Frampton, A. R., Goins, W. F., Nakano, K., Burton, E. A. & Glorioso, J. C. HSV trafficking and development of gene therapy vectors with applications in the nervous system. *Gene Therapy 2005 12:11* **12,** 891–901. https://www.nature.com/articles/3302545 (11 May 2005).

90. Velarde, K., Hogue, I. B., Manfredsson, F., Sandoval, I. & Varsani, A. *Herpes Simplex Virus 1 Amplicon Vectors* (Arizona State University, Apr. 2021).

91. Miyagawa, Y. *et al.* Herpes simplex viral-vector design for efficient transduction of nonneuronal cells without cytotoxicity. *Proc Natl Acad Sci USA* **112,** E1632–1641 (13 Mar. 2015).

92. Verlengia, G. *et al.* Engineered HSV vector achieves safe long-term transgene expression in the central nervous system. *Scientific Reports 2017 7:1* **7,** 1–11. https://www.nature.com/articles/s41598-017-01635-1 (1 May 2017).

93. Johnson, D. B., Puzanov, I. & Kelley, M. C. Talimogene laherparepvec (T-VEC) for the treatment of advanced melanoma. *http://dx.doi.org/10.2217/imt.15.35* **7,** 611–619. https://www.futuremedicine.com/doi/10.2217/imt.15.35 (6 June 2015).

94. Rehman, H., Silk, A. W., Kane, M. P. & Kaufman, H. L. Into the clinic: Talimogene laherparepvec (T-VEC), a first-in-class intratumoral oncolytic viral therapy. *Journal for ImmunoTherapy of Cancer* **4,** 1–8. https://link.springer.com/articles/10.1186/s40425-016-0158-5https://link.springer.com/article/10.1186/s40425-016-0158-5 (1 Sept. 2016).

95. Grandi, P. *et al.* Design and application of oncolytic HSV vectors for glioblastoma therapy. *http://dx.doi.org/10.1586/ern.09.9* **9,** 505–517. https://www.tandfonline.com/doi/abs/10.1586/ern.09.9 (4 Apr. 2014).

96. Shibata, T. *et al.* Development of an oncolytic HSV vector fully retargeted specifically to cellular EpCAM for virus entry and cell-to-cell spread. *Gene Therapy 2016 23:6* **23,** 479–488. https://www.nature.com/articles/gt201617 (6 Feb. 2016).

97. Krasnovskiĭ, A. A. & Kovalev, I. V. [Chlorophyll phosphorescence in leaves and cells of algae]. *Biofizika* **23,** 920–922. https://europepmc.org/article/med/698268 (5 Sept. 1978).

98. Hastings, J. W., Potrikusv, C. J., Gupta, S. C., Kurfürst, M. & Makemson, J. C. Biochemistry and Physiology of Bioluminescent Bacteria. *Advances in Microbial Physiology* **26,** 235–291 (C Jan. 1985).

99. Fasel, A., Muller, P. A., Suppan, P. & Vauthey, E. Photoluminescence of the African scorpion "Pandinus imperator". *Journal of Photochemistry and Photobiology B: Biology* **39,** 96–98 (1 May 1997).

100. Brasier, A. R., Tate, J. E. & Habener, J. F. Optimized use of the firefly luciferase assay as a reporter gene in mammalian cell lines. *Biotechniques* **7,** 1116–1122. https://europepmc.org/article/med/2698191 (10 Nov. 1989).

101. Gould, S. J. & Subramani, S. Firefly luciferase as a tool in molecular and cell biology. *Analytical Biochemistry* **175,** 5–13 (1 Nov. 1988).

102. Kendall, J. M. & Badminton, M. N. Aequorea victoria bioluminescence moves into an exciting new era. *Trends Biotechnol.* **16,** 216–224 (5 Dec. 1998).

103. Roy, R *et al.* Green Fluorescent Protein as a Marker for Gene Expression. *Science* **263,** 802–805. https://www.science.org/doi/10.1126/science.8303295 (5148 1994).

104. Inouye, S. & Tsuji, F. I. Aequorea green fluorescent protein: Expression of the gene and fluorescence characteristics of the recombinant protein. *FEBS Letters* **341,** 277–280 (2-3 Mar. 1994).

105. Cubitt, A. B. *et al.* Understanding, improving and using green fluorescent proteins. *Trends in Biochemical Sciences* **20,** 448–455 (11 Nov. 1995).

106. Matz, M. V. *et al.* Fluorescent proteins from nonbioluminescent Anthozoa species. *Nature Biotechnology 1999 17:10* **17,** 969–973. https://www.nature.com/articles/nbt1099_969 (10 Oct. 1999).

107. Shaner, N. C. *et al.* Improved monomeric red, orange and yellow fluorescent proteins derived from Discosoma sp. red fluorescent protein. *Nature Biotechnology 2004 22:12* **22,** 1567–1572. https://www.nature.com/articles/nbt1037 (12 Nov. 2004).

108. Zhang, J., Campbell, R. E., Ting, A. Y. & Tsien, R. Y. Creating new fluorescent probes for cell biology. *Nat. Rev. Mol. Cell Biol.* **3,** 906–918 (12 Dec. 2002).

109. Hogue, I. B. *et al.* Fluorescent Protein Approaches in Alpha Herpesvirus Research. *Viruses* **7** (11 2015).

110. Boncompain, G. & Perez, F. Fluorescence-based analysis of trafficking in mammalian cells. *Methods in Cell Biology* **118,** 179–194 (2013).

111. Weissman, T. A. & Pan, Y. A. Brainbow: New Resources and Emerging Biological Applications for Multicolor Genetic Labeling and Analysis. *Genetics* **199,** 293–306. https://academic.oup.com/genetics/article/199/2/293/5935802 (2 Feb. 2015).

112. Klingen, Y., Conzelmann, K.-K. & Finke, S. Double-Labeled Rabies Virus: Live Tracking of Enveloped Virus Transport. *Journal of Virology* **82,** 237–245. https://journals.asm.org/doi/10.1128/JVI.01342-07 (1 Jan. 2008).

113. Bauer, A. *et al.* Anterograde Glycoprotein-Dependent Transport of Newly Generated Rabies Virus in Dorsal Root Ganglion Neurons. *Journal of Virology* **88,** 14172–14183. https://journals.asm.org/doi/10.1128/JVI.02254-14 (24 Dec. 2014).

114. Isomura, M., Yamada, K., Noguchi, K. & Nishizono, A. Near-infrared fluorescent protein iRFP720 is optimal for in vivo fluorescence imaging of rabies virus infection. *Journal of General Virology* **98,** 2689–2698. https://www.microbiologyresearch.org/content/journal/jgv/10.1099/jgv.0.000950 (11 Nov. 2017).

115. Sarma, J. D., Scheen, E., Seo, S. H., Koval, M. & Weiss, S. R. Enhanced green fluorescent protein expression may be used to monitor murine coronavirus spread in vitro and in the mouse central nervous system. *Journal of NeuroVirology* **8,** 381–391. https://link.springer.com/article/10.1080/13550280260422686 (5 Oct. 2002).

116. Bauer, L. *et al.* The neuroinvasiveness, neurotropism, and neurovirulence of SARS-CoV-2. *Trends in Neurosciences* **45,** 358–368 (5 May 2022).

117. Cardona, G. C., Pájaro, L. D. Q., Marzola, I. D. Q., Villegas, Y. R. & Salazar, L. R. M. Neurotropism of SARS-CoV 2: Mechanisms and manifestations. *Journal of the Neurological Sciences* **412,** 116824. /pmc/articles/PMC7141641/https://www.ncbi.nlm.nih.gov/pmc/articles/PMC7141641/ (May 2020).

118. Jöns, A. & Mettenleiter, T. C. Green fluorescent protein expressed by recombinant pseudorabies virus as an in vivo marker for viral replication. *Journal of Virological Methods* **66,** 283–292 (2 July 1997).

119. Smith, B. N. *et al.* Pseudorabies virus expressing enhanced green fluorescent protein: A tool for in vitro electrophysiological analysis of transsynaptically labeled neurons in identified central nervous system circuits. *Proceedings of the National Academy of Sciences* **97,** 9264–9269 (16 2000).

120. Rinaman, L, Card, J. P. & Enquist, L. W. Spatiotemporal responses of astrocytes, ramified microglia, and brain macrophages to central neuronal infection with pseudorabies virus. *Journal of Neuroscience* **13,** 685–702 (2 1993).

121. Yang, M., Card, J. P., Tirabassi, R. S., Miselis, R. R. & Enquist, L. W. Retrograde, Transneuronal Spread of Pseudorabies Virus in Defined Neuronal Circuitry of the Rat Brain Is Facilitated by gE Mutations That Reduce Virulence. *Journal of Virology* **73,** 4350–4359. https://journals.asm.org/doi/10.1128/JVI.73.5.4350-4359.1999 (5 May 1999).

122. Pickard, G. E. *et al.* Intravitreal Injection of the Attenuated Pseudorabies Virus PRV Bartha Results in Infection of the Hamster Suprachiasmatic Nucleus Only by Retrograde Transsynaptic Transport via Autonomic Circuits. *Journal of Neuroscience* **22,** 2701–2710 (7 2002).

123. Ekstrand, M. I., Enquist, L. W. & Pomeranz, L. E. The alpha-herpesviruses: molecular pathfinders in nervous system circuits. *Trends in Molecular Medicine* **14,** 134–40 (3 2008).

124. Enquist, L. W. Exploiting Circuit-Specific Spread of Pseudorabies Virus in the Central Nervous System: Insights to Pathogenesis and Circuit Tracers. *The Journal of Infectious Diseases* **186,** S209–S214 (Supplement$_2$ 2002).

125. DeFalco, J. *et al.* Virus-Assisted Mapping of Neural Inputs to a Feeding Center in the Hypothalamus. *Science* **291,** 2608–2613 (5513 2001).

126. Yoon, H., Enquist, L. W. & Dulac, C. Olfactory Inputs to Hypothalamic Neurons Controlling Reproduction and Fertility. *Cell* **123,** 669–682 (4 2005).

127. Rosario, W. *et al.* The Brain–to–Pancreatic Islet Neuronal Map Reveals Differential Glucose Regulation From Distinct Hypothalamic Regions. *Diabetes* **65,** 2711–2723 (9 2016).

128. Jia, F. *et al.* Optimization of the Fluorescent Protein Expression Level Based on Pseudorabies Virus Bartha Strain for Neural Circuit Tracing. *Frontiers in Neuroanatomy* **13,** 63 (2019).

129. Kobiler, O., Lipman, Y., Therkelsen, K., Daubechies, I. & Enquist, L. W. Herpesviruses carrying a Brainbow cassette reveal replication and expression of limited numbers of incoming genomes. *Nature Communications* **1,** 146 (1 2010).

130. Nectow, A. R. *et al.* Identification of a Brainstem Circuit Controlling Feeding. *Cell* **170,** 429–442.e11 (3 2017).

131. Yeo, S.-H., Kyle, V., Blouet, C., Jones, S. & Colledge, W. H. Mapping neuronal inputs to Kiss1 neurons in the arcuate nucleus of the mouse. *PLOS ONE* **14,** e0213927 (3 2019).

132. Smith, G. A., Gross, S. P. & Enquist, L. W. Herpesviruses use bidirectional fast-axonal transport to spread in sensory neurons. *Proceedings of the National Academy of Sciences* **98,** 3466–3470 (6 2001).

133. Sankaranarayanan, S., Angelis, D. D., Rothman, J. E. & Ryan, T. A. The Use of pHluorins for Optical Measurements of Presynaptic Activity. *Biophysical Journal* **79,** 2199–2208 (4 2000).

134. Paroutis, P., Touret, N. & Grinstein, S. The pH of the Secretory Pathway: Measurement, Determinants, and Regulation. *Physiology* **19,** 207–215 (4 2004).

135. Llopis, J., McCaffery, J. M., Miyawaki, A., Farquhar, M. G. & Tsien, R. Y. Measurement of cytosolic, mitochondrial, and Golgi pH in single living cells with green fluorescent proteins. *Proceedings of the National Academy of Sciences* **95,** 6803–6808 (12 1998).

136. Rinaman, L, Roesch, M. R. & Card, J. P. Retrograde transynaptic pseudorabies virus infection of central autonomic circuits in neonatal rats. *Developmental Brain Research* **114,** 207–216 (2 1999).

137. Loncoman, C. A. *et al.* Natural recombination in alphaherpesviruses: Insights into viral evolution through full genome sequencing and sequence analysis. *Infection, Genetics and Evolution* **49,** 174–185 (Apr. 2017).

138. Tirabassi, R. S. & Enquist, L. W. Role of Envelope Protein gE Endocytosis in the Pseudorabies Virus Life Cycle. *Journal of Virology* **72,** 4571–4579. https://journals.asm.org/doi/10.1128/JVI.72.6.4571-4579.1998 (6 June 1998).

139. Brideau, A. D., Banfield, B. W. & Enquist, L. W. The Us9 Gene Product of Pseudorabies Virus, an Alphaherpesvirus, Is a Phosphorylated, Tail-Anchored Type II Membrane Protein. *Journal of Virology* **72,** 4560–4570. https://journals.asm.org/doi/10.1128/JVI.72.6.4560-4570.1998 (6 June 1998).

140. Schindelin, J. *et al.* Fiji: an open-source platform for biological-image analysis. *Nature Methods* **9,** 676–682 (7 2012).

141. Meijering, E., Dzyubachyk, O. & Smal, I. Methods for Cell and Particle Tracking. *Methods in Enzymology* **504,** 183–200 (Jan. 2012).

142. Johnson, D. C., Webb, M., Wisner, T. W. & Brunetti, C. Herpes Simplex Virus gE/gI Sorts Nascent Virions to Epithelial Cell Junctions, Promoting Virus Spread. *Journal of Virology* **75,** 821–833 (2 2001).

143. DuRaine, G., Wisner, T. W., Howard, P., Williams, M. & Johnson, D. C. Herpes Simplex Virus gE/gI and US9 Promote both Envelopment and Sorting of Virus Particles in the Cytoplasm of Neurons, Two Processes That Precede Anterograde Transport in Axons. *Journal of Virology* **91,** e00050–17 (11 2017).

144. Scherer, J. *et al.* A kinesin-3 recruitment complex facilitates axonal sorting of enveloped alpha herpesvirus capsids. *PLOS Pathogens* **16,** e1007985 (1 2020).

145. Huang, H., Koyuncu, O. O. & Enquist, L. W. Pseudorabies Virus Infection Accelerates Degradation of the Kinesin-3 Motor KIF1A. *Journal of Virology* **94** (9 2020).

146. Wilson, D. W. & Purpura, D. P. Motor Skills: Recruitment of Kinesins, Myosins and Dynein during Assembly and Egress of Alphaherpesviruses. *Viruses 2021, Vol. 13, Page 1622* **13,** 1622. https://www.mdpi.com/1999-4915/13/8/1622/htmhttps://www.mdpi.com/1999-4915/13/8/1622 (8 Aug. 2021).

147. Elliott, G. & O'Hare, P. Intercellular Trafficking and Protein Delivery by a Herpesvirus Structural Protein. *Cell* **88,** 223–233 (2 1997).

148. Foster, T. P., Rybachuk, G. V. & Kousoulas, K. G. Expression of the enhanced green fluorescent protein by herpes simplex virus type 1 (HSV-1) as an in vitro or in vivo marker for virus entry and replication. *Journal of Virological Methods* **75,** 151–160 (2 1998).

149. Desai, P. & Person, S. Incorporation of the Green Fluorescent Protein into the Herpes Simplex Virus Type 1 Capsid. *Journal of Virology* **72,** 7563–7568. https://journals.asm.org/doi/10.1128/JVI.72.9.7563-7568.1998 (9 Sept. 1998).

150. Crump, C. M. *et al.* Alphaherpesvirus glycoprotein M causes the relocalization of plasma membrane proteins. *Journal of General Virology* **85,** 3517–3527 (12 2004).

151. Song, R. *et al.* Two Modes of the Axonal Interferon Response Limit Alphaherpesvirus Neuroinvasion. *mBio* **7,** e02145–15 (1 2016).

152. Flomm, F. J. *et al.* Intermittent bulk release of human cytomegalovirus. *PLOS Pathogens* **18,** e1010575. https://journals.plos.org/plospathogens/article?id=10.1371/journal.ppat.1010575 (8 Aug. 2022).

153. Llewellyn, G. N., Hogue, I. B., Grover, J. R. & Ono, A. Nucleocapsid Promotes Localization of HIV-1 Gag to Uropods That Participate in Virological Synapses between T Cells. *PLOS Pathogens* **6,** e1001167. https://journals.plos.org/plospathogens/article?id=10.1371/journal.ppat.1001167 (10 Oct. 2010).

154. Llewellyn, G. N., Grover, J. R., Olety, B. & Ono, A. HIV-1 Gag Associates with Specific Uropod-Directed Microdomains in a Manner Dependent on Its MA Highly Basic Region. *Journal of Virology* **87,** 6441–6454. https://journals.asm.org/doi/10.1128/JVI.00040-13 (11 June 2013).

155. Pais-Correia, A. M. *et al.* Biofilm-like extracellular viral assemblies mediate HTLV-1 cell-to-cell transmission at virological synapses. *Nature Medicine 2009 16:1* **16,** 83–89. https://www.nature.com/articles/nm.2065 (1 Dec. 2009).

156. Tarasevich, A., Filatov, A., Pichugin, A. & Mazurov, D. Monoclonal antibody profiling of cell surface proteins associated with the viral biofilms on HTLV-1 transformed cells. *Acta Virologica* **59,** 247–256. https://europepmc.org/article/med/26435148 (3 Sept. 2015).

157. Millen, S. *et al.* Collagen iv (Col4a1, col4a2), a component of the viral biofilm, is induced by the htlv-1 oncoprotein tax and impacts virus transmission. *Frontiers in Microbiology* **10,** 2439 (OCT Oct. 2019).

158. Nakamura, H. *et al.* Initial human T-cell leukemia virus type 1 infection of the salivary gland epithelial cells requires a biofilm-like structure. *Virus Research* **269,** 197643 (Aug. 2019).

159. Norrild, B., Virtanen, I., Lehto, V. P. & Pedersen, B. Accumulation of herpes simplex virus type 1 glycoprotein D in adhesion areas of infected cells. *Journal of General Virology* **64,** 2499–2503. https://www.microbiologyresearch.org/content/journal/jgv/10.1099/0022-1317-64-11-2499 (11 Nov. 1983).

160. McMillan, T. N. & Johnson, D. C. Cytoplasmic Domain of Herpes Simplex Virus gE Causes Accumulation in the trans -Golgi Network, a Site of Virus Envelopment and Sorting of Virions to Cell Junctions. *Journal of Virology* **75,** 1928–1940 (4 2001).

161. Tomishima, M. J. & Enquist, L. W. A conserved α-herpesvirus protein necessary for axonal localization of viral membrane proteins. *The Journal of Cell Biology* **154,** 741–752 (4 2001).

162. Diefenbach, R. J. *et al.* The Basic Domain of Herpes Simplex Virus 1 pUS9 Recruits Kinesin-1 To Facilitate Egress from Neurons. *Journal of Virology* **90,** 2102–2111 (4 2016).

163. Kratchmarov, R. *et al.* Glycoproteins gE and gI Are Required for Efficient KIF1A-Dependent Anterograde Axonal Transport of Alphaherpesvirus Particles in Neurons. *Journal of Virology* **87,** 9431–9440 (17 2013).

164. Kramer, T. *et al.* Kinesin-3 Mediates Axonal Sorting and Directional Transport of Alphaherpesvirus Particles in Neurons. *Cell Host Microbe* **12** (6 2012).

165. Homma, Y. *et al.* Comprehensive knockout analysis of the Rab family GTPases in epithelial cells. *Journal of Cell Biology* **218,** 2035–2050. https://doi.org/10.1083/jcb.201810134 (6 June 2019).

166. Nyitrai, H., Wang, S. S. H. & Kaeser, P. S. ELKS1 Captures Rab6-Marked Vesicular Cargo in Presynaptic Nerve Terminals. *Cell Reports* **31,** 107712 (10 June 2020).

167. Scheper, W. *et al.* Rab6 is increased in Alzheimer's disease brain and correlates with endoplasmic reticulum stress. *Neuropathology and Applied Neurobiology* **33,** 523–532. https://onlinelibrary.wiley.com/doi/full/10.1111/j.1365-2990.2007.00846.xhttps://onlinelibrary.wiley.com/doi/abs/10.1111/j.1365-2990.2007.00846.xhttps://onlinelibrary.wiley.com/doi/10.1111/j.1365-2990.2007.00846.x (5 Oct. 2007).

168. Piacentini, R. *et al.* HSV-1 and Alzheimer's disease: More than a hypothesis. *Frontiers in Pharmacology* **5 MAY,** 97 (May 2014).

169. Harris, S. A. & Harris, E. A. Molecular mechanisms for herpes simplex virus type 1 pathogenesis in Alzheimer's disease. *Frontiers in Aging Neuroscience* **10,** 48 (MAR Mar. 2018).

170. Protto, V. *et al.* Role of HSV-1 in Alzheimer's disease pathogenesis: A challenge for novel preventive/therapeutic strategies. *Current Opinion in Pharmacology* **63,** 102200 (Apr. 2022).

171. Opdam, F. J. *et al.* The small GTPase Rab6B, a novel Rab6 subfamily member, is cell-type specifically expressed and localised to the Golgi apparatus. *Journal of Cell Science* **113,** 2725–2735. https://journals.biologists.com/jcs/article/113/15/2725/26177/The-small-GTPase-Rab6B-a-novel-Rab6-subfamily (15 Aug. 2000).

172. Deinhardt, K. *et al.* Rab5 and Rab7 Control Endocytic Sorting along the Axonal Retrograde Transport Pathway. *Neuron* **52,** 293–305 (2 Oct. 2006).

173. Grigoriev, I. *et al.* Rab6 Regulates Transport and Targeting of Exocytotic Carriers. *Developmental Cell* **13,** 305–314 (2 Aug. 2007).

174. Gillingham, A. K., Bertram, J., Begum, F. & Munro, S. In vivo identification of GTPase interactors by mitochondrial relocalization and proximity biotinylation. *eLife* **8.** /pmc/articles/PMC6639074//pmc/articles/PMC6639074/?report=abstracthttps://www.ncbi.nlm.nih.gov/pmc/articles/PMC6639074/ (July 2019).

175. Miserey-Lenkei, S. *et al.* Rab6-interacting Protein 1 Links Rab6 and Rab11 Function. *Traffic* **8,** 1385–1403. https://onlinelibrary.wiley.com/doi/full/10.1111/j.1600-0854.2007.00612.xhttps://onlinelibrary.wiley.com/doi/abs/10.1111/j.1600-0854.2007.00612.xhttps://onlinelibrary.wiley.com/doi/10.1111/j.1600-0854.2007.00612.x (10 Oct. 2007).

176. Guichard, A., Nizet, V. & Bier, E. RAB11-mediated trafficking in host–pathogen interactions. *Nature Reviews Microbiology 2014 12:9* **12,** 624–634. https://www.nature.com/articles/nrmicro3325 (9 Aug. 2014).

177. Kawabe, H. *et al.* ELKS1 localizes the synaptic vesicle priming protein bMunc13-2 to a specific subset of active zones. *Journal of Cell Biology* **216,** 1143–1161. https://doi.org/10.1083/jcb.201606086 (4 Apr. 2017).

178. Scherer, J., Yaffe, Z. A., Vershinin, M. & Enquist, L. W. Dual-Color Herpesvirus Capsids Discriminate Inoculum from Progeny and Reveal Axonal Transport Dynamics. *Journal of Virology* **90,** 9997–10006. https://journals.asm.org/doi/10.1128/JVI.01122-16 (21 Nov. 2016).

179. Diwaker, D., Murray, J. W., Barnes, J., Wolkoff, A. W. & Wilson, D. W. Deletion of the Pseudorabies Virus gE/gI-US9p complex disrupts kinesin KIF1A and

KIF5C recruitment during egress, and alters the properties of microtubule-dependent transport in vitro. *PLOS Pathogens* **16,** e1008597. https://journals.plos.org/plospathogens/article?id=10.1371/journal.ppat.1008597 (6 June 2020).

APPENDIX A

COAUTHOR PERMISSION FOR PREVIOUSLY PUBLISHED WORK IN CHAPTER 3

The co-authors listed in Chapter 3 have given permission for the previously published work entitled "Live-cell Fluorescence Microscopy of HSV-1 Cellular Egress by Exocytosis" to be included in this dissertation work.

APPENDIX B

COAUTHOR PERMISSION FOR PREVIOUSLY PUBLISHED WORK IN CHAPTER 4

The co-authors listed in Chapter 4 have given permission for the previously published work entitled "Herpes Simplex Virus 1 (HSV-1) Uses the Rab6 Post-Golgi Secretory Pathway For Viral Egress" to be included in this dissertation work.